T-PM-Sym1 **ELECTROCHEMICAL ION GRADIENTS AND ACTIVE TRANSPORT: PASSAGE TO PERMEASE.** **H. R. Kaback. Roche Institute of Molecular Biology, Roche Research Center, Nutley, NJ 07110.**

β-Galactoside:H^+ symport (co-transport) is mediated by the *lac* permease, a hydrophobic membrane protein encoded by the *lac y* gene that has been purified to homogeneity in a functional state. Since proteoliposomes reconstituted with purified permease catalyze transport with turnover numbers and kinetic properties comparable to those observed in right-side-out membrane vesicles, it is clear that a single polypeptide species is responsible for β-galactoside transport. Based on circular dichroic studies and on the hydropathic profile of the permease, a secondary structure has been proposed in which the permease consists of 12 α-helical segments that traverse the membrane in a zig-zag fashion connected by shorter, hydrophilic domains that contain most of the charged residues in the protein. Preliminary support for the model has been obtained from proteolysis experiments and from binding studies with monoclonal antibodies and site-directed polyclonal antibodies. Furthermore, one of the monoclonal antibodies binds quantitatively to an externally disposed epitope and inhibits all translocation reactions that involve net H^+ movement with no effect on exchange or binding. The role of histidine and certain sulfhydryl residues in the permease has been evaluated by oligonucleotide-directed, site-specific mutagenesis.

T-PM-Sym2 MOLECULAR MECHANISM OF HISTIDINE TRANSPORT IN BACTERIA. G. Ferro-Luzzi AMES, Department of Biochemistry, University of California, Berkeley, California 94720

Bacterial periplasmic transport systems are typically composed of a periplasmic substrate-binding protein and three membrane-bound proteins. The periplasmic histidine permease from Salmonella typhimurium has been extensively characterized genetically, physiologically, and biochemically. The operon coding for the four transport proteins has been cloned and sequenced. The histidine-binding protein has been purified and shown to undergo a conformational change upon binding of histidine; it has also been shown by genetic means to interact directly with one of the membrane-bound proteins. This latter protein has also been shown to bind ATP. Since in all cases tested one protein from several unrelated periplasmic permeases is known to interact with ATP, it has been suggested that these proteins are responsible for the mechanism of energy-coupling. Interestingly, all of these ATP-binding proteins show strong sequence homology, indicating a common evolutionary origin and a similar function. The other two membrane-bound components are very hydrophobic and are presumably embedded in the cytoplasmic membrane. Two alternative models are presented. One suggests the formation of a pore which allows passage of substrate only when the liganded binding protein interacts with the membrane-bound proteins. According to the other model substrate-binding sites on the membrane-bound components become available when the liganded binding protein interacts with one or more of them.

The genes coding for the membrane-bound components have been subcloned and the proteins greatly overproduced. The purification of these proteins and their reconstitution into membrane vesicles is being attempted. In vitro mutagenesis and genetics are also being used to help characterize the molecular mechanism of action of these proteins.

T-PM-Sym3 GENETIC STUDIES OF AMINO ACID TRANSPORT IN CHINESE HAMSTER OVARY CELLS, Dale L. Oxender, Biological Chemistry, University of Michigan, Ann Arbor, MI 48109

The major transport systems for the uptake of neutral amino acids into mammalian cells are designated A, ASC and L. The transport systems and their regulation have been characterized in several cell types including the Chinese Hamster Ovary (CHO) cells. System A is Na^+-dependent and serves for low molecular weight amino acids such as glycine, proline and alanine. System ASC is also Na^+-dependent and shows a preference for alanine, serine and cysteine. System L is sodium-independent and serves for the uptake of branched-chain and aromatic amino acids. Since these systems show significant overlap in specificity, the availability of mutations in one or more of the Systems would greatly facilitate their characterization. We have been using genetic approaches to study the transport systems in CHO cells. In the present study we have isolated and characterized CHO mutants defective in the regulation and activity of System L. We have also used hamster-human cell hybrids to show that human chromosome 20 is responsible for System L transport activity. Using a cosmid library constructed from total human genomic DNA we have obtained transformants that show increased leucine transport as a result of the stable integration of one or more of the cosmid vectors containing human DNA sequences. These transformants are currently being characterized and attempts are being made to rescue the human DNA from the high transport transformed CHO cells. (Supported by NIH Grant GM-20737)

T-PM-Sym4 RECENT WORK ON BACTERIORHODOPSIN. H. G. Khorana, Massachusetts Institute of Technology, Cambridge, Massachusetts 02139.

(a) Studies at the Protein Level. BR is a single polypeptide chain of 248 amino acids whose sequence is known both by protein and gene sequencing. The protein can be completely delipidated and, subsequently, reconstituted into vesicles that translocate protons efficiently. Following complete denaturation, the protein refolds quantitatively to regenerate the BR chromophore. The molecule can be selectively cleaved to form fragments that also reassociate to regenerate the native BR structure. Using a photolabeled analog of retinal, approximate orientation of the chromophore in the membrane has been deduced. (b) Expression of the BR Gene in E. coli and Site-specific Mutagenesis. Using a cDNA fragment as the probe, the BR gene has been identified. It has been inserted into an expression vector under the control of the lipoprotein and Lac promoters in tandem. These constructions gave fusion proteins containing extensions of 8-25 amino acids at the N-terminus of BR. Using other vectors, bacterio-opsin without extension at N-terminus has been prepared. A variety of methods have been used for specific amino acid replacements in the protein and mutants containing such replacements have been prepared. (c) Effects of Amino Acid Replacements on Properties of Bacteriorhodopsin. A variety of amino acid replacements in helices F and G have been carried out. By the reconstitution procedure described above, three types of effects have been characterized; (1) the chromophore does not regenerate; (2) the regenerated chromophore shows a shift in the λmax; (3) the original chromophore is reformed. Effects on proton translocation are being studied.

T-PM-A1 K CURRENTS IN PERFUSED AXON ARE MODIFIED BY ATP. Christina Webb and F. Bezanilla. Dept. of Physiology, UCLA, Los Angeles CA.

ATP has been shown to modulate the K currents in the dialyzed and voltage-clamped squid giant axon (Biophys. J. 47:222a, 1985). The modulation in the perfused squid giant axon is presented here. The internal perfusion medium contained (in mM): 2 Mg^{++}, 20 $PO_4^{=}$, 160 Glutamate, 200 K^+, 1 EGTA, and 10 TRIS, pH 7.4 (19-20°C); in some cases $PO_4^{=}$ and Mg^{++} were replaced by 40 mM F^-. ATP was added as ATP-Mg (2 mM) and, in some cases, protein kinase (catalytic subunit of cAMP dependent from Sigma) was added. The external medium contained (in mM): 50 Ca^{++}, 520 TRIS, 600 NO_3^- and 2 K^+, with 300 nM TTX, pH 7.6. ATP, alone or with kinase, caused an increase in the conductance (g) of up to 3 times, depending on the axon and the holding potential; at more positive holding potentials the effect was larger, consistent with a decrease in the amount of inactivation. The kinetics are changed by ATP; the currents turn on more slowly (up to 2 times slower). This is not just a shift of the time constants on the voltage (V) axis as currents with comparable time constants still do not superimpose. The fact that ATP with or without kinase modified the K currents suggests that the kinase is not removed by the perfusion. Removal of ATP did not reverse the effect indicating that the phosphatase is washed out. The effects of ATP were partially reversed by alkaline phosphatase (Sigma) - the conductance decreased at positive potentials and increased at negative potentials. The time constants for turning on also became faster after phosphatase was added. Without ATP the g-V curve e-folds in about 5 mV; with ATP the curve e-folds in about 9 mV suggesting that with ATP fewer charges are involved in the gating of the K conductance. (Supported by MDA and USPHS GM30376. C.W. was a Grass fellow)

T-PM-A2 ATP MODIFICATION OF K CURRENTS IN DIALYZED SQUID AXONS. E. Perozo, R. DiPolo, C. Caputo H. Rojas and F. Bezanilla. CBB, IVIC, Apartado 1827, Caracas 1010A, Venezuela and Dept. of Physiology, UCLA, Los Angeles CA, USA.

We reported previously that ATP modifies both the amplitude and kinetics of K currents in dialyzed squid axons under voltage clamp conditions. (Bezanilla et al. 1985 Biophys. J. 47:222a). Further characterization of the effects of phosphorylation is presented here. Internal dialysis solution contained (in mM): 310 K^+, 15 $PO_4^{=}$, 3 Mg^{++}, 110 glycine, 1 EGTA, pH=7.3; external medium was artificial sea water with 300 nM TTX and 1 mM cyanide. The previously reported large variation in the effect of ATP on the current amplitude was found to be correlated with the membrane holding potential suggesting that ATP may modify the K slow inactivation. This was confirmed since the K inactivation curve was found to be shifted in ATP by 15 to 20 mV towards more positive potentials. A similar shift could be observed at pH=9 in the absence of ATP, suggesting that a charged group is involved in the ATP effect. The activation curve is also displaced to more positive potentials but the effect cannot be fully explained by a simple shift. The analysis of the current kinetics for a pulse to 0 mV from a holding potential of -60 mV shows an increase in the time constant, in the lag and in the steady fraction of open channels. Experiments buffering the ATP concentration with 5 mM Phosphoarginine shows a K_m of 10 uM for the amplitude effect. ITP and GTP were found to have little or no effect. The selectivity of the ATP modified conductance was tested by measuring reversal potentials in media containing NH_4^+. The selectivity ratio NH_4^+/K^+ was 0.31 in absence of ATP and it was not modified by the addition of ATP. (Supported by NSF-CONICIT joint program, MDA and USPHS GM30376.)

T-PM-A3 EFFECTS OF PHORBOL ESTER ON SLOW POTASSIUM CURRENTS OF BULLFROG GANGLION CELLS. Paul R. Adams and D. A. Brown* , Department of Neurobiology and Behavior, State University of New York at Stony Brook, Stony Brook, New York 11794 and Laboratory of Cellular Biology,* NIMH, Building 36, NIH, Bethesda, Maryland 20205.

We have examined the effects of a brief (1-2 minute) application of phorbol dibutyrate (PDB, 1-4 μM) on the voltage dependent slow K-current I_M and the calcium-dependent slow K-current I_{AHP} using a single electrode switching voltage clamp. I_{AHP} was unaffected. I_M was usually reduced in amplitude, but to a highly variable extent (10 to 90%). The reduction continued to progress after washing out PDB, and I_M could not be restored by prolonged washing (>1/2 hour). The remaining I_M showed normal voltage sensitivity, kinetics and reversal potential. Effects of muscarine, LHRH and Ba on I_M were tested prior to and at various times following brief exposures to PDB. The variable residual I_M left after PDB treatment showed greatly reduced sensitivity to muscarine and LHRH but not to Ba. These effects are probably attributable to C-kinase activation since they were not seen with phorbol applications (4 μM). These data have at least 2, non-exclusive, interpretations: (1) C-kinase may phosphorylate and inhibit an intermediate in the receptor - M channel control pathway. (2) This pathway may itself work partly by C-kinase activation.

Supported by NS18579 and a Fogarty International Scholarship to D.A.B.

T-PM-A4 A NEW INTERPRETATION OF THE EFFECTS OF TEA^+ ON POTASSIUM CHANNELS IN SQUID AXONS. John R. Clay. Lab. of Biophysics, NINCDS, NIH, MBL, Woods Hole, MA 02543.

Blockade of potassium channels in nerve membrane by internal tetraethylammonium ions (TEA^+) is thought to occur only after the channels have been opened by membrane depolarization (C.M. Armstrong. J. Gen. Physiol. 50:491, 1966). This mechanism is based on the time dependent effects of blockade, especially with relatively low concentrations of TEA^+ (.2-1 mM). Under these conditions, potassium current rises subsequent to membrane depolarization, and then declines in a manner suggestive of channel inactivation. This result is logically consistent with Armstrong (1966) model. However, the link between channel activation and TEA^+ blockade could be fortuitous, since membrane depolarization is required for both processes to occur. Tail current kinetics in the presence of relatively large concentrations of TEA^+ (10-20 mM) demonstrate that blockade is independent of channel gating. The tail current time constant, τ_{tail}, under these conditions is identical to the control, which is to be expected if TEA^+ can occupy its binding site within the channel even when the channel gates are closed. The Armstrong (1966) model predicts a significant increase in τ_{tail} for these conditions, which is not observed. The kinetics of blockade can be readily explained from an Eyring rate theory description of the interaction of TEA^+ with its binding site. The model is consistent with the voltage dependence of the TEA^+ kinetics as well as the voltage dependence of blockade.

T-PM-A5 K CHANNEL INTEGRITY DEPENDS ON EXTRACELLULAR CALCIUM. C.M. Armstrong and J. Lopez-Barneo. Dept. Physiology, Univ. of Pennsylvania, Philadelphia, Pa. 19104 and Dept. de Fisiologia, University of Seville.

Isolated cells from the giant fiber lobe of squid stellate ganglion have large potassium currents, and much smaller calcium and sodium currents, when studied with whole-cell patch-clamp technique. Standard solutions were 440 NaCl + 10 $CaCl_2$ + 50 $MgCl_2$ externally, and KF + K-glutamate internally. When external calcium is removed, K channel activity quickly disappears and a large current develops through non-selective ("leak") channels that are open at the holding potential (-80 mV). The leak channels conduct Tris and N-methyl glucamine about as well as sodium. On restoring calcium the leak current disappears and K channel activity reappears. Two facts suggest that the leak current is carried through K channels that have lost their gating and selectivity properties. First, K channel disappearance and leak current appearance have the same time course. Second, barium ions prevent the leak current, but only if barium is allowed time to block the K channels before calcium is removed. Strontium and magnesium cannot substitute for calcium. Previous evidence has suggested that K channels contain a calcium ion when they close. The present results imply that the maintenance of the functional conformation of the K channel depends on the availability of calcium ions to occupy the channels in the closed state.

T-PM-A6 SINGLE K CHANNELS RECORDED FROM SQUID GFL NEURONS. Isabel Llano, Richard J. Bookman and Clay M. Armstrong. U. of Pennsylvania, Phil., PA and Biozentrum, Basel, Switzerland.

We have used neuronal cell bodies dissociated from the GFL of the squid stellate ganglion to observe the activity of single voltage-dependent K channels. Recordings were obtained from excised outside-out patches bathed in $5K^+$-ASW at 10°C; pipettes were filled with solutions containing 475 K Glutamate, 25 KF, 10 KCl, 10 EGTA, 10 Hepes. Depolarizing pulses from a holding potential of -60 mV elicit mainly a single type of unitary event, with a conductance (γ) of 22 pS. For 50 ms depolarizations the probability of a channel being open, P(o), increases sharply with membrane potential (0.2 at -20 mV, 0.3 at 0 mV, 0.6 at 20 mV). After 50 ms P(o) decreases with time presumably as channels inactivate. Reconstruction of the macroscopic currents from single channel records shows that the average current declines to approx. 40% of its peak by the end of a 100 ms pulse, in accord with our previous observations of I_K inactivation in whole-cell clamp recordings from this preparation. When an excised outside-out patch is bathed in 440 K^+-ASW, single channel currents reverse direction between -10 and 0 mV (expected E_K=-5 mV). In these ionic conditions γ appears to increase (in agreement with Standen et. al., J. Physiol, 364), rising to a value of approx. 54 pS. Preliminary analysis of the kinetics of this channel shows that two exponentials are required to fit the histograms of open times (τ in the order of 0.6 and 1.5 ms at -20 mV) suggesting that there may be two open states. At least two closed states are suggested from the distribution of closed times. In the presence of 18 mM external Ba^{2+}, P(o) is reduced while γ is not altered. This seems to occur as a result of complete occlusion of the channel (rather than high frequency flicker) since the proportion of blank records is increased at all potentials.

T-PM-A7 **SINGLE CHANNEL RECORDING FROM NORMAL RAT LACTOTROPHS.**
T.L. Croxton, N. Ben-Jonathan, and W.McD. Armstrong, Dept. of Physiol. and Biophys., Indiana Univ. Sch. of Med., Indianapolis, IN 46222.

Primary anterior pituitary cell cultures were inititated by trypsin digestion and 24 hr. were allowed for cell attachment to the bottom of the culture dish. Prolactin-secreting cells were identified by a reverse hemolytic plaque assay and their locations on a grid were recorded. Single channel recordings were obtained after an additional 24-72 hr. in culture. Two channel types with large conductances were identified and partially characterized. The first had characteristics resembling those of Ca^{2+}-activated "maxi" K^+ channels (R. Latorre and C. Miller, 1983, J. Memb. Biol., 71, 11). Records showed complex gating kinetics with both prolonged and "flicker" closed intervals. Conductances were ~150 pS. In detached patches, channel currents had crossover potentials near the Nernst potentials for K^+. With 130 mM KCl and 10 mM NaCl in the pipette, channel currents in cell-attached patches became zero at ~-45 mV applied potential. These results, with reasonable assumptions for membrane potential and cellular K^+ activity, imply K^+-selectivity. The second channel type was tentatively characterized as Cl^--selective. Crossover potentials of currents through these channels were near zero in detached patches exposed to symmetrical Hank's solutions or to solutions assymetrical in Na^+ and K^+ but with similar Cl^- concentrations. Single channel conductances were ~400 pS. Supported by USPHS F32 AM07554.

T-PM-A8 TOW TYPES OF POTASSIUM CURRENTS IN VASCULAR SMOOTH MUSCLE AS DISTINGUISHED BY TEA AND BETHANIDINE. G. Bkaily, M.D. Payet, R. Sauvé, M.B. Bacaner, and N. Sperelakis. Department of Biophysics, Faculty of Medicine, University of Sherbrooke, Sherbrooke, Québec, CANADA. Department of Physiology, Faculty of Medicine, University of Montréal, Montreal, Québec,CANADA. Department of Physiology, University of Minnesota, Minneapolis, MN, USA and Department of Physiology and Biophysics, College of Medicine, University of Cincinnati, Cincinnati, Ohio, USA.

Single potassium channel and membrane currents through the K channel were studied in rabbit aortic single vascular smooth muscle (VSM) cells in culture using the cell-attached patch clamp and whole-cell voltage clamp techniques. A potassium channel with a very large amplitude of opening was found with a slope conductance of 80 pS. The single channel I/V curve was linear over the entier applied voltage range. In whole-cell voltage clamp, two delayed rectifier K outward currents were found in VSM cell. Both K currents were voltage and time dependent and did reverse at the same reversal potential (-50 mV), and were TEA sensitive, and betanidine blocks only the higher g_K type, and increased the bethanidine insensitive-TEA or barium sensitive I_K and deplaced the I/V curve to more negative potentials. TEA and barium inhibited both types of potassium currents, and the betanidine activated potassium current. The present results demonstrated the presence of a very large potassium conductance in aortic vascular smooth muscle cells and the presence of two types of I_K; one is inhibited by bethanidine, however , the second type could be activated by bethanidine.
This study was supported by grants from MRCC, FQMC and FRSQ to Dr. Bkaily.

T-PM-A9 POTASSIUM CHANNELS IN HUMAN RETINAL PIGMENT EPITHELIUM, by J.A. Fox, B.A. Pfeffer, and G.L. Fain, Department of Ophthalmology, Jules Stein Eye Institute, UCLA School of Medicine, Los Angeles, CA 90024 USA.

We have recorded single channel currents from human retinal pigment epithelium (RPE) cells in tissue culture using patch clamp techniques. Recordings have been obtained from intact cells (on-cell patches) and from excised inside-out patches. Two types of potassium selective channels were observed in on-cell patches: a small channel (25 pS with the pipet filled with Ringer), with a maximum channel open time of around 7 msec at 40 mV negative to cell resting potential, and with the open time decreasing as potential is increased or decreased from that value; and a larger (100 pS) channel, which shows a marked increase in mean channel open time as the cell is depolarized, with a maximum open time greater than 15 msec. In excised patches, a larger potassium selective channel (250 pS in symmetric .1 M KCl) and a large non-selective channel are seen as well. The mean open time of the 250 pS channel increases with voltage in the hyperpolarizing direction, to an open time greater than 10-15 msec. These channels could account for the potassium permeability previously reported for both apical and basal membranes of RPE.

T-PM-A10 EFFECTS OF A HISTIDINE REAGENT ON POTASSIUM AND CHLORIDE EFFLUXES FROM DEPOLARIZED FROG SKELETAL MUSCLE. B.C. Spalding, J.G. Swift, D.J. Gefell and P. Horowicz, Department of Physiology, Univ. of Rochester School of Medicine and Dentistry, Rochester, NY 14642.

Lowering the external pH has no effect on the rate of K^+ efflux from frog skeletal muscle, but reduces Cl^- efflux 10-fold with the midpoint for the effect at pH 6.8. External Zn^{++} reduces both K^+ and Cl^- efflux. The reduction in K^+ efflux is strongly pH-sensitive: 5 mM Zn^{++} reduces K^+ efflux by 56% at pH 7.1 but by only 2% at pH 5.2. Because of the pH range over which these effects occur, we have studied K^+ and Cl^- fluxes after application of a histidine-modifying reagent, diethylpyrocarbonate (DEPC) at pH 6. All experiments were performed on depolarized frog sartorius muscles equilibrated in a solution containing 150 mM K^+, 120 mM Na^+ and 270 mM Cl^-.

Following treatment with 1.5 mM DEPC, the K^+ efflux rate does not differ from control, but Zn^{++} is much less effective in reducing K^+ efflux, mimicking the effects of low pH on untreated muscle. After DEPC treatment, Cl^- efflux at neutral or alkaline pH is reduced by about half, while efflux at pH 5 is slightly increased. The midpoint of the pH effect on the Cl^- efflux remaining after DEPC treatment occurs at pH 7.5.

We have also examined the effect of pH on the reduction of Cl^- efflux by Zn^{++} (without DEPC treatment). Zn^{++} is less effective at acid pH: Cl^- efflux is half-inhibited by 2.0 mM Zn^{++} at pH 7.5 but 5.2 mM Zn^{++} is required at pH 6.5.

We conclude that it is likely that a histidine group is involved in the reduction of K^+ efflux by Zn^{++} ions. Further, application of a histidine-modifying reagent alters the pH-dependence of Cl^- efflux. (Supported by grants from the USPHS and the MDA).

T-PM-A11 NON-STATIONARY FLUCTUATION ANALYSIS OF THE DELAYED RECTIFIER POTASSIUM CHANNEL IN THE CALF CARDIAC PURKINJE FIBER: INFLUENCE OF NOREPINEPHRINE ON SINGLE CHANNEL CURRENT. P. Bennett, T. Begenisich, & R. Kass. Dept. of Physiology, Univ. of Rochester, Rochester, NY 14642

We have used non-stationary fluctuation analysis to estimate single channel current in an intact cardiac preparation. Deactivating delayed rectifier current tails were measured at holding potentials near -30 mV after prepulses to voltages near 0 mV. Ensembles of tail currents were obtained by identical voltage pulses applied at 0.1 Hz. Variance and mean currents were determined for small groups of records to minimize possible errors due to slow changes in the currents. Control experiments identified these signals as fluctuations of currents through delayed rectifier potassium channels. The power spectral density of the current fluctuations of decaying I_K tails is well-fit by the sum of two Lorentzians whose cut-off frequencies are predicted by the time constants of the macroscopic currents. In two paired experiments in which we estimated single channel currents in the absence and presence of norepinephrine (NE), there was no significant change in single channel current. This is in sharp contrast to the large (3 to 4-fold) NE-induced increase in macroscopic currents. On average, in 4 mM K_o, control single channel current was 3.7 ± 0.4 pA (SEM N=5), and in the presence of NE it was 3.0 ± 0.9 pA (N=3). The analysis of our data provides information about single channel currents, but cannot yield estimates for channel number, because the probability of channel opening (p) is very small under the conditions of our experiments. Thus, from our results, we conclude that of three possible mechanisms for increasing currents through these I_K channels (increasing single channel current, increasing p, or increasing the number of functional channels), we can rule out an effect of this neurohormone on single channel current.

T-PM-A12 DETERMINATION OF MAGNITUDES OF VOLTAGE ACTIVATED CURRENTS IN ISOLATED IDENTIFIED SNAIL NEURONS. Bruce Yazejian (Intr. by Susumu Hagiwara) Section of Neurobiology, Department of Biological Sciences, University of Southern California, Los Angeles, CA 90089-0371.

Very little is known about the factors controlling differentiation of excitable membranes. We are pursuing these by studying adult molluscan nerve cell bodies that are completely isolated and grown in culture. The magnitudes of five voltage dependent currents are being determined for Lymnaea neurons using the internal perfusion voltage clamp technique. Since cells do not survive this procedure it is necessary to use identified neurons. The Na current and K currents are measured with external Cd^{2+} to block Ca currents. Ca and H^+ currents are measured with Na^+ and K^+ free solutions. Examined a few hours after isolation the fast inactivating K current varies by as much as an order of magnitude between cell types but does not vary as much within a cell type. On the other hand, the slowly inactivating K current shows no significant variation between cells studied. The Na and Ca currents are present in some cell types at five times the density as in others. Although the outward H^+ current does not vary much between cell types, the ratio between Ca current and H^+ current varies by as much as ten times. We are culturing these isolated neurons and developing techniques for the re-isolation of cells from culture. Observations that action potentials broaden after a week in culture lead us to expect changes in some of the currents. Supported by NS 15341.

T-PM-B1 STRUCTURAL STUDIES OF ACTO-S1 BY NEUTRON SCATTERING USING "INVISIBLE" ACTIN. Curmi,P.M.G.[1], Stone,D.B.[1], Schneider,D.[3], Spudich,J.A.[2], and Mendelson,R.A.[1]. [1]CVRI and Biochem/Biophys, University of California, San Francisco, CA, [2]Cell Biology, Stanford, CA and [3]Brookhaven National Laboratory, Upton, N.Y.

Neutron scattering from complexes of deuterated and protonated proteins allows structural data to be obtained from one member of the complex with minimal interference from the other. We have applied this approach to the study of muscle contraction.

Using cell techniques, highly deuterated actin has been extracted and purified in sufficient quantities to carry out neutron scattering experiments. The level of deuteration was set to make the actin appear 'invisible' to neutrons in a nearly 100% D_2O buffer. Under these conditions, the scattering from protonated myosin subfragment-1 (S1) was maximal and the background, due to incoherent proton scattering, was minimal. Difference scattering patterns were obtained between (a) solutions of acto-S1 complexes (at various stoichiometries) and (b) acto-S1 that had been dissociated by the addition of magnesium pyrophosphate. From these data sets, information has been obtained about the structure of S1 when it binds to F-actin and about the influence of the binding of one S1 monomer on the probability that other S1 monomers bind to neighbouring sites on F-actin.

Supported by NIH (HL-16683, GM-25240), MDA, AHA and Postgraduate Medical Foundation, Univ. of Sydney grants.

T-PM-B2 TOPOGRAPHY OF MYOSIN S-1 DOMAINS: THE LOCATION OF SH1 & SH2 IN RELATION TO 25K & 50K FRAGMENTS, Renné Chen Lu, Anna Wong, & Lauren Moo, Dept. of Muscle Res., Boston Biomed. Res. Inst. and Dept. of Neurology., Harvard Med. Sch., Boston, MA 02114

The thiol-specific photolabile reagent benzophenone iodoacetamide (BP-IA) can be incorporated into nicked myosin S-1 in the absence of nucleotide, accompanied by an increase of Ca^{2+} ATPase and the loss of K^+ ATPase activities. Upon photolysis, both 20K and 25K fragments disappeared and a new 45K band appeared on SDS-PAGE, indicating the N-terminal 25K fragment was crosslinked to the C-terminal 20K fragment via SH1. Crosslinking of SH1 and the 25K region was also demonstrated by labeling, photolysis, and subsequent proteolysis of intact S-1. The presence of actin and Tm+Tn during photolysis had no effect on crosslinking. Blocking thiols with iodoacetamide or 1,5- IAEDANS inhibits the crosslinking by BP-IA. If photolysis was carried out in the presence of ATP, a 70K band was also observed on SDS-PAGE, suggesting that the 50K region came closer to SH1 in the presence of ATP. When S-1 was labeled with BP-IA in the presence of ATP, a condition known to increase the reactivity of SH2, both 45K and 70K were formed upon photolysis in the absence of ATP. More of the 70K at the expense of 45K species was formed if the photolysis was carried out in the presence of ATP. Since SH1 and SH2 are only nine residues apart, these results show that SH1 and SH2 are located at the interface of all three putative domains, and the binding of ATP moves the 50K closer to 20K or 25K away from 20K regions. Using dibromobimane Mornet et al. (PNAS 82, 1658,1985) reported the crosslinking of SH1 to 50K. However, they were unable to look at the effects of nucleotide, since MgATP was required to prevent dimer formation. Supported by NIH grant AM-28401.

T-PM-B3 MYOSIN S1 HAS FLEXIBLY ATTACHED TERTIARY STRUCTURAL DOMAINS by S. HIGHSMITH (University of the Pacific) and D. EDEN (San Francisco State University), San Francisco, CA.

Transient electrical birefringence measurements were made on skeletal myosin subfragment-1 at 3.7°C in 10 mM tris-acetate, 0.1 mM $MgCl_2$, pH 7.0. Steady state birefringence signals were obtained with pulse-lengths above 5 μs. For 0.3 to 0.7 μM [S1], the Kerr law was obeyed for electric fields up to 12 statvolt/cm. Above 12 statvolt/cm partial saturation of the birefringence was observed. Alignment in the field was due to S1's large permanent electric dipole moment, $\mu_p = 8500 \pm 2000$ D.

The field-free rate of decay of the birefringence was analyzed after 0.35 and 7.0 μs pulses in the 2.5 to 25 statvolt/cm range. For 7.0 μs pulses, the single exponential decay was independent of the field strength. At 3.7°C, $\tau = 315 \pm 10$ ns, compatible with a prolate ellipsoidal S1 19-20 nm long. For 0.35 μs pulses, the observed rate of decay increased with increasing field strength. The rotational correlation coefficient, τ, was 236 ns after a 3.3 statvolt/cm pulse and decreased to 187 ns for a 19.7 statvolt/cm pulse.

We were unable to account for this data without evoking an S1 structure that has at least two tertiary structural domains connected by a flexible linkage with a restoring force. This model has S1 nearly fully extended at equilibrium and the dipole moments on the two segments arranged head-to-tail. Short weak pulses selectively align segments without distortion. Short pulses of sufficiently high field strength exert a torque that distorts S1 into a more compact structure with a corresponding lower τ-value. This bending of S1 may be involved in force generation and/or energy storage after force generation by actomyosin in situ.

Support: AHA (S.F. Chapter, Cal. Affil.) and NIH (GM31674 and a RCDA).

T-PM-B4 EVIDENCE FOR HINGING IN MYOSIN RODS FROM VARIOUS SPECIES BASED ON LIGHT SCATTERING AND OPTICAL ROTATION MELTING CURVES. Michael E. Rodgers and William F. Harrington. Department of Biology, The Johns Hopkins University, Baltimore, MD 21218.

Radius of gyration (R_g) vs. temperature (ramping) measurements for rabbit, frog, scallop and ice-fish myosin rods have been compared with optical rotation melting curves (unpublished results). M_r from SDS gels indicate that all particles have the same molecular weight (130 kD). All fragments are approximately 100% α-helical at low temperature (0-5°C). The melting profiles are qualitatively similar in shape but are shifted progressively to higher temperatures in the order: ice-fish (T_m=33.5°), scallop (T_m=37.5°), frog (T_m=45.5°), and rabbit (T_m=49.5°). The radius of gyration of all of these fragments decreases rapidly with increasing temperature and in each case the R_g vs. T profile is shifted to lower temperature (by about 5-8°C) with respect to the optical rotation melting curve. Both frog and rabbit rod give rigid rod lengths of ~136 nm at 15°C, whereas the estimated rigid rod lengths of ice-fish and scallop are substantially lower (~115 nm) at this temperature. Plots of R_g vs. %-helix for all species show a marked decrease in R_g for a relatively small change in f_h, consistent with hinging of the myosin rod. At temperatures above 55°C, all species behaved as random coils with R_g≅13-15 nm. The different melting profiles of the rod fragments parallel the working temperatures of their respective muscles.

T-PM-B5 THREE-DIMENSIONAL RECONSTRUCTION OF MYOSIN S1 BASED ON TILTED VIEWS OF THIN SECTIONED CRYSTALS. Donald A. Winkelmann, Timothy S. Baker, Harold Mekeel and Ivan Rayment. Rosenstiel Center, Brandeis University; Dept. of Biological Sciences, Purdue University; Dept. of Neurobiology, Harvard Medical School; Dept. of Biochemistry, University of Arizona.

Crystals of myosin subfragment-1 (S1) from avian skeletal muscle have been examined by X-ray diffraction and electron microscopy to determine the packing of S1 in the crystal lattice (Winkelmann et al., 1985, JMB 181, 487-501). There are eight molecules in the unit cell with two in the asymmetric unit related by a non-crystallographic or local two-fold axis. Image analysis of electron micrographs of thin sections of small crystals which were fixed and embedded with tannic acid reveal the approximate size and shape of the myosin head. The molecule is at least 16 nm long with a maximum thickness of 6 nm, and it has marked curvature. We have now collected a complete data set for three-dimensional structure determination of the myosin head in the crystal lattice to 3 nm resolution. Electron micrographs of the thin sections were recorded at angles up to 45° by tilting the sections about the two orthogonal unit cell axes in each of the three principal views. This approach provides redundant sampling of the three-dimensional Fourier transform and eliminates the "missing cone". Each tilt series was recorded with a total exposure of 12,000 electrons/nm^2; the sections appear quite insensitive to this level of irradiation. The data from six separate tilt series have been merged to form a complete set of crystallographic structure factors. At this resolution, the three-dimensional map confirms the results of the packing analysis and reveals the molecular envelope of myosin S1. This molecular envelope may provide a starting model for solving the low-resolution structure of the myosin head by X-ray crystallography. (Supported by grants from the NIH and NSF.)

T-PM-B6 THREE-DIMENSIONAL RECONSTRUCTION OF DECORATED THIN FILAMENTS IN A FROZEN HYDRATED STATE. R.A. Milligan and P.F. Flicker (Intr. by R.W. Aldrich), Department of Cell Biology, Stanford University School of Medicine, Stanford, CA 94305.

Recently developed techniques for preparing and examining frozen hydrated specimens in the election microscope allow visualization of unstained biological samples in physiological solutions (Taylor and Glaeser, J. **Ultrastruct. Res.** 55:448, 1976; Dubochet et al., **J. Microscopy 128**:219, 1982; Milligan et al., **Ultramicroscopy 13**:1, 1984). We applied these techniques, combined with image processing, to native thin filaments decorated with myosin subfragment-1 (S-1). In our reconstruction the actin subunit has a prolate ellipsoid shape with some separation into two domains distinguishable in sections parallel to the filament axis. The separation between the thin filament and S-1 clearly appears in our maps as a narrowing density located at about 50 Å radius. The S-1 has a long curved shape slewing away from the helix axis. A new feature in our maps is a weakly contrasted region centered at about 115 Å radius. This portion of the head extends azimuthally in the opposite direction to that of the bulk of the S-1. Our interpretation of this feature is that it is a smear of density from a region of the S-1 with a variable position arising from flexibility somewhere along the head. To distinquish the position of tropomyosin unambiguously in our map, we are examining decorated actin filaments and native thin filaments in a frozen hydrated state. (R.A.M. is supported by a fellowship from the Royal Society of London; P.F.F. is an MDA fellow.)

T-PM-B7 MODIFICATION OF MYOSIN SUBFRAGMENT-1 WITH IODOACETAMIDO TETRAMETHYLRHODAMINE THAT RECOGNIZES STRUCTURAL DIFFERENCES IN HEAVY CHAINS. Reiji Takashi, Kathleen Ue, Clark Waldrip. CVRI, UCSF, San Francisco, CA 94143

The thiol-specific fluorescent reagent, iodoacetamido tetramethylrhodamine (ITMR), was used to label and study myosin subfragment-1 (S1) heavy chain from rabbit skeletal muscle. Under controlled conditions only half a mole of thiol group per S1 is labeled by ITMR in the absence of MgADP[TMR(S1)], while one mole of thiol group is modified in its presence [TMR(S1)DP]. The labeling leads to a ca. 3-3.5 fold activation of the Ca^{2+}-ATPase activity and ca. 80% inhibition of the K^{+}(EDTA)-ATPase activity. Both the Ca^{2+}- and K^{+}(EDTA)-ATPase activities are fully affected when half a mole of thiol group per S1 is labeled and there after the ATPase acivities are virtually unaffected by additional labeling up to one mole of thiol group per S1. Chemical cleavages of the labeled S1 followed by peptide mappings were carried out to locate ITMR labeling site on TMR(S1) and TMR(S1)DP. These results were obtained: 1) The 10 kDa fragment (Elzinga and Collins, Proc. Natl. Acad. Sci. USA (1977) 74, 4281) produced by CNBr treatment, which contains only two thiols, SH_1 and SH_2, is labeled with TMR. 2) The 13 kDa fragment generated by NH_2OH cleavage (Sutoh, Biochemistry (1981) 20, 3281), which contains two thiols, SH_1 and a thiol other than SH_2, is labeled with TMR. These results indicate that on both TMR(S1) and TMR(S1)DP, the fast-reacting thiol, SH_1, is selectively labeled by ITMR. Similar results are obtained using myosin labeled with ITMR in the presence and absence of MgADP. From the above it is deduced that an ordinary S1 or myosin preparation is a 1:1 mixture of heavy chains functionally different from each other. Supported by HL-16683.

T-PM-B8 THE PRIMARY STRUCTURE OF SUBFRAGMENT-1 OF CHICKEN FAST SKELETAL MUSCLE MYOSIN Genji Matsuda, Tetsuo Maita, Masaki Hayashida and Yoshito Tanioka, Dept. of Biochemistry, Nagasaki University School of Medicine, Nagasaki 852, Japan

We have studied on the primary structure of myosin from chicken skeletal muscle to clarify the relationship between structure and function of muscle myosin. Thus far the primary structure of the three kinds of light chains of chicken skeletal muscle myosin have been determined in our laboratory. In this paper, we will report the study on the primary structures of subfragment-1 from the heavy chain of chicken skeletal muscle myosin.

Myosin was prepared from pectoral muscle of adult chicken (Hubbard type). The subfragment-1 was restrictively redigested by trypsin, and S-carboxymethylated after the reduction. The obtained 20K, 23K and 50K fragments were purified by using the gel filtration of Sephadex G-100 and chromatography of QAE-Sephadex A-50.

The purified 23K fragment was digested by trypsin. The tryptic peptides were isolated and sequenced, respectively, by the conventional methods. The ordering of the tryptic peptides in the fragment was deduced from the analytical results of the chymotryptic digests and BrCN hydrolysates of the fragment to determine the primary structure of the 23K fragment. The primary structures of the 20K and 50K fragments were also determined in a similar manner as above.

The heterogeneities in the 23K and 20K fragments were found at four and three positions respectively. The heterogeneity in the 50K fragment was found at least at three positions.

T-PM-B9 ENZYMATIC ACTIVITY OF MYOSIN ISOZYMES IN AVIAN MUSCLE DEVELOPMENT. Guillermina S. Waller and Susan Lowey. Rosenstiel Center, Brandeis University, Waltham, MA 02254.

It is well established that at least three myosin isoforms are expressed sequentially during muscle development: embryonic, neonatal and adult myosin. Recent immunological studies have revealed even more extensive polymorphism in chicken pectoralis muscles. Myosin from 10-day chick embryos was shown to be immunologically distinct from that present at 18 days' incubation by immunofluorescence, radioimmunoassay, Western blots and peptide mapping (Lowey et al., 1985, UCLA Symposia on Molecular and Cellular Biology). The existence of multiple forms of myosin raises the question of functional significance. It has generally been assumed that embryonic muscles are slow contracting, and that their myosins will be correspondingly low in enzymatic activity. Measurements of actomyosin ATPase were made using "minifilaments" formed in citrate/tris (Cheung and Reisler, 1983, J. Biol. Chem. 258, 5050), a system that yields more reproducible results than synthetic filaments. Unexpectedly, the actin-activated MgATPase activity of 10- and 18-day embryonic myosin was found to be equal to that of posthatch and adult pectoralis myosin (V_{max}=10s^{-1}), which was 10-fold higher than that of ALD myosin. Unfortunately, no physiological data are available for pectoralis muscles, but the speed of shortening for PLD muscles has been shown to increase by more than 2-fold between 15 days' in ovo and two weeks after hatching (Reiser et al., 1982, Am. J. Physiol. 243, C177). Since PLD muscles are too small to isolate purified myosin, CaATPase activity will be measured in non-denaturing gels in order to obtain a correlation between the enzymatic activity and speed of contraction in developing muscles.

T-PM-B10 LIGAND EFFECTS AND THE FUNCTIONAL ROLE OF THE LIGHT CHAIN ISOFORMS OF FAST MUSCLE MYOSIN
E. Wilck, M. Balish, and P. Dreizen. Biophysics Program and Department of Medicine, State University of New York Downstate Medical Center, Brooklyn, New York.

The inhibitory effects of ionic ligands on acto-S1 ATPase of rabbit fast muscle can be explained in terms of allosteric interactions at a single Mg inhibitory site and ca 3 mutually exclusive inhibitory sites for ATP and monovalent anions. We have further examined effects of major cytosol components creatine phosphate (CP), phosphate (Pi), and creatine on acto-S1 ATPase. In general, Ki values vary widely for ligands in the order: ATP < CP < Pi < Cl, lactate < creatine. Ki values are ca 2-fold greater for S1-LC3 than S1-LC1, except for Pi, where Ki is similar for both isozymes. The pattern of ligand effects for the 2 isoforms may be related to the classical physiological properties of fast muscle. Fast-twitch muscle is characterized by phasic contractions and glycolytic, anaerobic metabolism. Severe anaerobic exertion may deplete CP within several minutes, and sustained aerobic exercise may result in lactate accumulation and ATP depletion. In the case of S1-LC1 the kinetic values would predict that velocity increases significantly during CP depletion, and decreases during lactate accumulation/ATP depletion. In the case of S1-LC3 the kinetic values would predict unchanged velocity during CP depletion, and less marked decrease of velocity during lactate accumulation/ATP depletion. Thus, S1-LC1 would appear to undergo biologically disadvantageous velocity fluctuations during severe exercise, entering "overdrive" when CP becomes depleted, and being turned off as lactate accumulates. In contrast the LC3 isoform would appear to play a conservative role during the marked changes of ionic milieu that occur in fast muscle cytosol during severe exercise.

T-PM-B11 HYBRIDIZATION OF FAST SKELETAL MUSCLE MYOSIN HEAVY CHAINS AND SMOOTH MUSCLE MYOSIN LIGHT CHAINS.
S. P. Scordilis, Dept. Biol. Sci., Smith College, Northampton, MA 01063.

A protocol has been devised which allows for the hybridization of chicken gizzard myosin light chains with rabbit fast skeletal muscle heavy chains. The method involves the gentle stirring of column purified myosin with a 10 fold molar excess of purified homologous light chains in a solution of 36% deionized ethylene glycol, 540 mM KCl, 16 mM EDTA, 9 mM MgATP, 5 mM Tris-HCl (pH 7.4) and 0.1 mM dithiothreitol for 60 min at 25°C. The exchange was terminated by dialysis against saturated $(NH_4)_2SO_4$, 10 mM EDTA at 4°C. The hybridized myosin was pelleted, resuspended in a high ionic strength buffer and chromatographed on Sepharose Cl-4B to remove the contaminating light chains. SDS polyacrylamide gel electrophoresis demonstrated that between 30% to 65% of the light chains were exchanged from the rabbit fast skeletal muscle myosin [RSM] and replaced with the chicken gizzard smooth muscle light chains [CGLC]. The high ionic strength ATPase activities were decreased in the hybrid myosin [RSM+CGLC] over the control myosin [RSM] in the presence of EDTA, Ca^{2+} or Mg^{2+}. The actin-activated low ionic strength Vmax decreased in the the hybrid as well, whereas the K_{app} for actin was unchanged. Most striking, however, was the increase in calcium sensitivity of the actin activation in the hybrid. In short, this smooth/skeletal muscle hybrid demonstrated changes in the characteristic high ionic strength ATPase activity values and exhibited changes in the actin-activated ATPase activity.

This work was supported by grants from the Muscular Dystrophy Association of America, the Blakeslee Fund of Smith College and the Pew Memorial Fund.

T-PM-B12 A CENTRAL ROLE FOR IONIC INTERACTIONS IN THE LENGTH-REGULATION OF THICK FILAMENTS OF VERTEBRATE SKELETAL MYOSIN.
Julien S. Davis, Department of Biology, The Johns Hopkins University, Baltimore, MD 21218.

A mechanism that provides a structural basis for experiments (Davis (1985) Biochemistry 24, 5263-69) on the length-dependence of the extent of the ionic interactions between growing filament and dimer subunit is presented. The structural basis for the model was deduced from the effect of salt on mini-, synthetic and native filaments. Kinetically, length is regulated by a dissociation rate constant that increases exponentially as the filament grows bidirectionally from its center. Growth ceases at the point of equilibrium between invariant "on" and length-dependent "off" rates. In the model, the three-subfilament structure of the parallel-packed region of the thick filament is fundamental to the proposed scheme. The intra-subfilament bonding is strong and predominantly ionic in character, whereas the inter-subfilament bonding is relatively weak. These strong and weak interactions participate directly in the strictly sequential mechanism of assembly of dimer subunit observed in the kinetic mechanism. A third domain, independent of the sequential mechanism, consists of opposing negative charges on the subfilament surface juxtaposed at or close to the thick filament axis. The weak and repulsive domains are additively coupled to each other through the rigidity in the subfilaments. Length regulation occurs through the repulsive component rising in intensity more rapidly with length than the initially stronger positive interactions. Growth ceases at the point where the repulsive interactions weaken the attractive interactions to the extent that equilibrium is established between head-to-tail dimer subunit and its binding sites at the tips of the arms of the thick filament.

T-PM-B13 MYOSIN INSERTION INTO AND EXCHANGE BETWEEN THICK FILAMENTS. A.D. Saad, J.E. Dennis, C.G. dos Remedios, J.D. Pardee and D.A. Fischman. Department of Cell Biology and Anatomy, Cornell University Medical College, New York, NY 10021.

A fluorescence energy transfer (FET) assay has been established to examine the assembly of myosin into thick filaments and its exchange between thick filaments. Using synthetic filaments in which purified myosin molecules were labeled with either donor [5-(2-((iodoacetyl)amino)ethyl)-aminonapthalene-1-sulfonic acid; 1,5-IAEDANS] or acceptor [5-iodoacetamidofluorescein; IAF] fluorochromes, rapid and extensive exchange of myosin between filaments was observed. The critical concentration of myosin, i.e., that concentration which remained unassembled at equilibrium with fully formed filaments, was measured to be 17.20ug/ml (S.D.=3.75) at 20°C. When ^{125}I-labeled myosin, at subcritical concentrations (5 or 10µg/ml), was mixed with unlabeled synthetic filaments comparable exchange was seen to that detected by FET. To visualize the sites of myosin exchange, biotinylation of SH-1 was performed by the method of Sutoh et al. (J. Mol. Biol. 178: 323-339, 1984) and the introduction of biotin-labeled myosin into unlabeled filaments was detected by ferritin-conjugated avidin. Since ferritin particles were visualized along most of the filaments without any discernible pattern of binding we conclude that all of the myosin molecules in the filament appear to be exchangeable. These data indicate that myosin within thick filaments is in a dynamic equilibrium with a small (40nM) but kinetically active pool of unassembled myosin molecules.

Supported by NIH grant AM 32147 and MDA.

T-PM-B14 THE SPECIFIC ASSOCIATION IN VITRO OF NEWLY SYNTHESIZED MUSCLE PROTEINS WITH PREFORMED MYOFIBRILS. M. Bouché and D.A. Fischman (Intr. by S. Goldfine). Department of Cell Biology and Anatomy, Cornell University Medical College, New York, NY 10021.

The association of nascent muscle proteins with adult myofibrils has been studied in a cell-free protein synthetic system. Total poly(A)$^+$ RNA, extracted from 19-day-old chick embryos, was translated in a reticulocyte lysate system in the presence of ^{35}S-methionine. After translation, myofibrils from adult chicken pectoralis muscle were added to the system and at selected time intervals, the samples were centrifuged at low speed to separate myofibrils from the soluble proteins. The proteins in the pellet and in the supernatant were then separated by SDS-PAGE and the labeled proteins visualized by fluorography. Specific ^{35}S-labeled contractile proteins, identified by molecular weight as myosin heavy chain, C-protein, alpha-actinin, actin, tropomyosin and light chain 2, were found associated with the myofibrillar pellet. This specific association of nascent contractile proteins with material in the myofibrillar pellet can be detected within 5 min and is proportional to the concentration of added myofibrillar protein up to 0.8mg/ml. Translated peptides of embryonic brain poly(A)$^+$ RNA (19-day-old chick embryos) do not exhibit any specific association with the muscle myofibrils. When synthetic thick filaments, prepared from adult myosin, are added to the muscle poly(A)$^+$ translation products, only ^{35}S-myosin cosedimented with the myosin filaments. Similarly, ^{35}S-actin was found to associate with purified F-actin filaments. We interpret these results to indicate that newly synthesized muscle proteins are assembly-competent in vitro and associate or exchange with their homologous adult counterparts in mature myofibrils. Supported by NIH grant AM 32147 and MDA.

T-PM-C1 THE BINDING OF ETHIDIUM BROMIDE TO THE NUCLEOSOME CORE PARTICLE: MODEL FOR NUCLEOSOME UNFOLDING IN DNA:PROTEIN INTERACTIONS. Cynthia T. McMurray,[1] W. D. Wilson,[2] and K. E. van Holde[1] (Intr. by G. Pearson[1]), [1]Department of Biochemistry and Biophysics, Oregon State University, Corvallis, Oregon 97331; [2]Department of Chemistry, Georgia State University, Atlanta, Georgia 30303

We have studied the interaction of ethidium bromide with the chicken erythrocyte core particle. The binding and intercalation of ethidium bromide result in a step-wise dissociation of the core particle structure which involves the initial release of one H2A•H2B histone dimer. Binding of a critical amount of drug is required for dissociation which, above the critical value, is both time-dependent and reversible. The binding of ethidium bromide to the core partiacle is characterized by an initial positive slope at low ratios of bound drug, a maximum near a ratio of 0.1 and a negative cooperative phase typical of neighbor exclusion. Prior to dissociation, drug binding appears to occur in specific regions within the core particle (the ends); regional binding corresponds to the initial cooperative phase. The cooperative maximum occurs at or near the same value as that required for the dissociation, the critical value. We discuss the details of dissociation and pre-dissociation events. Additionally, we present a model for the unpackaging transitions and mechanism which occur in the nucleosome core particle when ligand binding involves a stacking and/or intercalation mode of binding. We specifically consider RNA-polymerase interactions. Supported by grant BC504 from the American Cancer Society.

T-PM-C2 THE CONFORMATIONAL BEHAVIOR OF DNA IN HYPERACETYLATED CHROMATIN. M.R. Riehm and R.E. Harrington, Department of Biochemistry, University of Nevada, Reno, NV 89557

Information from circular dichroism and DNA thermal denaturation was used in concert to study the conformational behavior of DNA in the extended 11 nm fiber of chromatin. Large fragments of hyperacetylated or control chromatin were isolated from HeLa cells treated with or without sodium butyrate. To investigate the protein-dependent behavior of the system, the N-terminal histone tails (the acetylation sites) were selectively removed using trypsin.

The rotary strength of the positive exciton band for DNA above 260 nm shows an increase along the series of whole, H1-stripped, and trypsinized samples. This is interpreted as an increase in exciton coupling due to increases in the content of regular B DNA in our chromatin samples as protein is removed. Derivative melting curves were resolved into a sum of three Gaussians. The general trend indicated that removal of the histone tails resulted in a massive destabilization of the nucleosome, with about 70% DNA melting as if protein free. The ratio of percent hyperchromicity for each of the three melting transitions to sample rotatory strength provided additional information about the conformational behavior of DNA in the three principal regions of the nucleosome: central loop, flanking and linker. Both control and hyperacetylated chromatin had negative protein-dependent slopes for the central loop region. This suggests DNA in this region relaxes as protein is removed. The content of control whole and H1-stripped flanking DNA increased at a faster rate than the amount of regular B DNA in the sample. In contrast, hyperacetylated chromatin showed a monotonic decrease. Histone hyperacetylation evidently allows DNA to relax while control chromatin maintains DNA superhelicity in the flanking region as H1 is removed.

T-PM-C3 THE CROSSED-LINKER DOUBLE-HELICAL MODEL FOR CHROMATIN. S.P. Williams, B.D. Athey and J.P. Langmore, Biophysics Research Division, The University of Michigan, Ann Arbor, 48109.

Species specificity of chromatin fiber structure was studied using low angle x-ray scattering and Fourier image analysis of electron micrographs. Low angle x-ray diffraction patterns of 9 tissues indicated a linker length (N) dependence of the 20 nm^{-1} peak position which was interpreted as the fibers scattering as cylinders having diameter, D, and leading to a relation $D = 19.3 + 0.23N$. Histograms of measured diameters from micrographs of negatively stained isolated fibers of the two most ordered tissues, Necturus maculosus erythrocytes (N = 48 bp; D = 30 ± 3nm by EM vs. 31 ± 2nm by x-ray) and Thyone briareus sperm (N = 88 bp; D = 38 ± 4nm by EM vs 39 ± 2nm by x-ray) confirmed this interpretation. This close agreement suggests a good degree of structural preservation of isolated fibers. Fourier transforms of negatively stained Necturus fibers showed definite left handed helical symmetry with a pitch of 25.8 ± 0.8 nm and a pitch angle of 32 ± 3.0°; consistent with a two-start helix. Micrographs of Pt:Pd shadowed fibers were also consistent with left handed helical symmetry. We propose a crossed-linker model having two left handed helical ramps separated by 13nm along the fiber axis. The nucleosomes are alternately arranged such that each helical ramp contains every other core, and the linker DNA crosses the fiber center as it connects the cores in both ramps. Scanning transmission electron microscopy of unstained fibers indicated a mass per unit length of 19.0 ± 3.2 nucleosomes per helical repeat for Necturus and 33.0 ± 5.4 nucleosomes per helical repeat for Thyone. This variable mass per unit length suggests conserved interactions among nucleosomes for all tissues. (Supported by NIH GM27937. BDA by NIH T32 GM07315. We thank all members of the Brookhaven Stem Facility, NIH RR 0177).

T-PM-C4 UPSTREAM OPERATOR SITES ENHANCE REPRESSION OF THE lac PROMOTER.
Michael C. Mossing and M. Thomas Record, Jr., Depts. of Chemistry and Biochemistry, University of Wisconsin, Madison, WI. 53706.

Plasmids have been constructed which contain a lac promoter under the control of a constitutive operator driving, expression of galactokinase. At various positions 100-300 base pairs upstream of the promoter a wild type operator has been inserted. Galactokinase levels as well as β-galactosidase levels (from an intact chromosomal lac operon - to control for variation in free repressor concentrations due to binding to the multi copy plasmids) were measured in cells bearing these plasmids. Up to 40 fold enhancement of repression has been observed due to the presence of an upstream operator. This effect is strikingly length dependent. Operators located closer than ~100 base pairs from the promoter show very small effects. Our working hypothesis is that a loop in the DNA is required for cooperative interaction between operators and that DNA flexibility constraints account for the ineffectiveness of the nearest of the operators. These data suggest a simple thermodynamic mechanism for DNA regulatory sites located far from their site of action. Two proteins which have the capacity to interact may be driven to do so by the high relative concentrations which arise due to their binding to sites which are tethered by DNA. Conversely the cooperative interaction of proteins can drive binding to a DNA site which is localized in the vicinity of an already occupied DNA site.

T-PM-C5 DNA TOPOLOGY INFLUENCES THE TEMPLATE BINDING PREFERENCE OF RNA POLYMERASE II.
Michael G. Fried, Department of Biochemistry, The University of Texas Health Science Center at San Antonio, San Antonio, Texas 78284

Transcription by eucaryotic RNA polymerase II proceeds far more efficiently from closed circular templates than from linear forms in vivo (1). Curiously, the opposite preference is generally observed in vitro. In order to determine whether this effect occurs at the DNA binding step or at some later stage in transcription, we have used binding competition assays to compare the affinity of wheat germ RNA polymerase II for the linear, nicked circular, and closed circular forms of plasmids pBR322 and pCMB13 (pBR322 containing a eucaryotic promoter insert). We found that linear and nicked circular forms are bound with 1/30 and 1/5 the affinity, respectively, of closed circular DNA. The presence of a strong RNA polymerase II promoter in pCMB13 had little effect on this structural preference. Thus the topological specificity of binding in vitro follows the same order as transcription in vivo.

Since in vitro binding and transcription exhibit different preferences, factors other than polymerase affinity must determine the transcriptional activity of a given template. In addition, it is clear from these results that the cofactors required for specific transcription are not necessary for the appropriate topological specificity of RNA polymerase II.

(1) Harland, R., Weintraub, H. and McNight, S. (1983) Nature 302, 38-43.

Supported in part by American Cancer Society grant IN-116G.

T-PM-C6 Isolation of an Msp-1 Transcription Complex: Nancy Lynn Rosenberg Dept. of Pharmacology, Baylor College of Medicine, 1 Baylor Plaza, Houston, Tx. 77030.

A deoxribonucleoprotein was isolated from a minimally perturbed nucleolus by restriction digestion with Msp-1. This structure was shown to contain a relatively homogeneous DNA, 39 kbp, as shown by second dimension DNA electrophoresis. Second dimension protein electrophoresis indicated that this complex contained 12 major tightly bound proteins. Identification of some of the proteins by the use of ELISA, monoclonal , and polyclonal antibody techniques showed that RNA polymerase 1 and its cofactors are associated with this particle. In addition topoisomerase 1 was shown to be bound to the complex. Electron microscopic analyses showed that the complex was approximately 340 angstroms in diameter. In vitro transcription studies demonstrated that this structure was capable of specific transcription. Hybridization studies with known rDNA clones were used to map the constituent DNA.

T-PM-C7 THE CRYSTAL STRUCTURE OF TRP REPRESSOR, A LIGAND ACTIVATED GENETIC REGULATORY PROTEIN. R.W. Schevitz, Z. Otwinowski, A. Joachimiak, C.L. Lawson, R.-g. Zhang, R. Marmorstein and P.B. Sigler, (Intr. by M.W. Makinen), Department of Biochemistry and Molecular Biology, University of Chicago, 920 East 58th Street, Chicago Illinois 60637.

The crystal structure of the E.coli trp repressor has been solved to 2.2 A. The two subunits (107 residues each) are related by an exact crystallographic dyad. Each subunit is composed of six helices, five of which intertwine about each other in a way that may make it impossible to disengage the subunits without altering their tertiary structure. The two symmetrically related L-tryptophan binding sites are formed by this interface.

Tryptophan must bind to the protein for repressor function. Tryptophan acts as an allosteric effector as follows:(i) L-tryptophan is wedged between the amino end of the C helix of one subunit and the side of the E helix of the dimer-related subunit fixing the orientation of the E helix, the most important element in recognizing the operator; (ii) The polar substituents of the bound tryptophan mold the protein's polar residues near the region of the repressor surface where the DNA backbone most closely approaches the protein.

To understand how repressor actvity is induced by tryptophan, we are analyzing crystals of (i) aporepressor, the inactive dimeric protein that has no bound tryptophan; and (ii) pseudorepressor, a nearly isomorphous inactive adduct formed when tryptophan is displaced by analogues. Comparison of repressor and these inactive variants should show why bound tryptophan is essential for sequence-specific binding.

T-PM-C8 ^{1}H NMR STUDIES OF THE AVIAN MYELOBLASTOSIS VIRUS PP12 PROTEIN. Joyce E. Jentoft, Jonathan Leis and Xiangdong Fu, Department of Biochemistry, Case Western Reserve University, Cleveland, OH 44106.

Type C RNA tumor viruses contain a small, basic nucleocapsid protein that forms a complex with the single-stranded genomic RNA within the virion. These nucleocapsid proteins may comprise an as yet uncharacterized class of nucleic acid-binding proteins, as they show little sequence homology with other proteins that bind RNA or DNA. The pp12 nucleocapsid protein from Avian myeloblastosis virus has been shown to undergo a pH dependent change in RNA binding properties that is probably associated with ionization of P-Ser 40 (Leis, J. & Jentoft, J. (1983) J. Virol. 48, 361-369). ^{1}H NMR spectroscopy has been used to investigate the pp12 protein as a function of pH. Virtually all the resonances in the aliphatic region of the spectrum are shifted from the positions of the corresponding peptide resonances, indicating that the protein is highly structured. In addition, while some broad resonances are evident, most of the aliphatic resonances are relatively narrow, suggesting that the majority of the aliphatic side chains have similar mobilities. The pattern of the aliphatic resonances changes noticeably with pH; this may reflect a pH-dependent change in protein conformation. The aromatic region of the spectrum has been investigated in detail. The resonance pattern is relatively simple, since the protein has only 5 aromatic amino acids, His 29, His 55, Tyr 22, Tyr 30, and Trp 80. The aromatic resonances for the individual amino acids have been identified and initial assignments of resonances to the amino acids will be presented.

T-PM-C9 STRUCTURE AND PROPERTIES OF DISK AGGREGATES OF TOBACCO MOSAIC VIRUS PROTEIN (TMVP) IN SOLUTION. K.Raghavendra*, D.M.Salunke§, D.L.D.Caspar§ and T.M.Schuster*. * Molecular and Cell Biology Department, University of Connecticut, Storrs, CT 06268. § Rosenstiel Research Center, Brandeis University, Waltham, MA 02254.

TMV protein crystallizes as an aggregate of a pair of 2-layer cylindrical disk structure with 17 subunits (M_{π} = 17560) per layer (Finch et al., J. Mol. Biol., 1974, 86, 183). We have investigated by electron microscopy the structure and sizes of these protein aggregates in solution under crystal growing conditions, pH 8.0 and high ionic strength (Leberman et al., J. Mol. Biol., 1974, 86, 179). The aggregates appear as short stacks of disks of different sizes. Majority of the images from the micrographs of the disk aggregates lying on their sides corresponds to 3-, 4- and 5-disk stacks and the remaining few longer stacks, upto 12 disks, may be interpreted as a combination of the short stacks. These disk aggregates are very stable to changes in solution conditions, such as, pH, ionic strength and temperature which makes possible spectroscopic and hydrodynamic measurements in low ionic strength, pH 7.0, virus reconstitution buffer. The inherent metastability of the stacks of disks is not due to proteolysis or other irreversible changes as indicated before (Durham, A.C.H., FEBS Lett., 1972, 25, 147). Further, the disk aggregates do not participate in either the nucleation or the elongation phase of TMV assembly in virus reconstitution buffer. Electron microscopy observations presented here are consistent with the characteristics of disk aggregates obtained by sedimentation velocity and near-UV circular dichroism techniques (Raghavendra et al., Biochemistry, 1985, 24, 3298). [Supported by NIH grants AI 11573 (TMS) and CA 15468 (DLDC)].

T-PM-C10 SELF-ASSEMBLY OF CLONED POLYOMA VIRUS CAPSID PROTEIN. Dinakar M. Salunke, Donald L. D. Caspar, Rosenstiel Basic Medical Sciences Research Center, Brandeis University, Waltham, MA 02254 and Robert L. Garcea, Division of Pediatric Oncology, Dana Farber Cancer Institute, Binney St., Boston, MA 02115.

The polyoma virus major capsid protein VP1 has been purified after high level expression in E. coli (Leavitt et al., J. Biol. Chem., 1985, in press). The cloned protein, as seen in electron micrographs, consists of donut-shaped units with an outer diameter of about 80 Å which can be identified with the pentameric capsomeres of polyoma virus. Image analysis using correlation averaging methods shows that the morphology of these units is very similar to that of capsomeres in the intact virus capsid as seen from the X-ray structure and the electron microscope images of the frozen-hydrated samples. The cloned VP1 capsomeres can assemble to form capsid-like and other polymorphic aggregates under conditions favoring association. Results of the ultracentrifuge studies carried out on aggregated capsomeres are consistent with the electron microscopic observations. The mean sedimentation constant of the distribution of aggregates is about 15% less than that of intact capsids. Our electron microscopic and sedimentation experiments suggest that the post-translational modifications or the interactions with minor protein components are not essential for self-assembly of VP1 in a surface lattice with six as well as five coordinated pentameric units. (This investigation was supported by PHS Grants CA15468 to D.L.D.C. and CA37667 to R.L.G. awarded by the National Cancer Institute.)

T-PM-C11 THE EFFECT OF AN AMINO ACID SUBSTITUTION ON THE STRUCTURE, FOLDING AND POLYMERIZATION PROPERTIES OF THE SIMIAN VIRUS 40 MAJOR CAPSID PROTEIN, Veronica Blasquez, Marla Behm, and Minou Bina, Chemistry Department, Purdue University, West Lafayette, IN 47907, U.S.A.

We have used a temperature-sensitive assembly mutant of Simian Virus 40 as a model to study how a change in a critical amino acid residue in a polypeptide chain alters the folding and polymerization properties of proteins and influences the interaction of structural proteins with chromatin. VP1, a 40 kda protein, is the major protein of the icosahedral shell which surrounds SV40 chromatin. Our DNA sequencing studies of the mutant tsB265 have revealed a single point mutation in the VP1 gene resulting in the substitution of Thr for Ala at residue 74. We have conducted thermodynamic and kinetic studies to examine the effect of this substitution on the structure and assembly of nucleoprotein complexes formed in tsB265-infected cells at various temperatures. At 33°C, tsB265 mutants assemble 220S nucleoprotein complexes which resemble the wild-type virions. However, although the conformation adapted by VP1 at 40°C enables the protein to function in initiation, it does not allow propagation of virus assembly. Improper propagation is reflected in the loss of cooperativity in shell assembly around the minichromosomes and the accumulation of nucleoprotein complexes which appear as semiassembled virions (SAV) in the electron microscope. The results of pulse-chase kinetic studies conducted at 37°C and temperature shift experiments (33° to 40° and 40° to 33°) indicate that the temperature-induced conformation changes of VP1 can not be readily accommodated after the protein has polymerized around the minichromosomes. That is, nucleoprotein complexes assembled at a given temperature--e.g., the 220S virions at 33° or SAV at 40°--must first dissociate and go through a "chromatin pathway" before they can be converted into another type of nucleoprotein complex.

T-PM-C12 PREDICTION OF T-CELL IMMUNOGENIC SEQUENCES IN PROTEINS: APPLICATION TO HTLVIII ENVELOPE PROTEIN AND IMPLICATIONS FOR DESIGN OF VACCINES. John N. Weinstein and H. Robert Guy. LTB, DCBD, NCI, NIH, Bethesda, MD 20892.

T-cells recognize processed peptides, rather than the tertiary conformation of an intact protein. Prediction of the T-cell immunogenic peptide sequences in a protein may be important to the design of vaccines. It has been suggested that T-cell activation is correlated with the ability of a peptide to form an α-helix (Pincus, et al., PNAS 80:3297,1983), or, more particularly, an amphipathic α-helix (Watts, et al., PNAS 82:5480,1985; DeLisi and Berzofsky, PNAS, in press) in association with MHC molecules on an antigen-presenting cell. We have developed new semi-empirical methods for scanning a protein and analyzing a posteriori the relative amphipathicity of its component sequences, given that they are indeed helical. Although a hydrophobic surface might induce helix, the a priori probability of helix formation was assessed using the DELPHI algorithm and (when available) crystallographic structures. We have analyzed the HTLVIII envelope protein using 3 different hydrophobicity scales, 5 different criteria of merit for amphipathicity, and 7 assumed sequence lengths. Four amphipathic sequences are identified as present in all 4 HTLVIII isolates analyzed; one of those sequences is strongly predicted a priori to be helical. We suggest that any causal relationship between amphipathicity and T-cell response could relate either to antigen presentation or to protection during antigen processing. Additional factors (e.g., genetics, immunologic history) determine whether T-cells of a given animal or human will, in fact, respond to a particular peptide. Also, it is clear that antigens to be included in a vaccine should be as nearly conserved as possible among isolates. Those issues await further data.

T-PM-C13 THE RATIONAL DESIGN OF A SEQUENCE-SPECIFIC DNA-BINDING PEPTIDE. T. Abel, H. Wolfe, J. Wendoloski, W. DeGrado, and S. Brenner, E. I. du Pont de Nemours & Company, Central Research & Development Department, Experimental Station, Wilmington, DE 19898.

We have begun the design of a site-specific DNA-binding peptide. Using information gleaned from crystallographic and genetic studies of Cro and lambda repressor, a peptide has been designed which shares minimal homology with either of these two proteins, and yet which should compete with them for binding to the OR1 DNA sequence. The peptide was designed using CPK models, computer graphics, distance geometry, and energy minimization techniques. The criteria chosen for the design of this helical peptide were 1) maximization of hydrogen bond formation between residues in the major groove of DNA and the peptide, 2) matching the electrostatic surface topology of one face of the helix with that of the major groove of the DNA, 3) maximization of the helix-forming potential of the peptide by using residues which favor helix formation, and by placing negatively charged residues at the N-terminus of the helix and positively charged residues at its C-terminus, and 5) minimization of non-specific interactions with the DNA by making the peptide electrically neutral. The peptide we designed represents a compromise of these conflicting requirements (EEENEKQSEQSRRVNRQRQA). This peptide has been synthesized and its interaction with specific and non-specific DNA sequences is being evaluated.

T-PM-C14 X-RAY DIFFRACTION STUDIES OF BLACK BEETLE VIRUS. M. V. Hosur, T. Schmidt, R. C. Tucker, E. S. C. Lee, and J. E. Johnson (Intr. by T. S. Baker). Department of Biological Sciences, Purdue University, West Lafayette, Indiana 47907 U.S.A.

Black beetle virus (BBV) is a nodamura virus causing fatal paralysis in a variety of Lepidoptera. The virus is 312Å in average spherical diameter and displays an icosahedral shape in electron micrographs. The protein capsid consists of 180 subunits of molecular weight 44 Kd which have been post translationally cleaved to give two polypeptides per subunit of molecular weight 39 Kd and 5 Kd. BBV has been the subject of intense study at the University of Wisconsin, Madison, by the groups of Roland Rueckert and Paul Kaesberg. The bipartite genome has been fully sequenced and cloned and infectious RNA has been produced from the cloned DNA. A variety of site directed mutation studies are planned by the Madison groups to explore replication, translation, and assembly strategies.

Crystals of BBV have been obtained that diffract to 2.8Å resolution. The space group is $P4_232$ a = 362Å with two particles/cell each occupying tetrahedral symmetry sites in the lattice. A native data set to 2.8Å resolution has been collected at LURE, Orsay, France, and processed at Purdue. The overall R factor for data with $I/\sigma(I) \geq 2.0$ is 13.9% for 390,714 observations. There were 130,261 independent reflections corresponding to 70% of the data at 2.8Å resolution. Two derivatives of the virus crystals have been characterized to 5.0Å resolution. The DIR map so obtained is currently being improved in quality and resolution, using phase refinement by non-crystallographic symmetry.

T-PM-D1 SUPPRESSION OF VOLTAGE-DEPENDENT NOISE BY A GLUTAMATE ANALOG IN DEPOLARIZING BIPOLAR CELLS OF THE GOLDFISH RETINA. S. Nawy and D. Copenhagen, Div. of Neuroscience, University of Calif, San Francisco, 94143.

Responses to steps of light and current were recorded intracellularly from rod-driven depolarizing bipolar cells in the isolated goldfish retina. Small rapid fluctuations in membrane potential were often observed. The magnitude of these fluctuations are highly voltage-dependent, peaking at about -40 mV. They are often completely absent at potentials above -25 mV or more negative than -60 mV, and are usually not seen when recording from cells impaled with electrodes containing TEA+, which is known to block gated K+ conductances. Superfusion of the retina with 1 mM Co++ also blocks these fluctuations.

Superfusion of the retina with 2 μM 2-amino-4-phosphono-butyric acid (APB) hyperpolarizes the bipolar cell and blocks the light response. I-V plots constructed in darkness, light or during APB application crossed at the same potential, about -15 mV, suggesting that both APB and the rod transmitter act by decreasing a conductance with a reversal potential positive to the cell's resting potential. We have found that at concentrations which block the light response, APB also completely suppresses the voltage-dependent fluctuations. We postulate that these fluctuations arise from the activity of voltage-gated channels, possibly Ca++-activated K+ channels. APB appears not only to turn off a transmitter-gated conductance but to block, either directly or indirectly, the voltage-gated channels as well. It remains to be seen if the rod transmitter itself can modulate these voltage-gated channels.

T-PM-D2 KINETICS OF SIGNAL TRANSFER FROM RODS TO SECOND-ORDER NEURONS IN BUFO RETINA J. H. Belgum and D. R. Copenhagen, Dept of Ophthalmology, University of California, San Francisco, 94143

The synaptic transfer of signals from rods to horizontal cells (HC) and to hyperpolarizing bipolar cells (HBC) was determined using paired simultaneous recordings. For dim diffuse flashes postsynaptic responses could be simulated by scaling and low-pass filtering the response of the paired rod. For brighter flashes the same linear transformation was sufficent to simulate the initial rise and the decay of the postsynaptic response but did not predict two striking features of these responses: saturation and slowed HC kinetics. Rod hyperpolarizations of 5-7 mV produced a maximal postsynaptic potential; further rod hyperpolarization, including the rod "nose", produced no detectable postsynaptic response. This static saturation can be fitted by the model of Falk and Fatt. This model plus filtering simulates HBC responses at all flash intensities. HC responses became much slower than model reponses as flash intensities increased. This lag could be simulated by increasing the time-constant for low-pass filtering in proportion to modelled input resistance. Light is presumed to cause a resistance increase and a concomitant increase in membrane time-constant.

Satisfactory simulation of responses required the assumption that a 4.5 to 7 mV change in rod potential caused a ten-fold change in synaptic conductance and that synaptic conductance was about 1/2 of total conductance in the dark.

T-PM-D3 GTP AND INOSITOL 1,4,5-TRISPHOSPHATE MEDIATE INTRACELLULAR CALCIUM RELEASE FROM N1E-115 NEURONAL CELLS. Donald L. Gill, Teruko Ueda, & Sheau-Huei Chueh. Dept. Biol. Chem., Univ. Maryland Sch. Med., Baltimore, MD 21201. Release of Ca^{2+} from an intracellular organelle within the N1E-115 neuroblastoma cell line is shown to be mediated by both inositol 1,4,5-trisphosphate (IP_3) and GTP. Cells permeabilized with 0.005% saponin (37°C, 20 min) were loaded with Ca^{2+} (containing 80 Ci/mol ^{45}Ca) via the (ATP + Mg^{2+})-dependent Ca^{2+} pump characterized in detail in recent studies (Gill & Chueh, J.B.C. **260**, 9289). After Ca^{2+} uptake for 5 min at 37°C, 2 μM IP_3 effects release of approximately 30% of accumulated Ca^{2+} within 30 seconds. Half-maximal Ca^{2+} release occcurs with 0.5 μM IP_3, the effect being maximal at 3 μM. Addition of 10 μM GTP, in the absence of any added IP_3, effects release of 60-70% of accumulated Ca^{2+} within 20 seconds, the rapidity of GTP-mediated Ca^{2+} release equaling that effected by 5 μM A23187, although the latter mediating release of 90-95% of accumulated Ca^{2+}. The effect of GTP is half-maximal at 0.8 μM. Neither ITP, CTP or ATP at 10 μM effect any Ca^{2+} release. Although 20 μM GppNHp or 20 μM GMP are also ineffective, 20 μM GDP does induce Ca^{2+} release. GDP-mediated Ca^{2+} release, although maximal, is much slower than GTP-mediated release, with a significant lag of 30 seconds. During this time GDP-GTP conversion is suspected. 100 μM GDP completely blocks the effect of 5 μM GTP, indicating that while GDP has no direct effect on Ca^{2+} release, it competes for the same site as GTP. The addition of IP_3 together with GTP does not appear to result in additional release compared to GTP alone. Thus the actions of the two agents, although probably on the same intracellular Ca^{2+} pool, are apparently noninterdependent. We believe the intracellular Ca^{2+}-pumping organelle contains a Ca^{2+} channel opening of which is dependent on GTP hydrolysis. (Supported by NIH Grant NS19304).

T-PM-D4 CHANGES IN THE CONCENTRATION OF INTRACELLULAR FREE CALCIUM INDUCED BY EXTRACELLULAR CALCIUM OR MAGNESIUM IN PARATHYROID CELLS AS MEASURED BY QUIN 2 OR FURA 2. E.F. Nemeth and Antonio Scarpa, Dept. Biochem/Biophysics, Univ. of Penna., Philadelphia, PA 19104.

Intracellular concentrations of free Ca^{2+} ($[Ca^{2+}]_i$) were measured in dissociated bovine parathyroid cells (PTCs) using the fluorescent indicators quin 2 or fura 2. Previous studies using PTCs loaded with 700-900 μM intracellular quin 2 have shown that small increases in the concentration of extracellular Ca ($[Ca]_0$) are associated with slow and sustained increases in $[Ca^{2+}]_i$. In PTCs loaded with 75-100 μM intracellular fura 2, however, a qualitatively different pattern emerges which reveals the presence of two components contributing to the regulation of $[Ca^{2+}]_i$ by $[Ca]_0$. In fura 2-loaded PTCs, increasing $[Ca]_0$ from 1.0 to 1.5 or 2.0 mM caused a rapid and transient 4- to 5-fold increase in $[Ca^{2+}]_i$ that was followed by a lower yet sustained increase in $[Ca^{2+}]_i$. Increasing $[Mg]_0$ likewise elicited a rapid and transient increase in $[Ca^{2+}]_i$, whereas in quin 2-loaded PTCs, $[Mg]_0$ caused only very small, monophasic increases in $[Ca^{2+}]_i$. PTCs loaded with fura 2 had higher $[Ca^{2+}]_i$ at all $[Ca]_0$ than did quin 2-loaded PTCs. The different steady-state levels of Ca^{2+}_i and the absence of transient increases in $[Ca^{2+}]_i$ in quin 2-loaded PTCs appear to result from the greater buffering capacity in these cells rather than from some unique property of either indicator. Transient increases in $[Ca^{2+}]_i$ induced by extracellular Ca or Mg were depressed by pretreatment with ionomycin and could be interpreted as the mobilization of Ca from a common intracellular pool. Because these intracellular Ca transients are seen only at extracellular concentrations of Ca or Mg that modulate secretion of parathyroid hormone, such transients may contribute importantly to the regulation of secretion in PTCs. Supported by NIH grant AM-33928.

T-PM-D5 SIMULATIONS of CALCIUM FLUXES and BINDING at NERVE TERMINALS

John W. Moore, Halina Meiri and Michael L. Hines. Dept. of Physiology, Duke Univ. Med. Cntr., Durham, NC 27710 and Dept. of Physiology, Hadassah Med. School, The Hebrew University, Jerusalem, Israel.

Recent experiments (Meiri et.al., in press) with the frog neuromuscular junction suggest that the sodium-calcium exchange mechanism (NaCaX) is contributing to the regulation of $[Ca]_i$. To examine this possibility, we extended our computer program for intracellular diffusion of Ca^{++} (in axoplasm with Ca^{++} binding sites) at synapses to add detailed descriptions of transmembrane fluxes. In addition to the Na-CaX, mechanisms included are: 1) temperature and voltage sensitive Na, K & Ca channels, and 2) an ATP driven (temperature sensitive) Ca pump.

NaCaX allows extra Ca to enter during a membrane action potential and exit at rest. With reduction of $[Na]_0$, the peak level of $[Ca]_i$ increases, but not as much as observed in experiments. With increasing $[Ca]_0$, the peak value of $[Ca]_i$ increases linearly with E_{Ca}, not with $[Ca]_0$ as is generally inferred from the 4th power relation between release and $[Ca]_0$ (frog). With literature values of binding sites, the $[Ca]_i$ peak is rather insensitive to the pump and exchange coefficients. A 10°C increase in temperature decreases the peak $[Ca]_i$.

These simulations aid in the evaluation of current ideas about the role of calcium in secretion and transmission.

Supported by NIH grants NS 03437 (JWM) & NS 11613 (MLH)

T-PM-D6 EFFECTS OF ACIDIFICATION ON Ca^{2+}_i, Ca FLUXES, AND DOPAMINE RELEASE IN SYNAPTOSOMES. Daniel Nachshen and Pierre Drapeau, Department of Physiology, Cornell University Medical College, New York, N.Y. 10021.

When pinched-off presynaptic nerve terminals (synaptosomes) from rat brain are acidified by the addition of HCl, there is a gradual drop in pH_i from ~7.2 to 6.2 within 3-4 min., as monitored with the intracellular fluorescent pH indicator BCECF (2',7'-bis(carboxyethyl)-5.6-carboxyfluorescein). When the acidification is done in the presence of acetate (20 mM), the drop in pH_i is almost instantaneous, since the undissociated acetate anion can serve to shuttle H^+ across the plasma membrane. Lowering pH_o from 7.4 to 5.5 in the absence of acetate has no significant effect on baseline ^3H-dopamine release from synaptosomes measured within 30 sec., but in the presence of acetate, lowering pH_o increases dopamine release by a factor of 5-8. Thus, intra- but not extra-synaptosomal acidification is responsible for the increase in dopamine release. This increase is not dependent on extracellular Ca, and is not accompanied by an increase in baseline ^{45}Ca uptake or cytosolic Ca (as monitored with the intracellular Ca fluorescent indicator Fura-2). Lowering pH_o blocks depolarization-dependent dopamine release from the synaptosomes. This block is paralleled by a decrease in depolarization-dependent Ca uptake. When pH_o is lowered from 7.4 to 6.0, both Ca uptake and dopamine release are inhibited by ~50% (Ca_o=0.2 mM). This block is not increased by intracellular acidification in the presence of acetate. In conclusion, lowering pH_o but not pH_i blocks voltage- (Ca-channel) dependent Ca uptake and dopamine release, whereas lowering pH_i but not pH_o increases baseline dopamine release in a Ca-independent manner.

T-PM-D7 POLYMER PHASE TRANSITION: A NOVEL MECHANISM OF PRODUCT RELEASE IN SECRETION.

Pedro Verdugo, Center for Bioengineering, University of Washington, Seattle, Washington 98195.

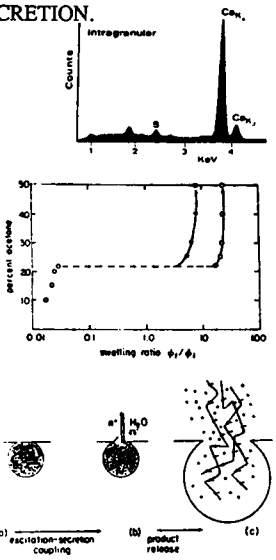

Mucus is a polymer gel that functions as a hydrated shell coating a variety of epithelial surfaces in a large number of animal species. It is made of high molecular weight polyionic mucins which are tangled together forming a three-dimensional random network (Biorheology 20, 223, 1983). Mucins swell upon release from secretory cells following a characteristic first order kinetic similar to other polymer gels (CIBA Symp. 109, 212, 1984). Thus we have proposed that inside the secretory granule musins must form a condensed polymer network, their anionic charges being shielded by a cation; and that the molecular mechanisms of product release may be a phase transition as found in other polymer gels. The following experiments were designed to test this hypothesis: The presence of a shielding cation was investigated in giant mucin granules of the slug *Ariolimax Columbianus*. X-ray microanalysis spectra of quick frozen thin sections of these granules confirm the presence of 2.4±0.8 M Calcium (M/Kg dry material) inside the secretory granule (Fig. 1). Experiments using videomicroscopy show that giant mucins secretory granules equilibrated in solutions containing different water/acetone ratios can reversibly expand as much as 100 times their original volume. The observed volume change reveals a characteristic discontinuity. The critical point take place at 26% water, 74% acetone (pH 7, 20° C) and it varies with temperature and Ca^{2+} concentration following the typical features of a polymer gel phase transition (Fig. 2).

Thus mucins must be in condensed phase in secretory granules. Their charges being shielded by Ca^{+2}. The release of secretory product from the granule must be driven by molecular forces stored in a cation-shielded condensed polyionic network. The triggering mechanism would be the release of the shielding cation or entrance of an anion into the granule; and the driving force would result from a phase transition phenomenon whereby the mucins polymer network would go from a condensed phase to an expanded hydrated phase (Fig. 3).

T-PM-D8 IMPROVED METHODS OF SERIES RESISTANCE COMPENSATION FOR VOLTAGE CLAMPS.

Ronald Millecchia and Gunter N. Franz. Department of Physiology, West Virginia University Medical Center, Morgantown, WV 26506.

The two-port equivalent of a voltage clamp is characterized by the open-circuit output voltage Voc = k Vcmd (k=voltage transfer gain, Vcmd=command voltage) and the output impedance, Zo, which is a function of the access resistance and the inner impedance of the amplifier. With a membrane of impedance, Zm, and series resistance, Rs, connected to the clamp circuit, the membrane potential is Vm = k Zm Vcmd / (Zo + Rs + Zm). The normal methods of Rs compensation add a term equal or approximately equal to -Rs to the denominator. Complete fidelity, however, would require that Zo be made zero too. This poster offers two methods of complete Rs compensation: (1) "split compensation", i.e. separate terms are added to the denominator to cancel Zo and Rs, respectively; (2) the clamp circuit is transformed into a negative impedance device of output impedance Zo = -Rs. A collection of circuit schemes is given.

T-PM-D9 THREE-DIMENSIONAL COMPUTER RECONSTRUCTION OF MICROCAPILLARY MODULES IN THE MEDIAN EMINENCE. L.S. Hibbard, B.J. Dovey-Hartman, and R.B. Page, Departments of Radiology, Anesthesia, and Surgery, The M.S. Hershey Medical Center, The Pennsylvania State University, Hershey, Pennsylvania 17033 (Intr. by Sally Carty).

The capillary plexus in the median eminence forms a humoral connection between the hypothalamus and the pituitary, capable of blood flow in both directions, and may exercise control over hormonal communication between these centers. To determine whether the physical means for such control exists (smooth muscle sphincters located strategically in loops and arbors) we have developed a program system for the 3D reconstruction of capillaries from digitized transmission electron micrographs (TEM) of thin sections of the rabbit median eminence. Using digital imaging techniques, capillary features are extracted from the serial TEM images, mosaics of multiple overlapping images are generated, and the images are placed in register. The feature detection is carried out in the spatial domain using point operators. Mosaics are formed with fast Fourier transform (FFT) correlation of capillary lumen edges. Image registration is carried out in two stages: 1. coarse alignment is effected by superposition of capillary-feature principal axes, and 2. fine alignment is produced by rotation and translation refinements of the coarse alignment transformation with FFT correlation. In two preliminary reconstructions, capillary bundles were observed to consist of parallel tubes interrupted at intervals by changes in the connections among them. (Supported by NSF Grant BNS-8506479 and by NIH Grant NS 15926.)

T-PM-D10 MEASUREMENT OF A $[Na]_o$-DEPENDENT $[Ca]_i$-ACTIVATED MEMBRANE CURRENT IN SQUID AXONS. C. Caputo, R. DiPolo and F. Bezanilla. CBB, IVIC, Apartado 1827, Caracas 1010A, Venezuela, Dept. of Physiology, UCLA, Los Angeles, CA and MBL, Woods Hole MA 02543.

We have measured a $[Na]_o$-dependent $[Ca]_i$-activated current in intracellularly dialyzed squid axons under membrane potential control with a low noise voltage clamp. TTX was used to block Na channels and prolonged exposure to K-free media was used to eliminate K conductance. In most experiments the solutions were (in mM); External: $NaNO_3$, 200; NMG-NO_3 (N-methylglucamine), 240; $Ca(NO_3)_2$, 10; $Mg(NO_3)_2$, 50; TRIS-MOPS, 10; pH=7.8. Internal: NMG-aspartate, 290; Na-asp 20; $MgCl_2$, 4; TRIS-MOPS, 50; TRIS-EGTA, 1; pH=7.3; osmolality=1000 mOsm. Membrane resistance was 2000 to 7000 Ωcm^2. With these solutions, addition of 200 μM free internal Ca caused the development of an inward current of 1.3± 0.13 $\mu A/cm^2$ (mean ± SEM, n=10) at -10 to -15 mV, 20° C with a time course consistent with Ca diffusion to the membrane from the dialysis capillary. This current disappeared upon Ca_i removal. When NaCl was used instead of $NaNO_3$, the current was smaller by 30%. The current was not present when Li substituted for external Na, or in the presence of 1 mM external La. Internal Ba did not activate the current. Decreasing the temperature from 20 to 14° C reduced the current by 50 to 40% in two axons. The magnitude and direction of the current could be modified by changing the Na gradient and/or the membrane potential. Thus with 100 mM $[Na]_o$ and 100 mM $[Na]_i$, a fiber clamped at -11 mV developed an outward current of 300 nA/cm^2, and when it was clamped at 0 mV a current of 470 nA/cm^2, also in the outward direction, was obtained. These results indicate that a sizeable fraction of this current is related to the Na/Ca exchange. (Supported by NSF-CONICIT, S1-1556 joint program, MDA and USPHS grant GM30376)

T-PM-D11 THE IONIC MECHANISM OF ACTION POTENTIALS OF MOTORNEURONS IN RAT EMBRYOS. Lea Ziskind-Conhaim, Dept. Physiol., Univ. Calif. Med. Sch., San Francisco, CA 94143.

The ionic mechanism of the regenerative potentials was studied at various gestational stages (14-20 days of gestation, birth is at 21-22 days). Spinal cords were removed from the vertebral column leaving the ventral and dorsal roots intact. Membrane excitability was determined by injecting depolarizing current pulses to the soma. At 14 days of gestation, 2 days after motorneurons are generated, depolarizing currents evoked slow and small action potentials in most motorneurons.

The relative contribution of each ionic current to the action potential was examined by adding selective ionic channel blockers to the recording medium. To study the contribution of sodium ions tetrodotoxin (TTX, 1-3 uM) was added to the recording solution or sodium ions were replaced by equimolar concentrations of Tris. Action potentials were reversibly abolished in the presence of TTX or Tris which provides a strong indication that starting at Day 14 sodium is a major ion carrying the inward current. Potassium contribution was determined by application of tetraethylammonium (TEA, 10 mM), a potassium channel blocker. TEA induced a prolonged shoulder on the falling phase of the action potential evoked by intracellular stimulation of the soma. The appearance of long duration action potentials suggested that blocking potassium current unmasked an inward current, most likely caused by calcium. In the presence of 2 uM TTX and 10 mM TEA the rate of rise of the action potential decreased and its duration was prolonged. Substitution of external calcium with strontium increased even further the duration of the potential and replacement of calcium with cadmium (200 uM) abolished the regenerative response. These results strongly suggest that the prolonged inward current is due to calcium influx. Calcium contribution persisted at least until birth. Supported by NS 05988.

T-PM-D12 MODULATION OF SUBTHRESHOLD INWARD CURRENT BY SEROTONIN AND CYCLIC NUCLEOTIDES IN THE APLYSIA BURSTING NEURON R15. Edwin S. Levitan and Irwin B. Levitan, (Intr. by R. Kramer) Graduate Department of Biochemistry, Brandeis University, Waltham, MA 02254

At concentrations below 5 μM serotonin (5-HT) hyperpolarizes the bursting Aplysia neuron R15. This has been shown to be due to activation of the inward rectifying K^+ current (I_R) by cAMP dep. protein kinase. At higher concentrations 5-HT is excitatory and causes the cell to tonically spike. Here we report that 2-50 μM serotonin causes an increase in voltage dependent subthreshold inward current (SIC) measured under voltage clamp. This effect persists in 230 mM Mg suggesting that it is not synaptic. Both basal and serotonin evoked SIC are blocked by the calcium channel blockers Cd and Mn, but are unaffected by iontophoretically loading the cell with EGTA. Lowering external Cl and blocking K currents, with internal Cs or external TEA and 4-AP, fail to block the serotonin effect. Removing 90% of external Na also does not block basal and serotonin evoked SIC if the cell is preloaded with Cs-EGTA. These results suggest that 5-HT acts to increase basal subthreshold calcium current. The effect of 5-HT on SIC is mimicked by bath application of the adenylate cyclase activator forskolin with RO20-1724, a phosphodiesterase inhibitor. This result implies that 5-HT's effects on I_R and SIC are both mediated by cAMP. Interestingly, preliminary experiments indicate that 8-PCPT-cGMP decreases SIC without affecting the inward rectifier.

T-PM-D13 THE RELATION BETWEEN ELECTRODE PLACEMENT AND THE AMPLITUDE OF EXTRACELLULARLY-RECORDED ACTION POTENTIALS. D. W. Tank & D. Kleinfeld, AT&T Bell Laboratories, Murray Hill, NJ 07974.

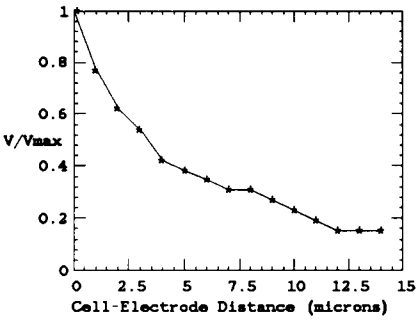

The amplitude of extracellularly-recorded action potentials was measured as a function of electrode to cell surface distance in cultures of dissociated mouse spinal cord neurons [1]. Borosilicate glass microelectrodes with tip diameters of 2-10μm were pressure-filled with a molten mixture of 75% Woods alloy/25% In to within 5μm of the tip; after cooling, the void at the tip was filled with electroplated Au. In mammalian Ringer, the electrode impedance at 1 kHz was 1MΩ (10μm tip) and exhibited a ν^{-1} frequency dependence (10Hz-1kHz). Electrodes were positioned at calibrated heights above the dorsal surface of neurons in 7-14 day old cultures, and extracellular potentials generated by spontaneously occurring action potentials were measured. The amplitude of the measured signals decayed with a characteristic half-amplitude distance of ~3-4μm from the cell surface (Fig.). However, the shape of the signal and the detailed form of the amplitude vs. distance relation depended upon cell type and geometry. These data suggest design parameters for photolithographically-defined extracellular electrode arrays [2] for monitoring activity in cultured spinal cord neurons.

[1] B.R.Ransom, E.Neale, M.Henkart, P.N.Bullock & P.G.Nelson. 1977. J.Neurophysiology 40:1132.
[2] R.S.Pickard. 1979. Trends NeuroSci. 2:259.

T-PM-D14 CONTROL OF NEURONAL-SUBSTRATUM ADHESION USING SURFACE MODIFICATION AND PHOTOLITHOGRAPHIC TECHNIQUES. D. Kleinfeld and D. W. Tank, AT&T Bell Laboratories, Murray Hill, NJ 07974.

The adhesion of dissociated mouse spinal cord cells [1] cultured on silicon and glass substrates was controlled by chemical modification of the substrate surface. Organoalkoxy silanes and/or organochloro silanes were used to covalently link small molecules to substrate surfaces. Surfaces functionalized with alkyl chains (1-18 carbons) inhibit the adhesion of neurons [2]. Surfaces functionalized with amines, however, were found to promote adhesion. In particular, the adhesion characteristics of neurons cultured on surfaces linked with ethylenediamine mimicked that of neurons cultured on conventional substrates, e.g., polylysine or polyornithine coated glass. These chemical methods for controlling neural adhesion were combined with photolithographic techniques to selectively pattern the location of neurons on substrates. Cells uniformly dispersed on patterned substrates adhered according to the chemical nature of the substrate surface (Fig.). At present, neurons can be localized with 100 μm resolution. Methods for increasing this resolution and extending these techniques to metallic substrates are under development.

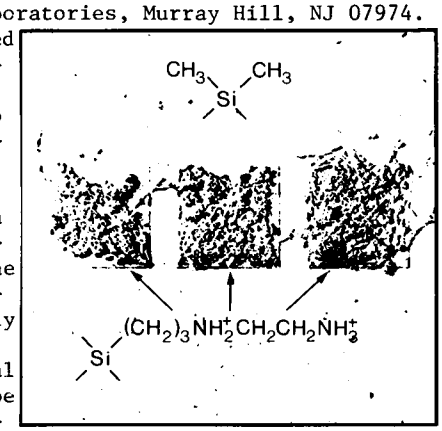

Photomicrograph of neurons cultured for 20 hrs on a patterned (400 μm squares) silicon substrate. Scale: — 100 μm.

1- B.R.Ransom, E.Neale, M.Henkart, P.N.Bullock & P.G.Nelson. 1977. J.Neurophysiology 40:1132. 2- D.Bray. 1984. Dev.Biol. 102:379.

T-PM-E1 SEQUENCE ANALYSIS OF PHOSPHOLAMBAN (PLB): IDENTIFICATION OF PHOSPHORYLATION SITES AND PRESENTATION OF A 3-D STRUCTURAL MODEL. Heather K.B. Simmerman[#], John H. Collins[*], Janet L. Theibert[*], Adam D. Wegener[#], and Larry R. Jones[#]. [#]Indiana Univ. Sch. of Medicine and Krannert Inst. of Cardiology, Indpls., IN 46202 and [*]Clarkson Univ., Dept. of Biology, Potsdam, NY 13676

Canine cardiac phospholamban purified from sarcoplasmic reticulum was examined by gas phase protein sequence analysis and found to possess a free NH_2-terminus, allowing direct identification of 20 NH_2-terminal residues. Overlap peptides produced by trypsin or papain digestion were purified, and used to extend the sequence by 16 residues. PLB phosphorylated by either cAMP-dependent or Ca/calmodulin-dependent protein kinase (PK) was cleaved with trypsin and the major phosphorylated peptide (comprising >70% of incorporated ^{32}P label) was purified by reverse phase HPLC and sequenced. The identical sequence was revealed for the phosphorylated peptide obtained from PLB phosphorylated by either PK. In combination with phosphoamino acid analysis and manual Edman degradation techniques to identify phosphorylated sites, the adjacent residues Ser-7 and Thr-8 of PLB were identified as the unique sites phosphorylated by cAMP-PK and Ca/calmodulin-PK, respectively. These results indicate that the PLB monomers are identical through residues 1-36 and that PLB has a cytoplasmically oriented NH_2-terminal domain containing the unique adjacent sites phosphorylated by cAMP-PK and Ca^{2+}/calmodulin-PK. Hydropathic profiling and secondary structure prediction suggests each PLB monomer also contains an amphipathic helix sufficiently long to traverse the SR membrane. A 3-D model of PLB is presented in which the amphipathic rod of each monomer is part of a pentameric, transmembrane domain comprised of an exterior hydrophobic surface and an interior, largely hydrophilic channel.

T-PM-E2 TOPOLOGY OF THE CALCIUM BINDING SITE REGION OF THE Ca-ATPase OF SARCOPLASMIC RETICULUM Terrence L. Scott, Dept. of Muscle Research, Boston Biomedical Research Institute, Boston, MA 02114.

The SR Ca-ATPase was labeled in the Ca binding domain with carbodiimide (FCD's) derivatives whose fluorescence is sensitive to Ca occupancy of the high affinity transport sites (Chadwick & Thomas, BBA, 769, 291, 1984). Quenching of the fluorescence of the FCD-labeled ATPase with a series of doxyl stearates (n-NS), fatty acid derivatives with spin labels located at different positions along the hydrocarbon chain, was used to determine the depth of the Ca site region within the membrane. After correction for differences in the partition coefficients among the n-NS's, an order of quenching efficiency of 16- >12- >10- >7- >5-NS was found. The depth of the labeled site did not change due to Ca binding. Quenching of the same probes by the water-soluble agents KI and acrylamide was quite efficient and this aqueous accessibility changed significantly as a result of Ca binding. The results suggest that the Ca binding domain is located near the center of the bilayer, in an aqueous filled pore which is accessible to the external aqueous milieu. The binding of Ca alters the external access to the sites.

In contrast, the ATPase Trp residues appear to be localized primarily at the level of the lipid polar head groups, as deduced from the 5- >7- >10- >12- >16-NS order of quenching efficiency of intrinsic fluorescence. The Trp residue(s) whose fluorescence changes due to Ca binding is shown to be near the aqueous-membrane interface at the depth of the polar head groups. Supported by NIH GM-32247.

T-PM-E3 THE ROLE OF ACIDIC RESIDUES IN THE SPECIFIC CALCIUM BINDING BY SARCOPLASMIC RETICULUM (SR) ATPase. Marwan K. Al-Shawi and Giuseppe Inesi, Department of Biological Chemistry, University of Maryland School of Medicine, Baltimore, MD 21201.

The pH dependence of high affinity Ca^{2+} binding by SR ATPase was investigated potentiometrically by difference titrations. The titrations were done, at various H^+ concentrations, by sequential Ca additions to suspensions of Ca^{2+} free vesicles in a pH stat. Aliquots were sampled for measurements of $^{45}Ca^{2+}$-binding. It was found that the stoichiometry of H^+ release to Ca^{2+} bound drops from 1.6 to 0, as the pH is increased from 5.9 to 8.1. The data is best fit assuming two independent acidic residues participating in complexation of one Ca^{2+}, and dissociating H^+ with pK_{app} values of 6.1 and 7.3. H^+-Ca^{2+} exchange specificity was further demonstrated by the lack of H^+ release upon addition of μM Ca^{2+} to ATPase in the presence of 100μM vanadate. Furthermore, transient kinetic studies following the addition of ATP to SR vesicles, revealed direct H^+ extrusion and inward Ca^{2+} transport. The pH dependence of low affinity Ca^{2+} binding by SR ATPase was investigated by studying the Ca^{2+} activation of ATP synthesis following ADP addition to enzyme phosphorylated with Pi in the absence of Ca^{2+}, and by determining the Ca^{2+} concentration dependence of ATPase "back inhibition". It was found that Ca^{2+} binding to the phosphorylated ATPase in the low affinity state, retains a pH dependence similar to that of the non-phosphorylated ATPase in the high affinity state. It is concluded that acidic residues participate in calcium complexation by SR ATPase both in the high and low affinity states, and that a protein conformational change, rather than a large change in the pK of pertinent acidic residues, determines the change in affinity following enzyme phosphorylation. Supported by USPHS (HL 27867) and MDA.

T-PM-E4 REGULATION OF CALCIUM RELEASE FROM CARDIAC SARCOPLASMIC RETICULUM BY CALCIUM•CALMODULIN -DEPENDENT PHOSPHORYLATION. Hae Won Kim*, Do Han Kim**, Noriaki Ikemoto**, and Evangelia G. Kranias*. *Dept. of Pharm. & Cell Biophys, Univ. of Cinn. Col. of Med., Cinn. OH 45267 and **Dept. of Muscle Res., Boston Biomed. Res. Inst., Dept. of Neurol, Harvard Med. School, Boston, MA 02114.

Canine cardiac sarcoplasmic reticulum (SR) contains an endogenous calcium•calmodulin CAM-dependent protein kinase and a substrate, phospholamban. Phosphorylation of SR by Ca^{2+}•CAM-dependent protein kinase is associated with an increase in the initial rates of Ca^{2+} transport, which reflects an increased affinity of the transport protein for Ca^{2+}. To determine the effect of Ca^{2+}•CAM-dependent phosphorylation on Ca^{2+} release, SR vesicles were preincubated under conditions for optimal phosphorylation while control vesicles were preincubated under identical conditions but in the absence of ATP. Both control and phosphorylated vesicles were centrifuged and subsequently used for Ca^{2+} release studies after passive or active Ca^{2+} loading. Passive Ca^{2+} loading occurred at 4°C for 4 hrs in the presence of 5 mM $CaCl_2$ and Ca^{2+} release was induced by dilution of the loaded SR to achieve 2 μM free Ca^{2+}. Ca^{2+}•CAM-dependent phosphorylation was associated with an increase in the rate and level of Ca^{2+} released at 20°C. Active Ca^{2+} loading occurred at 37°C for 9 min, in the presence of 0.37 μM Ca^{2+} and 2 mM ATP. Ca^{2+}•CAM-dependent phosphorylation was associated with increased levels of Ca^{2+} loaded into SR and increased levels of Ca^{2+} released by SR (at 2 and 4 μM Ca^{2+}). These findings indicate that calcium release from cardiac SR may be under regulation by Ca^{2+}•CAM-dependent protein kinase and this may represent an important control mechanism for the myocardium. Supported by NIH grants AM 16922, HL 26057 and HL 22619. Dr. D.H Kim was supported by an NIH postdoctoral fellowship.

T-PM-E5 ROLE OF CARBOHYDRATE RESIDUES IN THE REGULATION OF CALCIUM RELEASE FROM SARCOPLASMIC RETICULUM N. Ikemoto, B. Antoniu, M.E. Cifuentes, L.G. Mészáros, and C. Hidalgo Dept. Muscle Res., Boston Biomed. Res. Inst.; Dept. Neurol. Harvard Med. Sch.; Dept. Physiol. Biophys., Fac. Med., Univ. Chile

We have investigated the effects of several lectins [e.g. concanavalin A (ConA) and wheat germ agglutinin (WGA)] on two types of Ca^{2+} release from a microsomal fraction enriched in the T-tubule/SR complexes: 1) depolarization-induced Ca^{2+} release produced by choline Cl replacement of K gluconate, and 2) (Ca^{2+} plus caffeine)-induced Ca^{2+} release. Incubation of the vesicles with ConA or WGA reduced the amount of depolarization-induced Ca^{2+} release with a half-maximal inhibition at 0.5-0.8 mg per mg membrane protein. ConA had little effect on (Ca^{2+} plus caffeine)-induced Ca^{2+} release, but in sub-optimal conditions (e.g. [Ca^{2+}]-dependent passive efflux) it produced a considerable activation. Digestion of the carbohydrate moiety with neuraminidase led to significant changes in the [Ca^{2+}]-dependence profile of depolarization-induced Ca^{2+} release: the amount of Ca^{2+} released was higher than control at [Ca^{2+}] less than 10 uM, but lower than control at [Ca^{2+}] higher than 10 uM. The neuraminidase treatment produced little effect on the [Ca^{2+}]-dependence profile of (Ca^{2+} plus caffeine)-induced Ca^{2+} release. These results suggest that glycoproteins located in the T-tubule are involved in the mechanism by which depolarization-induced Ca^{2+} release is regulated by the extravesicular [Ca^{2+}]. The fact that ConA potentiates (Ca^{2+} plus caffeine)-induced Ca^{2+} release in some conditions suggests that glycoproteins (or glycolipids) in SR are also involved in the regulation of Ca^{2+} release. Supported by grants from NIH (AM-16922, HL-23007) and MDA.

T-PM-E6 PROTEINS INVOLVED IN THE REGULATION OF CA^{2+} RELEASE FROM SKELETAL MUSCLE SARCOPLASMIC RETICULUM (SR) Do Han Kim, Karen L. Brown and Noriaki Ikemoto. Dept. of Muscle Res., Boston Biomed. Res. Inst.; Dept. of Neurol., Harvard Med. School, Boston, Ma

The effects of calmodulin (CaM)-dependent phosphorylation of SR components on Ca^{2+} release from SR (Kim, D. H. and Ikemoto, N., Biophys. J. 47, 56a, 1985) were further investigated. SR vesicles passively loaded with Ca^{2+} were phosphorylated by [γ-^{32}P] ATP and the phosphoproteins were identified by autoradiography. Ca^{2+} efflux was initiated by adjusting $[Ca^{2+}]_o$, and monitored by means of stopped-flow fluorometry and filtration method. Addition of protease inhibitors during Ca^{2+} loading decreased the number of phosphoproteins. Furthermore, at lower concentrations of ATP, only a 60 kDa protein was predominantly phosphorylated. Under these conditions, the extent of phosphorylation of the 60 kDa protein paralleled inhibition of Ca^{2+} efflux. Removal of the endogenous CaM amplified both the CaM effect on phosphorylation and the inhibition of Ca^{2+} efflux. One uM CaM in the loading solution without added ATP significantly decreased Ca^{2+} efflux, suggesting that CaM binding per se is also involved. The CaM binding protein was identified by passing detergent solubilized SR through the CaM affinity column. After EDTA elution, a single protein was recovered; the protein was identified as calsequestrin suggesting that calsequestrin may also be involved in the regulation. Supported by grants from NIH (AM 16922) and MDA. D.H.K. was supported by an NIH postdoctoral fellowship.

T-PM-E7 SOLVENT ACCESSIBILITY OF THE SR CaATPase ATP CATALYTIC SITE by S. HIGHSMITH (Univ. of the Pacific, San Francisco, CA 94115), Sponsored by Don Scales.

The CaATPase of rabbit skeletal SR was labeled at or near the ATP catalytic site with fluorescein isothiocyanate (FITC) and the accessibility of the attached probe to the bulk solvent was determined by I^- quenching of its fluorescence. The quenching of free FITC was also measured. In both cases the quenching was of the Stern-Volmer type and collisional quenching rate constants were obtained over the pH range 5-8 in the presence of EGTA, and with added Ca^{2+}, vanadate or phosphate.

The fluorescence intensity and susceptibility to quenching by I^- of free FITC were insensitive to the added ligands. The intensity decreased with pH, as predicted from the known properties of FITC mono- and dianions. The collisional quenching rate constants increased at lower pH, as expected for I^- quenching of a molecule with decreasing negative charge due to protonation.

Attached to the CaATPase, the FITC fluorescence intensity and I^- collisional quenching rate constants were sensitive to ligand binding and pH. The changes in fluorescence intensity with acidity indicated the pKa of the FITC was 5.8, when attached to the CaATPase. The ligand-induced changes in the collisional quenching rate constants appeared to be due to changes in steric hindrance to I^- colliding with bound FITC, rather than changes in local charge near the probe. At all pH values, the hindrance to I^- quenching of the fluorescence of the FITC at the ATP binding site, was vanadoenzyme < enzyme < phosphoenzyme. The effect of Ca^{2+} binding to the CaATPase was to decrease the hindrance. At pH 6.0, the transition from E-P to ECa_2 was consistent with an increase of 48% in the accessibility of the ATP binding site to the bulk solvent. (Am. Heart Assoc.)

T-PM-E8 PROTEOLYTIC ACTIVATION OF THE CALCIUM PUMP OF CANINE CARDIAC SARCOPLASMIC RETICULUM. M. A. Kirchberger, D. Borchman, C. Kasinathan, and R. G. Lanzara. Department of Physiology and Biophysics, Mount Sinai School of Medicine, NY 10029.

The calcium pump of sarcoplasmic reticulum (SR) vesicles prepared from canine ventricle was activated several fold by mild protease treatment. After 5 min of incubation with protease, a suitable protease inhibitor was added and an aliquot was assayed for the initial rate of oxalate-facilitated ^{45}Ca-uptake by a filtration procedure. Ca-uptake was stimulated by different proteases in the following order of effectiveness: trypsin > chymotrypsin > papain > elastase. The trypsin Ca^{2+} concentration dependency curve for Ca-uptake was identical to that produced by cAMP-dependent protein kinase (PK), both curves indicating higher Ca^{2+} sensitivity compared to untreated SR. The Hill coefficients of the Ca^{2+} dependency after treatment of SR with trypsin or PK were similar and were not different from untreated SR. Autoradiograms of sodium dodecylsulfate polyacrylamide electrophoretic gels indicate that phosphorylation of phospholamban (PL) (M_r=27.3K or its presumed monomeric subunit M_r=5.5K) was markedly reduced by prior treatment of the SR with trypsin. The trypsin concentration dependencies of the activation of Ca-uptake and the loss of ^{32}P-labelling ability of PL were identical. The effect of trypsin on Ca-uptake could not be attributed to a direct effect on the 100-kDa Ca pump protein. These findings provide evidence for the view that the cardiac SR Ca pump is in an inhibited state in the presence of unphosphorylated PL and that this inhibition can be relieved by either phosphorylation or proteolysis of phospholamban. Part of PL would appear to be accessible to the cytoplasm and may act as a sensor of the cytoplasmic environment and hence allow feedback modulation of SR membrane function. (NIH grant HL15764)

T-PM-E9 MODULATION BY POTASSIUM, TRIS, AND CHOLESTEROL OF THE CALCIUM ATPASE OF SARCOPLASMIC RETICULUM. P.L. Yeagle, B.S. Selinsky, C. Sprowl, and A. Messina, Department of Biochemistry, SUNY/Buffalo School of Medicine, Buffalo, NY 14214.

The effects of potassium and Tris in the medium, and cholesterol in the membrane, on the calcium pump protein in light rabbit muscle sarcoplasmic reticulum were assessed. Measurements were made of functional molecular weight by target size analysis, of conformation by tryptophan fluorescence, of the number of phospholipids bound to the protein in the membrane by P-31 NMR, and of activity by calcium transport and ATP hydrolysis assays. Potassium was found to change the ratio of calcium pumped to ATP hydrolyzed, to change the number of phospholipids bound to the membrane protein and to cause no change in the functional molecular weight. Tris was found to inhibit the enzyme, to change the conformation of the enzyme, to change the number of phospholipids bound to the protein and to increase the state of aggregation of the protein in the membrane. Cholesterol caused no discernable effects on the activity or the number of phospholipids bound to the calcium pump protein in the intact light sarcoplasmic reticulum. These results suggest that the state of aggregation of this membrane protein can be modified by the environment of the membrane with consequent changes in enzyme activity. These results suggest that the choice of buffer in which to study the membrane is important. These results also suggest that there is little interaction between cholesterol and the calcium pump protein.

T-PM-E10 EFFECTS OF MODIFICATION OF THE Ca-ATPase BY FLUORESCEIN ISOTHIOCYANATE OR VANADATE ON Ca RELEASE FROM SARCOPLASMIC RETICULUM; STUDIES WITH A RAPID FILTRATION SYSTEM L.G. Mészáros and N. Ikemoto Dept. Muscle Res., Boston Biomed. Res. Inst. and Dept. Neurol., Harvard Med. Sch.

A rapid filtration system with few-millisecond time resolution (Y. Dupont; Anal. Biochem. 142 504-510, 1984) was applied for the measurements of rapid Ca^{2+} release from sarcoplasmic reticulum (SR) loaded passively with $^{45}Ca^{2+}$. The time course of Ca^{2+} efflux showed biphasic kinetics. Release activators, such as adenine nucleotides and caffeine, affected different phases of the efflux; former ones potentiated the fast phase (rate constant up to 20 s^{-1}), while the latter potentiated the slow phase. Both phases were activated by μM extravesicular [Ca^{2+}], and blocked by μM ruthenium red or mM Mg^{2+}.

The Ca^{2+}-ATPase moiety of SR was selectively modified with fluorescein isothiocyanate (FITC) as determined by fluorometry of gel slices of the treated SR samples. The rate of the Ca^{2+} efflux in the rapid phase was significantly increased in the FITC-modified SR (up to k=20 s^{-1}). The extent of this increase paralelled the amount of the FITC incorporated into the Ca^{2+}-ATPase and the degree of the inhibition of the Ca^{2+}-ATPase activity caused by the chemical modification. It was found that ortho-vanadate (100 μM) also increased the Ca^{2+} efflux rate, but primarily affecting the slow phase. Both the FITC- and vanadate-accelerated Ca^{2+} efflux were completely blocked by ruthenium red or Mg^{2+}, and regulated by extravesicular [Ca^{2+}], as in the case of unmodified SR. These results suggest that the Ca^{2+}-ATPase is able to mediate rapid and ruthenium red-sensitive Ca^{2+} release from SR. Supported by grants from NIH (AM-16922) and MDA, L.G.M. is a post-doctoral fellow of MDA.

T-PM-E11 KINETIC IDENTIFICATION OF THE SITE ON THE SARCOPLASMIC RETICULUM Ca^{++}-ATPase BINDING TNP-AMP WITH HIGH FLUORESCENCE. James E. Bishop, Marwan K. Al-Shawi & Guiseppe Inesi. University of Maryland Medical School, Dept. of Biological Chemistry, Baltimore, MD 21201.

It is known that TNP-nucleotides bind to the Ca^{++}-ATPase resulting in a high fluorescence, when the enzyme is phosphorylated with micromolar levels of ATP. Millimolar ATP displaces the fluorescent nucleotide, engendering the proposal that TNP-nucleotide binds the regulatory nucleotide site. This site is identified operationally in that millimolar ATP accelerates steady state turnover, without increasing phosphoenzyme levels formed by micromolar ATP. We have found that at pH 8.0 and in the abscence of K^+, TNP-AMP competitively inhibits this acceleration with a K_i of 1 μM TNP-AMP and K_d= 4 mM ATP, showing that TNP-AMP binds to the regulatory site.

Transient kinetics were used to establish the location of the regulatory site on the enzyme. Addition of 5 mM Mg·ADP to the steady state enzyme phosphorylated with 100 uM [^{32}P]ATP resulted in a rapid decomposition of 30% of the phosphoenzyme to ATP within 3 msec, followed by a slower decomposition at k= 10 sec^{-1}. Inclusion of saturating TNP-AMP, which has a dissociation rate constant of about 150 sec^{-1} (τ = 7 msec), blocked the rapid phase of decomposition completely, showing that TNP-AMP was bound to the phosphorylated catalytic site.

Together, these results show that the catalytic nucleotide site of the Ca^{++}-ATPase is converted to the regulatory nucleotide site upon phosphorylation. Supported by NIH grant HL 27867 & the Muscular Dystrophy Association of America.

T-PM-E12 TRINITROPHENYL-ATP ABSORBANCE AND FLUORESCENCE IN COUPLED AND UNCOUPLED SKELETAL SARCOPLASMIC RETICULUM. Mervyn C Berman, MRC Biomembrane Research Unit, Univ. Cape Town Medical School, Observatory, Cape Town 7925

The ATP analog, TNP-ATP, binds to both catalytic and regulatory sites on the Ca^{2+}-ATPase of sarcoplasmic reticulum. ATP-induced E-P formation leads to enhanced fluorescence and shifts in the absorbance difference peak from 510 to 450 nm, with decreased absorbance that is reversed on ATP hydrolysis. EGTA-induced uncoupling of active transport abolishes ATP-dependent spectral shifts and fluorescence changes that are only partly due to decreased binding of the probe. The data are compatible with previous studies on tightly bound ATP and ADP in coupled and uncoupled SR (Aderem et al., Proc. Natl. Acad. Sci. (U.S.A.) 76, 3622-3626, 1979). The findings indicate that coupling of active Ca^{2+} transport to catalysis is dependent on restricted access of H_2O to the regulatory site during turnover and suggest that alternate pathways and intermediate species may be involved in both the uncoupled state and under conditions that result in submaximal stoichiometry of the Ca^{2+} pump (Meltzer, S. and Berman, M.C., J. Biol. Chem. 259, 4244-4253, 1984).

T-PM-E13 INHIBITION OF P-NITROPHENYL-PHOSPHATASE ACTIVITY IN LIGHT SARCOPLASMIC RETICULUM VESICLES BY MICROMOLAR CONCENTRATIONS OF ADP. A. Gafni and S.M. Boorstein, (Intr. by Robert Zand) Institute of Gerontology and Department of Biological Chemistry, University of Michigan, Ann Arbor, MI 48109.

The p-nitrophenyl-phosphate (p-NPP) supported transport of Ca^{2+} into light sarcoplasmic reticulum (SR) vesicles from rabbit muscle is 30-40 times slower than the corresponding ATP-supported process. Vesicles which appear to be fully coupled when ATP is used as substrate may therefore have Ca^{2+} efflux rates which are large enough to effectively abolish the p-NPP supported accumulation of significant concentrations of Ca^{2+} in the intravesicular space. Under these conditions the hydrolysis of p-NPP proceeds at a constant rate until the substrate is exhausted. This p-NPPase activity, in a light fraction of SR vesicles was found to be inhibited by ADP in a biphasic manner. A steep decrease in the rate of p-NPP hydrolysis occurred with increasing ADP concentrations in the micromolar range until a ratio of ADP/ATPase ~ 1 was reached. As the concentration of ADP was further increased the corresponding decline in p-NPPase activity was greatly reduced. The concentrations of ADP required to produce the steep decrease in activity described above correlate well with those involved in the ADP-dependent dephosphorylation of the ATPase and it is suggested that both effects reflect the binding of ADP to a regulatory site on the enzyme outside the active site.

T-PM-E14 REACTION BETWEEN ADP AND EP IN SKELETAL SARCOPLASMIC RETICULUM (SR). KINETIC EVIDENCE FOR A DIMERIC REACTION MECHANISM. T. Wang, Department of Pharmacology and Cell Biophysics, University of Cincinnati College of Medicine, Cincinnati, Ohio 45267-0575.

Using ADP as a probe for investigation of the phosphorylated enzyme (EP) intermediate formed by ATP phosphorylation of the SR Ca^{2+}-ATPase in the presence of K^+, we have obtained strong kinetic evidence for the enzyme reacting as a dimer through the dimeric phosphoenzyme PE'E"P. The reaction ADP + PE'E"P $\rightleftarrows$ ADP•PE'E"P $\rightarrow$ [ATP•E'E"P $\rightarrow$ ATP•E'E"P•ADP $\rightarrow$ E'E" + 2 ATP (or ATP + Pi)], describing a rapid equilibrium (K_d) between the reactants (ADP + PE'E"P) and the first-formed "half-complex" (ADP•PE'E"P) and a rate-determining decomposition (k) of the half-complex in a manner presumably through sub-unit interaction resulting in the subsequent loss of the adjacent P in a fast step (shown in the bracket), is in accordance with the experimental observations. An exact kinetic equation can be derived from the reaction to account for the observed hyperbolic relationships between [ADP•PE'E"P] (detected as the missing [EP] = $1/2([PE']_o + [E"P]_o - [PE'] - -[E"P])$) and [ADP], and between the observed first-order rate constant k_b for the disappearance of the sum of [PE'] + [E"P] + [ADP•PE'E"P] and [ADP]. The equilibrium constants (Kd) obtained from the above two hyperbolic plots are the same, 100 μM, as expected from the mechanism. At 100 μM ADP, half of the PE'E"P is converted to ADP•PE'E"P; whereas at the saturating ADP, all of the PE'E"P is converted to ADP•PE'E"P, giving the maximum possible missing EP as half of the sum of PE' + E"P. Such half saturation of the PE'E"P by ADP is observed regardless of the time of EP formation and decomposition. The rate-determining constant k is the $k_{b\ max} = 43.5\ s^{-1}$ at $[ADP]_{max}$. The results suggest that the phosphoenzyme intermediate is composed of two kinetically distinguishable ADP-sensitive EP's. (Supported by NIH PO1 HL22619 IVA-1.)

T-PM-F1 PROTEIN DYNAMICS AND REACTIVITY IN HEMOGLOBIN: TRANSIENT RAMAN AND PICOSECOND RAMAN HOLE BURNING STUDIES. Blair F. Campbell and Joel M. Friedman, AT&T Bell Laboratories, Murray Hill, N. J. 07974

The picosecond geminate recombination of oxygen in hemoglobins is highly responsive to the tertiary structure of the heme environment.[1] In particular, the geminate yield changes in response to changes in the heme-proximal histidine geometry as reflected in the frequency of the iron-proximal histidine stretching mode (ν(Fe-His). Non-exponential kinetics for the ps geminate recombination are observed.[1] Since ν(Fe-His is the same at 30 ps and 10 ns subsequent to photodissociation,[2] the non-exponential kinetics cannot originate from a subns structural diffusion involving the heme histidine geometry. One alternative explanation is that the dynamics associated with conformational heterogeneity are sufficiently slow that the initial geminate recombination reflects preferential binding to specific substate conformations. Because of the suggested relationship between ν(Fe-His) and the innermost barrier controlling geminate rebinding,[3] we have monitored the lineshape of ν(Fe-His) of the surviving population of the deoxyheme photoproduct during the picosecond geminate rebinding in order to determine whether this Raman band is inhomogeneous broadened with respect to functional selectivity. Our preliminary results reveal only a monotonic decrease in the intensity without any change in lineshape. Thus it appears that for ligand binding dynamics that there is no indication of conformational heterogeneity on the 10's of ps time scale at least for the heme-histidine geometry. A similar study at cryogenic temperatures is currently in progress.

1. J. M. Friedman, et al. Science 229, 187 (1985).
2. E. W. Findsen, et al. Science 229, 661 (1985).
3. J. M. Friedman, et al. Science 228, 1273 (1985).

T-PM-F2 INTERSPECIES VARIATIONS AND SIMILARITIES IN THE DYNAMICS OF HEME-PROTEIN INTERACTIONS SUBSEQUENT TO CO PHOTOLYSIS. S. D. Carson[a,*], C. A. Wells[a], J. M. Friedman[b], and M. R. Ondrias[a], [a]Department of Chemistry, University of New Mexico, Albuquerque, NM 87131 and [b]AT&T Bell Laboratories, Murray Hill, NJ 07974

Hemoglobins display wide interspecies variations in both the thermodynamics and kinetics of ligand binding. Using transient Raman spectroscopy it is possible to examine the dynamic evolution of heme-protein interactions subsequent to ligand photolysis. The demonstrated sensitivity of resonance Raman spectroscopy to heme structure and environment make it an ideal probe of ligand binding dynamics. It is possible to examine how specific vibrational modes change with time and correlate this with solution conditions and protein structural and conformational differences. Those modes which exhibit the greatest change with ligand photolysis are also indicative of possible paths of cooperative energy dissipation within the protein. The changes which occur in the vibrational modes of the heme within 10 nsec of CO photolysis have been determined for a wide variety of mammalian and reptilian hemoglobins. The modes most affected by this process, are, without exception, ν(Fe-His), ν_4, and the vinyl bending modes, $\delta(c_b\text{-}s)$ and $\delta(c_b\text{-}c_\alpha\text{-}c_\beta)$. Furthermore, a direct correlation exists between the shift in porphyrin π^* electron density upon CO photolysis (as indicated by the transient changes in ν_4) and the Hill coefficient of cooperativity. The implications of those results concerning ligand binding cooperativity in hemoglobins will be discussed. This work supported by the NIH (GM33330 and RR08189).
*Present address: BDM Corporation, Albuquerque, NM 87123.

T-PM-F3 TRANSIENT PHOTOLIGATION BEHAVIOR OF NICKEL PROTOPORPHYRIN RECONSTITUTED MYOGLOBIN AND HEMOGLOBIN. E. W. Findsen[a,c], K. Alston[b], J. A. Shelnutt[c], and M. R. Ondrias[a]. [a]Department of Chemistry, University of New Mexico, Albuquerque, NM 87131, [b]Department of Natural Science, Benedict College, Columbia, SC 29024, and [c]Solid State Materials Division, Sandia National Laboratories, Albuquerque, NM 87185.

Time-resolved Raman spectroscopy has been used to study the photoinduced ligation behavior of nickel protoporphyrin (NiPPIX) in reconstituted sperm whale myoglobin (NiMb) and human hemoglobin (NiHb) and contrast it to the behavior observed from NiPPIX in coordinating solvents and detergent micelles. We present results that demonstrate that the local protein environment can exert profound effects upon the photoinduced ligation dynamics of nickel protoporphyrin in reconstituted myoglobin and hemoglobin. NiPPIX in axially ligating solvents will, upon laser excitation, undergo complex excited state photochemistry resulting in net metal d-d transitions between a ligand binding $^3B_{1g}$ state and a dissociative $^1A_{1g}$ state. The dynamics of this process can be monitored by changes in the positions of porphyrin vibrational modes, sensitive to ligation state. We find that the photodynamics of the equilibrium 4-coordinate sites in NiHb are quite similar to those of 4-coordinate Ni-porphyrin models in solution. However, photoexcitation of the 5-coordinate sites in NiHb and NiMb does not yield any observable 4-coordinate excited state species within our 10 nsec timescale. This behavior is in sharp contrast to that observed for model Ni-porphyrins in coordinating solvents and micellar systems. This anomalous behavior can be explained by the effects of the hemepocket environment on the excited state reactivity of the Ni-porphyrin. This work supported by NIH (GM3330).

T-PM-F4 AXIAL COORDINATION IN NICKEL PORPHYRINS AND NICKEL-RECONSTITUTED HEME PROTEINS INVESTIGATED BY RAMAN DIFFERENCE SPECTROSCOPY. J. A. Shelnutt, Sandia National Laboratories, Albuquerque, NM; K. Alston, Benedict College, Columbia, SC; J. M. Rifkind, NIA/NIH Baltimore, MD.

Nickel porphyrins are of interest because of their occurrence in coal and petroleum deposits and because of their key role in biological conversion of CO_2 to methane. Nickel-porphyrin complexes and Ni(II)-reconstituted hemoglobin (^{Ni}Hb) and myoglobin (^{Ni}Mb) have been investigated using resonance Raman difference spectroscopy. The state of axial coordination at the metal is determined using the characteristic frequencies of Raman marker lines arising from the porphyrin moiety. The Raman frequencies distinguish between 4- and 6-coordination of Ni-porphyrins in non-coordinating and coordinating solvents and give evidence of a novel 5-coordinate species in the reconstituted proteins. The existence of only one axial ligand in the proteins is supported by identification of the axial ligand-Ni stretching vibration by isotopic substitution. The frequency of the Ni-ligand mode (236 cm^{-1} in ^{Ni}Hb and ~ 241 cm^{-1} in ^{Ni}Mb) is consistent with histidine as the fifth ligand. T→R structural changes in the protein conformation result in structural changes at the Ni-histidine bond as evidenced by a ~ 5-cm^{-1} increase in frequency of ν(Ni-his) for ^{Ni}Mb (R-like structure) with respect to ^{Ni}Hb (T-structure). Changes in the electronic structure of the porphyrin ring are evidenced by a shift in the oxidation-state marker line ν_4 which for the Fe globins anticorrelates with shifts in ν(Fe-his). Contrary to the Fe case, for the Ni-reconstituted globins ν(Ni-his) and ν_4 correlate. A correlation is also observed for the peroxidases.

This work supported by the U. S. Department of Energy under contract DE-AC04-756DP00789 and the Gas Research Institute Contract 5082-260-0767.

T-PM-F5 RESONANCE RAMAN EVIDENCE FOR A LACK OF EXTENSIVE DEHYDRATION EFFECTS AT THE HEME IN HEMOGLOBIN. E. W. Findsen[a], P. Simons[b], and M. R. Ondrias[a]. [a]Department of Chemistry and [b]Department of Biochemistry, University of New Mexico, Albuquerque, NM 87131

The ligand binding heme proteins Hb and Mb have been shown to exhibit both conformational and kinetic behavior at the heme active site which can be directly related to their ligand binding properties. Liganded Hb and Mb display a number of different heme-CO conformers which are interconvertible and their relative stability has been found to be quite solvent dependent. Pulsinelli and coworkers (Biochemistry (1983) 22, 2914) have demonstrated that removal of the globin hydration sphere profoundly affects the bound C-O frequency in both Hb and Mb. We have used resonance Raman spectroscopy to examine Hb in various stages of dehydration. Its molecular specificity allows for the direct assessment of the local heme structure. Specifically, the Fe-C bond strength and the C-O vibrational frequency of bound CO can be determined. Moreover, by using time-resolved techniques, the response of the proximal hemepocket immediately subsequent to ligand photolysis can be monitored. Our results indicate that the frequency of the C-O stretching motion of bound CO is markedly affected by dehydration and thus corroborate the previous IR studies. However, the Fe-C mode frequency is largely insensitive to these effects. The spectra of photolytic transients of dehydrated Hb are quite similar to solution spectra leading us to conclude that the initial proximal hemepocket geometry following photolysis is not highly dependent upon extent of hydration. Thus, the observed solvent dependence of C-O stretching must derive primarily from distal pocket effects and not from changes in the degree of proximal hemepocket strain or heme geometry. This work supported by the NIH (GM33330).

T-PM-F6 ACTIVE SITE DYNAMICS AND LIGAND BINDING IN MYOGLOBIN. William Bialek[1] and Robert F. Goldstein[2]; [1]Institute for Theoretical Physics, University of California, Santa Barbara CA 93106, and [2]Department of Cell Biology, Stanford University School of Medicine, Stanford CA 94305.

Recent Mossbauer and Raman measurements provide several independent pieces of information about the active site of carbonmonoxymyoglobin (Mb-CO). Within a quasi-harmonic description (1,2) these data are sufficient to determine all the parameters in simple models of active site dynamics if we restrict our attention to motions perpendicular to the heme plane. A remarkable feature of these models is that the dynamics are described by a small number of vibrational modes, including both high frequency localized vibrations and low frequency breathing of the protein; we discuss the evidence for this conclusion and outline some implications. Extending the single-mode approach in (1) we calculate the rate for CO binding to Mb in these multi-mode models. Special attention is payed to the temperature dependence of the apparent activation enthalpies and entropies, to the question of classical vs. quantum dynamics, and to the origin of reaction rate distributions in frozen solution.

(1) William Bialek and Robert F. Goldstein, Biophys. J. (Dec. 1985).
(2) Robert F. Goldstein and William Bialek, Comments Mol. Cell Biophys. (to appear).

Work supported by NSF PHY82-17853, supplemented by NASA, by NIH GM 24032, and by the Bank of America Giannini Fellowship (to R.F.G.).

T-PM-F7 SPECTROSCOPIC EVIDENCE FOR NONLINEAR EFFECTS IN MYOGLOBIN. Erramilli Shyamsunder, Department of Physics, University of Illinois at Urbana-Champaign, 1110 West Green Street, Urbana, IL 61801

We have found evidence for unusual nonlinear effects in the near infrared spectrum of deoxy sperm whale myoglobin. We have measured the temperature dependence of the charge-transfer band in the 760 nm region (band III) and find that, as we cool the sample, (i) the peak position moves to shorter wavelengths; (ii) the full width at half maximum decreases; (iii) the area under the curve increases dramatically. This last feature is reminescent of polarons or solitons. However, we note that this is a charge-transfer band and present the following alternative interpretation: The band arises from electron transfer between two sites coupled by an anharmonic oscillator, and not a polaron or a soliton. We have in addition measured the spectrum of the out-of-equilibrium long-lived photodissociated state Mb*. The peak position of Mb* at low temperature is characteristic of a deoxy peak position at a much higher temperature. The time-dependence of the decay of this apparently "hot band" to deoxy Mb leads us to propose a new model for the longevity of out-of-equilibrium states in proteins: The states are long-lived because they have to go through many structural levels of relaxation. This behavior is an example of a "kinetically frozen state" and is quite different from a dynamically trapped state. This work was supported in part by the U.S. Department of Health, Education and Welfare under Grant No. GM18051 and the National Science Foundation under Grant No. DMB82-09616.

T-PM-F8 EXPRESSION AND SITE-DIRECTED MUTAGENESIS OF HUMAN MYOGLOBIN. R. Varadarajan, David Lambright, and Steven G. Boxer, Dept. of Chemistry, Stanford University, Stanford, CA. 94305.

We have developed a very efficient expression system for the human Mb cDNA in E. coli (1). Using this method, it is possible to produce gram quantities of this protein.

Using site-directed mutagenesis, the Val-E11 codon was changed to Glu, Asp, and Ala. Val-E11 is a highly conserved residue located on the distal side of heme ring I within van der Waals contact. These mutant DNAs were expressed and the mutant proteins have been isolated. Detailed optical and magnetic resonance data will be presented on the unusual properties of these mutant proteins. In addition, heme has been replaced with chlorophyllide (2) in order to investigate the consequences of local charge perturbations on the properties of the chlorophylls.

(1) R. Varadarajan, A. Szabo, S.G. Boxer (1985) PNAS 82, 5681; (2) S.G. Boxer and K.A. Wright (1982) Biochem. 20, 7546.

T-PM-F9 TEMPERATURE DEPENDENCE OF OXIDIZED HEMOGLOBIN OPTICAL SPECTRA: IMPLICATIONS FOR THE (FE, ZN) HEMOGLOBIN HYBRID ELECTRON TRANSFER SYSTEM. S. E. Peterson-Kennedy, J. L. McGourty, B. M. Hoffman. Department of Chemistry, Whitworth College, Spokane, WA 99251; Department of Biochemistry, Molecular Biology and Cell Biology, Northwestern University, Evanston, IL 60201

The full temperature dependence of electron tunnelling across a crystallographically known distance (25Å) was measured by flash photolysis. The rate constants for the (α-Zn, β-met) Hb hybrid are a smooth function of the temperature. In contrast, the rate constants for the opposite (α-met, β-Zn) Hb hybrid show a plateau region from 240K to 270K. Prompted by these results, we measured the optical spectra of five liqated Met-Hb tetramers (H_2O, CN, F, OH, and Imidazole), several fully-metal-substituted and mixed-metal-substituted Hb hybrids as well as individual oxidized α and β chains. These studies reveal that a bismidazole species is formed in the α-met Hb chain as temperature is decreased through 250K, which directly correlates to the plateau in the electron transfer rate constant for the (α-met, β-Zn) Hb hybrid. Thus an increased room temperature rate constant for electron tunnelling within the bisimidazole species compared to that of the aquomet hybrid, is expected and in fact is experimentally supported by an increased electron transfer rate constant for the bisimidazole species formed upon the addition exogenous imidazole.

T-PM-F10 SPECTROPHOTOMETRIC ANALYSIS OF THE KINETICS OF OXYHEMOGLOBIN ASSEMBLY. Melisenda J. McDonald & Susan M. Turci. Hematology Division, Brigham & Women's Hospital, Boston, MA 02115.

Dissociation of the oxygenated non-α-chain tetramer to monomer can be the rate limiting step in the overall reconstitution of oxyhemoglobin A. Here we investigate the kinetics of assembly under conditions of 0.1M Tris, 0.1M NaCl, 1mM Na_2 EDTA, pH 7.4 and 21.5°C and find that over a protein concentration range of 10-100μM in heme the assembly process conforms to first order kinetics. Upon mixing of equivalent concentrations (heme basis) of oxygenated α and β subunits, the absorbance change (583 nm) versus time yielded a rate of constant of 0.069 (±0.0073) sec^{-1} for the dissociation of oxygenated chain tetramers of Hb A. This value agrees well with that of Kawamura and Nakamura (J. Biochem. 94:1851-1856, 1983) who reported a value of 0.064 (±0.0072) sec^{-1} for this rate using circular dichroism technique under identical buffer conditions.

At lower protein concentrations a predominance of β monomers exist and the subunit assembly process of Hb A follows second order kinetics presumably reflecting the α,β monomer combination reaction. An apparent value of 0.18 (±0.005)$\mu M^{-1}sec^{-1}$ has been determined spectrophotometrically in the Soret region for this rate constant. This value is an order of magnitude lower than that obtained by CD studies and suggests that an assembly dependent structural transition which perturbs the heme environment (resulting in spectroscopic change) may occur at a non-diffusion controlled rate in oxyhemoglobin A.

The kinetics of assembly of selective human hemoglobin variants has also been analyzed.

(Supported by NIH Grant HL 36089 and RCDA Award HL01727 to M.J.M.)

T-PM-F11 CARBON MONOXIDE INHIBITION OF INTRACELLULAR MYOGLOBIN FUNCTION IN ISOLATED CARDIAC MYOCYTES. Beatrice A. Wittenberg, Chui Fan Wong and Jonathan B. Wittenberg, Department of Physiology and Biophysics, Albert Einstein College of Medicine, Bronx, N.Y. 10461.

Carbon monoxide blockade of intracellular myoglobin (Mb) of isolated adult rat cardiac myocytes is complete in suspensions gased with 10% CO in air (75 torr pCO, 70 torr pO_2 in suspension medium). Steady state oxygen uptake drops to 70% of control values. At extracellular oxygen pressure (1-5 torr) where intracellular Mb would be partially saturated with oxygen (Wittenberg and Wittenberg, 1985, J. Biol. Chem. 260, 6548-6554), exposure of resting myocytes to carbon monoxide (75 torr) does not affect steady state levels of intracellular ATP and creatine phosphate nor does it affect the rate of lactate accumulation. In the presence of 1 uM CCCP (an uncoupler of mitochondrial respiration), oxygen uptake is reversibly increased 2-3-fold and a new steady-state level of lowered ATP and creatine phosphate is established and maintained during the 1-2 hour incubation. Carbon monoxide blockade of intracellular Mb (75 torr pCO, 1-5 torr pO_2) now brings about a doubling in the rate of lactate accumulation and a further decrease in the level of intracellular creatine phosphate, without further change in the ATP level. These changes in creatine phosphate level and lactate accumulation are partially reversed when the oxygen pressure is increased to more than 10 torr. Myoglobin remains fully saturated with carbon monoxide, so that the effect of increased pO_2 probably is to overcome a deficiency in oxygen transport. We conclude: At respiratory rates and extracellular oxygen pressures near those which may obtain in the working heart, the steady-state rate of oxidative high energy phosphate generation is enhanced in the presence of functional myoglobin. Supported in part by a Grant-in-Aid from the New York Heart Association and in part by NIH-HL-19299 from the United States Public Health Service.

T-PM-F12 HEMOGLOBINS WHICH SUPPLY OXYGEN TO INTRACELLULAR PROKARYOTIC SYMBIONTS. Jonathan B. Wittenberg, Beatrice A. Wittenberg, Department of Physiology and Biophysics, Albert Einstein College of Medicine, Bronx, N.Y. 10461, Quentin H. Gibson, Cornell University, N.Y., Michael Trinick, Anthony I. Fleming and Cyril A. Appleby, CSIRO, Canberra, Australia.

Cytoplasmic hemoglobin assures the supply of oxygen to intracellular nitrogen-fixing symbionts of plants and to intracellular carbon-fixing symbionts housed in the modified gills of certain bivalve molluscs living in environments where hydrogen sulfide and oxygen occur together. We discern a common pattern among the hemoglobins of diverse plants: Very great oxygen affinity is achieved by very rapid combination with oxygen together with a modest rate of dissociation. In contrast, the one clam hemoglobin so far examined achieves high oxygen affinity by very rapid combination with oxygen in the face of rapid dissociation.

Oxygen Reactions of Some Hemoglobins at 20°

	Combination k' ($M^{-1}\ s^{-1} \times 10^{-6}$)	Dissociation k (s^{-1})	Equilibrium K_{diss} (nM)	Equilibrium p1/2 (torr)
SYMBIONT-HARBORING PLANTS				
Soybean (legume/bacterium)	116	5.55	47	0.026
Parasponia (non-legume/bacterium)	165	14.8	89	0.05
Casuarina (dicot/actinomycete)	45	5.5	120	0.07
SYMBIONT-HARBORING CLAM				
Lucina pectinata (mollusc/bacterium)	155	55	360	0.2[a]
HORSE MYOGLOBIN	14	11	770	0.7

a) Read, KRH (1962) Biol. Bull. (Woods Hole) 123, 605-617.

T-PM-G1 BAYESIAN IMAGE PROCESSING OF DATA FROM QUANTITATIVELY CONSTRAINED SOURCE DISTRIBUTIONS. H. Hart and Z. Liang*, Dept. of Physics, City College of New York, New York 10031 and Dept. of Nuclear Medicine, Albert Einstein College of Medicine.

If source distributions can be characterized in terms of probability distributions in the source variables and/or spatially correlated probability patterns $P(\emptyset)$ in the source elements, image processing algorithms can be derived by maximizing $P(\emptyset/N) = P(N/\emptyset)\ P(\emptyset)/P(N)$ where $\emptyset$ is the source vector and N the data vector. The algorithms are very effective in exhibiting patterns which might otherwise be obscured by noise.

T-PM-G2 BAYESIAN IMAGE PROCESSING OF DATA FROM GENERICALLY CONSTRAINED SOURCE DISTRIBUTIONS. Z. Liang* and H. Hart, Dept. of Physics, City College of New York, New York 10031 and Dept. of Nuclear Medicine, Albert Einstein College of Medicine, Bronx, New York 10467.

If source distributions can be characterized in terms of the existence of finite non-vanishing ranges in the values of the source elements, and/or the existence of means and variances as statistical indices, maximum entropy considerations can be used to specify probability distributions $P(\emptyset)$ in the source elements. Image processing algorithms can then be derived by maximizing $P(\emptyset/N) = P(N/\emptyset)\ P(\emptyset)/P(N)$ where $\emptyset$ is the source vector and N the data vector. The results obtained compare favorably with maximum likelihood methods concerned only with $P(N/\emptyset)$.

T-PM-G3 EXPRESSION OF RADIOPHARMACEUTICAL UPTAKE IN VIVO AS A FUNCTION OF BLOOD FLOW OR THE REGIONAL BLOOD VOLUME: THEORY AND DEVIATIONS. Richard P. Spencer. Department of Nuclear Medicine. University of Connecticut Health Center, Farmington, CT 06032.

Intravenously administered radiopharmaceuticals distribute in a manner that depends upon blood flow and local extraction. When a gamma ray emitter is utilized, detection can be made externally. Quantification is made difficult by machine sensitivity and by the dual factors of attenuation and scattering of the gamma rays by tissue. It is possible to avoid these latter complex factors by using ratios; with the scattering and attenuation factors in both numerator and denominator, for the same radionuclide,they cancel. Extraction of the radiolabeled pharmaceutical can be expressed in terms of blood flow, regional blood volume, or mean transit time. The initial assumption is that the quantity of radiolabel extracted (E) is given by the measured activity (M) times the scattering and attenuation factor (A) that includes machine sensitivity. Thus: $E = M.A$. Consider the volume of blood in the region (as measured by a labeled blood element). The volume (V) is given by the recorded counts (C) times the attenuation-scatter factor. We can write: $V = C.A$. The ratio of the 2 expressions is given by: $E/V = M/C$. For certain systems with a single inlet, the mean transit time (T) is the ratio of local volume (V) divided by flow (F). Therefore: $T = V/F$. This expression can be used with the others, to obtain further measurable ratios. For example, an E/F expression appears to give a reasonable description of splenic radiocolloid extraction in vivo. Deviations from the simple predictions may represent dual inflow (liver) or intervening compartments. (Supported by USPHS CA 17802 from the National Cancer Institute).

T-PM-G4 THE USE OF CONTINUUM DIFFUSION THEORY TO DESCRIBE DIFFUSION ACROSS MEMBRANES CONTAINING DISCRETE DIFFUSION CHANNELS. T. L. Schwartz, Dept. of Mol. & Cell Biol., The Univ. of CT., Storrs, CT 06268

An analysis is presented that shows that the failures of several popular expressions long used to examine the properties of transmembrane ionic diffusion are actually due to the effect of the insertion of untested physical assumptions in the course of their derivation from the parent, and quite general thermodynamic theory. Thus: the Goldman-Hodgkin-Katz equations sometimes become inadequate to their task because of the assumptions of constant intramembrane electrical field and of permeabilities that are postulated to be unaffected by either the extramembrane concentrations of the permeant species or the membrane potential; the "independence principle" collapses for the same reasons; the Ussing-Teorell unidirectional flux ratio suffers from the assumption of no interflux coupling between the tracer and tracee. These theoretical inadequacies thus have nothing to do with a purported inapplicability to such membranes of the thermodynamic theories which, for more than a century, have demonstrated their applicability to passive diffusion in media going from liquids to solids to gases and have included such things as clays, glasses, aqueous media and artifical membranes of various sorts. Indeed, the general, parent, thermodynamic theory is shown to predict permeability to be a function of intramembrane electrical field, and, therefore of both the membrane potential and the extramembrane concentration of the permeant specie. This immediately dispels the mystery that has surrounded the observed phenomenon of saturation. With the caution that it must be used in a manner that is physically compatible with actual membrane conditions, an important research tool: thermodynamic continuum diffusion theory is thus shown still to be useful in our studies.

T-PM-G5 MODELS OF THE DISTRIBUTIONS OF SCORES FROM PROTEIN SEQUENCE DATABASE SEARCHES. David G. George and Winona C. Barker, National Biomedical Research Foundation, Washington, DC 20007

Because of the large amount of sequence information now available and the sophistication of the computer methods being used to search large sequence databases, many interesting relationships between proteins have recently been discovered. As a result, the use of database searching techniques has become increasingly popular and these methods are beginning to be employed on a regular basis. Methods for correctly assessing the statistical significance of the similarities found in database searches are presently lacking, however. It is generally assumed that scores from comparisons of a large population of unrelated real sequences will be randomly distributed and can thus be modeled by a 'normal' (Gaussian) distribution. Unfortunately, this has not been found to be the case; thus, the commonly used measures of significance are at best dubious. We have begun to investigate this problem by modeling the results of our SEARCH program. This program compares a test segment of a specified length with all possible segments in the database. For each comparison a score is computed using a similarity scoring matrix. We have previously reported that the distributions of comparison scores generated from randomly constructed sequences of random composition are not 'normal.' In principle, as the segment length increases, the model distribution should approach a 'normal' distribution; however, with the segment lengths generally used, this is not the case. The model distribution also does not conform to the distributions found in real database searches. We have continued these studies and will report the results of modeling studies aimed at understanding the additional factors contributing to real distributions. This work is supported by NIH grant RR01821.

T-PM-G6 NATURAL MODELS OF INTELLIGENCE, Charles Walter and Michael Parks, Houston, Tx.

Biological evidence is used to suggest a model for intelligent behavior. Since physiological studies of brain function suggest that symmetry and synergism are important to design, the model incorporates two different sites with different information processing modes interacting cooperatively. It is proposed that the different roles assigned to each hemisphere is not the important factor per se, but that co-operative interactions between the two hemispheres may be an important character of intelligence. This synergistic coupling between the dynamical mode and the linguistic mode results in introreflection. An important feature of introreflection is that the situations before and afterwards contain different information. Unlike usual models of artificial intelligence, models incorporating coupled dualistic processing are capable of generating information and goals. Such teleogenic processes are important in reasoning and other intelligent behavior. Specific models for the dynamical and linguistic modes are suggested. The logic for representing open-textured concepts is formulated for parallel processing.

T-PM-G7 A MATHEMATICAL MODEL OF AIDS-POPULATION-DYNAMICS AND THE BREAKDOWN OF COMMENSALISM. Hans J. Bremermann, Department of Biophysics and Medical Physics, University of California, Berkeley, CA 94720.

A persistent endoparasite supposedly evolves towards commensalism: If it kills its host prematurely it destroys its means of sustenance and replication and reduces its fitness. It is shown by means of a mathematical model that selection towards commensalism breaks down when several different strains (or species) simultaneously infect the same host. The AIDS viruses (HTLV-III, LAV, ARV) have been reported as being unusually heterogeneous, and clones with different restriction maps have been isolated from the same patient. The model indicates that a small number of simultaneous infections are compatible with commensalism but that a breakdown occurs when a threshold is exceeded. The prevalence of multiple infections depends critically upon contact rates with different partners. The model predicts a possible virulizing effect on opportunistic infections. A full dynamic model of host-parasite dynamics for multiple infections is intractible because of combinatorial complexity. Instead a game-theoreticcal argument is combined with a model tnat estimates the prevalence of different degrees of multiplicity of infection as a function of partner contact rate.

T-PM-G8 A REPRESENTATION OF THE GENERATOR REGION OF THE HODGKIN-HUXLEY EQUATIONS BASED ON PHASE SPACE METHODS. Alvin Siger (Intr. by D. Junge), Foundation for Cardiovascular Research, 85 N. El Molino Ave., Pasadena, CA. 91101.

A small modification of the FitzHugh transformation of the Hodgkin-Huxley variables V, m, n, h (Biophys. J. 1:445-466, 1961) produces a set of variables convenient for describing the physiological properties of excitable membranes in the generator region. The new variables are e (excitation) and r (refractoriness), similar respectively to FitzHugh's u and w; and f (fast damping) and s (slow damping), orthogonal respectively to e and r. The generator region being rather flat in the f direction, a convenient 3-d representation is obtained. The rhythmicity of the system depends on the relative positions of the stable and unstable singularities, determined by a controlling variable (e.g., steady current or a Frankenhaeuser-Hodgkin calcium shift). The semi-quantitative performance of the system can be obtained visually by applying the principles of phase-space analysis. For non-rhythmic modes, the classic properties, from the existence of a threshold to break re-excitation, as well as the existence of multiple gaps in the stimulus-delay relationship are clearly displayed. For rhythmic modes, the cyclic character and its perturbations, such as phase resetting and abolition (Best, Biophys. J. 27:87-104, 1979), as well as the existence of multicyclic delays are displayed. All of the above can be seen in projections onto the e-r plane. For phenomena where the projected trajectories necessarily intersect, such as the occurrence of finite spike trains, the 3-d e-r-s representation provides a clear display.

T-PM-G9 A NOVEL PROPOSAL FOR THE REAL-TIME VISUALIZATION OF NERVE FUNCTION. E. A. Kimble, ITT Educational Services, Fort Wayne, IN, 46825

Real-time measurement of nerve function using x-rays, RF, or ultrasound techniques is complicated by high background and symmetry related noise. A method is proposed for overcoming the symmetry related problems while reducing background noise. In this method a magnetically orientable membrane dye, with a distinct electic dipole, would be introduced into the tissue. Through application of an external magnetic field a competition would be established between the electric field of the nerve membrane and the external magnetic field. Directional scattering of x-rays, RF, et cetera, could then be used to detect changes in dye orientation which should in turn reflect real-time changes of membrane electric fields. An experimental system for testing this concept will be presented and candidates for possible dye molecules will be discussed. This technique would overcome a variety of symmetry related problems by using the external magnetic field to induce a detectable change in molecular symmetry as a function of membrane voltage. Research and medical uses for such a method could be unlimited.

T-PM-G10 Computer Simulation of Steady State and Transient Kinetics of Sarcoplasmic Reticulum Ca^{++} ATPase, Mark Kurzmack and Giuseppe Inesi, University of Maryland, School of Medicine, Department of Biological Chemistry, 660 West Redwood Street, Baltimore, Maryland 21201.

The Sarcoplasmic Reticulum Ca^{++} ATPase is a well characterized transport enzyme. The ability to measure the acid-stable phosphoenzyme intermediate, sequestration of calcium ion within the membrane, and formation of P_i derived from substrate utilization has allowed the experimental determination of many of the rate and equilibrium constants associated with individual partial reactions.

An interactive computer program has been developed to allow the simulation of both steady state and transient pre-steady state kinetics of all intermediate enzyme species levels and their change with time. The program allows the user to enter all foward and reverse rate constants, and the following substrate concentrations: $[Ca_{out}]$, $[Ca_{in}]$, [ATP], [ADP], and $[P_i]$. Steady state levels of all enzyme intermediates are then calculated directly for the given substrate conditions. Transient kinetic simulations are calculated using an iterative Runge-Kutta algorithm with suitable corrections for round-off error and a limited automatic step size adjustment. Two types of transient simulation are provided: simulation of phosphoenzyme formation upon addition of substrate; and reequilibration of the enzyme from the steady-state levels when the substrate concentrations are changed. This allows simulation of both the usual E ~ P formation type of experiments, and of concentration jump and E ~ P decay procedures. This work was supported by NIH grant HL 27867 and The Muscular Dystrophy Association of America.

T-PM-G11 EVIDENCE THAT MICROSCOPIC FLUCTUATIONS AFFECT RATES OF EXCHANGE OF K & NA IN LYMPHOCYTES. W.Negendank, Dept. of Medicine, Wayne State Univ.,Detroit,MI 48201.

A cooperative interaction between ion-adsorbing sites in lymphocytes is manifested by sigmoidal isotherms of K and Na described by a 1-d Ising model, a critical temperature transition of K/Na exchange, and kinetics of net K/Na exchange that are described by a time-dependent Ising model. The self-exchange rates of adsorbed ions have a complex dependence on chemical potential (BJ 46:331,1984). Human blood lymphocytes were preequilibrated 24-48 hr at 37°C at 0-30 mM K_{ex} ($K_{ex}+Na_{ex}$ = 150 mM), and preloaded with ^{42}K or ^{22}Na. Self-exchange of K or Na was then determined by isotopic efflux. For K, a minimum rate occurs at 5 mM K_{ex}, and sharp peaks in the rates of self-exchange of both K and Na occur at 0.4 mM K_{ex}, the critical transition point of the cooperative adsorption isotherms of K and Na. Since at 37° net K/Na exchange is faster ($t_{½}$ 40 min) than self-exchanges of K or Na ($t_{½}$ 100-200 min), it is postulated that around the critical transition at 0.4 mM K_{ex} there occurs an increased rate of fluctuations between K- and Na-adsorbing states within microscopic islands of ion-adsorbing biopolymers. These fluctuations may be intrinsic or due to a high susceptibility to slight changes of the chemical potentials of K or Na in cell water. Since observed isotopic self-exchange is a weighted average of exchange with all elements in the ensemble, increased fluctuations result in an increase in the apparent rate of self-exchange observed macroscopically. A number of puzzling observations are explained by this simple concept.

T-PM-G12 THE VISCOSITY OF A SUSPENSION OF SPHERES. Max A. Lauffer, Dept. of Biological Sciences, University of Pittsburgh, Pittsburgh, PA 15260.

The viscosity of a pure liquid, η_o, is W, the work per sec. per c.c. required to maintain unit velocity gradient. When solid spheres are added, there are two contributions to W for the suspension. W_1 results from the fact that the gradient in the liquid must be greater than unity for the average for the suspension to be unity. $W_1=\eta_o/(1-\Phi)$, where Φ is the volume fraction of the spheres. W_2 resulting from the necessity of liquid to flow around the spheres can be evaluated from Stokes's law. If solvent viscosity is used in evaluating this contribution, $W_2=1.5\Phi\eta_o/(1-\Phi)^2$. The viscosity of the suspension, $\eta=W_1+W_2=\eta_o(1+0.5\Phi)/(1-\Phi)^2$, or $\eta/\eta_o=1+2.5\Phi+4\Phi^2+5.5\Phi^3$ etc., the Einstein equation. However, it is proposed that the correct viscosity to use to evaluate W_2 is the suspension viscosity, η, multiplied by $(1-\Phi)$. This is the work per sec. per c.c. when the liquid in the suspension has unit velocity gradient. Thus, W_2 becomes $1.5\Phi\eta(1-\Phi)/(1-\Phi)^2$. Now, $W_1+W_2=\eta=\eta_o/(1-2.5\Phi)$, or $\eta/\eta_o=1+2.5\Phi+6.25\Phi^2+15.625\Phi^3$ etc. Also, $\eta_o/\eta=1-2.5\Phi$. The data of Vand fit this theoretical equation beautifully for values of Φ up to 0.25.

(Work supported by U.S. Public Health Service Grant GM 21619)

T-PM-G13 COMPLETE POLARIZATION CALCULATIONS OF LIGHT SCATTERING FROM RANDOMLY ORIENTED SUSPENSIONS OF LARGE ASSEMBLAGES

W.M. McClain and W.A. Ghoul, Wayne State University, Detroit MI 48202, Intr. by D. L. Njus

We present calculational results for all ten of the angle-dependent observables that characterize completely the elastic scattering of light from randomly oriented suspension of dielectric assemblages of a size comparable to, or larger than, the wavelength of light. Our algorithm captures all of the physical effects included in the Mie solution for scattering by large homogeneous spheres, but it is not limited to spherical shapes or homogeneous materials. The model is a collection of anistropic point dipoles, imitating the size, shape, and local polarizability of a biological assemblage.

We call particular attention to the parameter P_{34}, which links oblique polarization modulation of incident radiation to circular modulation of the scattered radiation. This parameter is exactly zero in orientation averaged theories that ignore the retardation (or time delay due to the finite speed of light) of the electromagnetic interaction between subunits. It therefore reveals (against zero background) the "multiple echo" effects that occur as the incident wave bounces around inside the model before exiting. These effects are exquisitely sensitive to the tertiary structure of the scattering body. With suitable enhanced scattering from preresonant tags, parameter P_{34} holds promise as the basis of a new macrostructural method applicable to aqueous suspensions of assemblages of a size near but below theoptical resolving limit.

T-PM-G14 ION DISTRIBUTIONS IN INTERFACIAL REGIONS. V.S.Vaidhyanathan, Biophysics department, SUNYAB, Buffalo, N.Y. 14214. The equilibrium distribution of concentration, charge density $|-Y(x)|$ and electric potential, $\phi(x)$, in the vicinity of a negatively charged surface, as given by classic limiting expression for chemical potential is presented in fig.2. Similar profiles, when ion-ion interaction energy terms are included are presented in fig.1, for 1-1 ion system. The nonvalidity of fig.2 and Debye approximation will be presented. The value of dielectric coefficient at the interface is computed to equal 2.44, when $C_+ = 5 \times 10^{-5}$ m/cm^3 and $\phi(o) = -100$ mV.

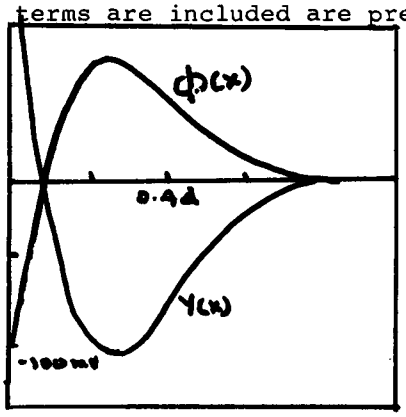

Figure 1

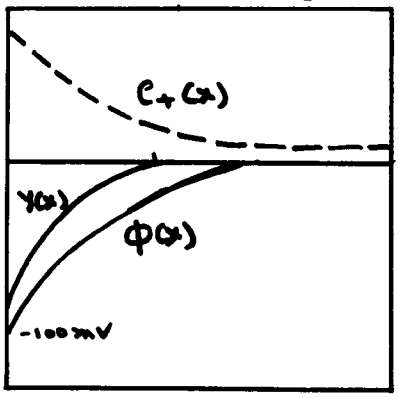

Figure 2.→

$\phi_{max} = 50mV$

$Y_{min} = -1.14 \times 10^{10}$ em/cm^3

T-PM-G15 CELLULAR RESPONSE TO A ROTATING FIELD

By Charles Polk, Department of Electrical Engineering, U. of Rhode Island, Kingston, RI 02881; and Herbert A. Pohl, National Magnet Laboratory, Bldg. NW-14, Massachusetts Institute of Technology, Cambridge, MA 02139.

We consider the problem of a living or dead cell rotating at an angular velocity Ω in a fluid medium when it is subjected to an electric field rotating at an angular velocity ω. It is observed in many experiments (1-4) that $\Omega << \omega$ and also that the sign of Ω can be opposite to that of ω. In fact for the same cell, as the frequency of ω is changed monotonically it is observed that Ω may go from positive to negative and back again. Moreover, the frequency response of the sign and magnitude of the cellular spin rate Ω differs for living and dead cells, and for differing cell types and physiological states.

All of these experimental results can be explained quantitatively by the mathematical development based upon the application of Maxwell's equations for conductive media, assuming a spherical cell.

1. M. Mischel, A. Voss & H. A. Pohl, J. Biol. Phys. 10 (1983) 227
2. H. A. Pohl, Int. J. Quantum Chem. 10 (1983) 161
3. M. Mischel & H. A. Pohl, J. Biol. Phys. 11 (1983) 98
4. H. Rivera & H. A. Pohl, "Cellular Spin Resonance", Chap. 15, in MODERN BIOELECTROCHEMISTRY, ed. by F. Gutmann & H. Keyzer, Plenum Press, 1985

T-Pos1 **MYOFIBRILLAR BOUND CREATINE KINASE ENHANCES THE KINETICS OF MgATP HYDROLYSIS BY THE MYOFIBRILLAR ATPase.** Stephen M. Krause and William E. Jacobus. The Johns Hopkins University School of Medicine, Baltimore, MD 21205.

In the heart, where the total ATP pool can turnover in as little as 3 seconds, the regulation of contraction and relaxation requires a tight control of both [ATP] and [ADP]. Phosphocreatine (PCr) is viewed as important for maintaining the intracellular ATP pool by buffering the MgADP to generate MgATP. The myosin-bound CK isozyme has been suggested to be very important in this regulation. The ability of this bound CK isozyme to provide MgATP to the myosin ATPase via transphosphorylation of PCr and MgADP was evaluated kinetically in isolated rabbit myofibrils. The inherent CK activity in the isolated myofibrils was 618 $\pm$ 31 mIU / mg myofibrillar protein. Experimental conditions were designed to closely mimic the normal intracellular environment. The free [Ca^{2+}] was maintained at pCa 4.5 while [MgATP] was varied from a pMgATP of 2.5 to 5.5 in the presence or absence of 12.2 mM PCr at pH 7.1 and 37° C. The steady-state maximal myofibrillar ATPase activity, measured as either Pi or creatine release, in the presence and absence of PCr was not significantly different, 124.8 $\pm$ 6.2 mIU / mg and 116.6 $\pm$ 5.7 mIU / mg, respectively. However, important differences were noted in the affinity of myosin for ATP. The extrapolated apparent Km for MgATP was 119 uM with MgATP alone, but decreased by an order of magnitude to 9.6 uM in the presence of both PCr and MgATP. These results demonstrate that the local regeneration of MgATP, mediated via the myofibrillar-bound CK, optimizes the nucleotide kinetics of the myosin ATPase. The data support the notion that PCr can play an important role in maintaining the local [ATP] required for the regulation of contraction.

T-Pos2 ESSENTIAL LIGHT CHAIN EXCHANGE IN SCALLOP MYOFIBRILS. Gaku Ashiba & Andrew G. Szent-Györgyi, Department of Biology, Brandeis University, Waltham MA 02254.

The essential light chains (SH-LCs) of scallop myosin are exchangeable in the absence of regulatory light chains (R-LCs)[1]. Since R-LCs can be readily removed from myofibrils, the method for SH-LC exchange could be extended to them. Aequipecten myofibrils were fully desensitized in advance by a 5 min. EDTA treatment at 37 °C. The myofibrils were then incubated at 37 °C for 10 min. with a 4-fold stoichiometric amount of either SH- or ϵ-amino modified SH-LCs in the presence of Mg^{2+} in low salt. More than 70% of SH-LCs were exchanged and the unbound SH-LCs were effectively removed by rinsing with the same medium at 0 °C. The myofibrils were then resensitized by an overnight incubation at 0 °C with a 2-fold stoichiometric amount of Mercenaria R-LCs. SH-LCs modified with a photosensitive cross-linking reagent (N-hydroxysuccinimidyl-4-azidobenzoate) were introduced by this method and formed large cross-linked products upon photolysis. These products contained myosin heavy chains and did not migrate into the usual SDS-polyacrylamide gel systems. The identification of the cross-linked complexes is in progress. (Supported by NIH AM-15903 and MDA grants).

1. Ashiba, G. & Szent-Györgyi, A. G. (1985) Biochemistry 24, in press.

T-Pos3 CHARACTERIZATION OF THE CALCIUM-INSENSITVE COMPONENT OF SCALLOP HMM. H. Shpetner and A. G. Szent-Gyorgyi, Graduate Program in Biophysics and Department of Biology, Brandeis University, Waltham, Massachusetts 02254.

The actin-activated Mg^{++}ATPase of scallop HMM is 75-80% calcium sensitive, although the parent myosin exhibits 90-95% sensitivity (% sensitivity = $(1-(v_{EGTA}/v_{Ca^{++}}))100$). Measuring single ATP turnovers, Wells and Bagshaw (FEBS Letters 164: 260, 1984) have shown that scallop HMM preparations are kinetically heterogeneous. 75% of the total actin-activated Mg^{++}ATPase activity is 99% sensitive; the remainder is completely insensitive, comprising a calcium-insensitive component (CIC). We have found that about two-thirds of the CIC is due to calcium-insensitive S1, and the remaining third to HMM. Native gels of HMM contain a species comigrating with scallop S1(+LC), comprising 6-7% of the total protein. Two-dimensional gels of this species indicate that it is composed of 95-100 and 75-80 kd peptides, as well as myosin light chains. The larger peptide comigrates with the heavy chain of scallop S1, and the smaller with an N-terminal product of S1 tryptic digests. This species was therefore identified as a tryptic variant of S1. HMM, chromatographed on Sephadex G-150, elutes in both fractions of higher and lower sensitivity than unfractionated HMM; native gel analysis of these fractions demonstrated a linear relation between the amounts of the CIC and tryptic S1 they contained. Extrapolation to 0 and 100% S1 indicated that the ATPase activity of the S1 component is comparable to that of S1(+LC), and that the HMM component is 90-95% sensitive, the same as the parent myosin. When desensitized myosin is digested with trypsin, S1 comprises 60-70% of the low-salt soluble products; thus, R-LCs protect the S1-S2 junction from proteolysis. Supported by NIH AM-15903 and MDA grants.

T-Pos4 INDEPENDENT REGULATION OF THE Mg^{++}ATPase SITES OF SCALLOP HMM. H. Shpetner and A. G. Szent-Gyorgyi, Graduate Program in Biophysics and Department of Biology, Brandeis University, Waltham, Massachusetts 02254.

Chantler and Szent-Gyorgyi (J. Mol. Biol. 138: 473, 1981) recombined desensitized scallop myofibrils with substoichiometric amounts of regulatory light chains (R-LCs) and found that myosin exhibits at least two forms of intramolecular cooperativity: binding of one R-LC to myosin substantially reduces the availability of the unfilled site to R-LCs, i.e., the binding is negatively cooperative, and inhibition of the actin-activated Mg^{++}ATPase does not occur unless both sites are filled. To determine whether these forms of cooperativity are also manifested by a soluble species, scallop HMM was desensitized by chromatography on Sephadex G-150, in 10mM EDTA, and recombined with R-LCs at various R-LC: HMM ratios, in the presence of actin and 1mM Mg^{++} at 4°. Unbound R-LCs were removed by centrifugation. Desensitized HMM readily rebound one mole of R-LC per mole HMM. Further uptake required large excesses of R-LC, stoichiometric rebinding occurring in the presence of 10-20 moles R-LC per mole HMM. Thus, like desensitized myofibrils, desensitized HMM binds R-LCs in a negatively cooperative manner, in 1mM Mg^{++}. However, the actin-activated Mg^{++}ATPase decreased linearly as function of the amount of R-LC bound, full sensitivity being restored at R-LC ratios of 1.7:1 or greater. These findings imply that the two actin-activated Mg^{++}ATPase sites of scallop HMM are independently inhibited by R-LCs, although their activation by calcium occurs cooperatively (Chantler et. al., Biochem. 20: 210, 1981). Supported by NIH AM-15903 and MDA grants.

T-Pos5 AGENTS WHICH AFFECT THE S_1-S_2 AND S_2-BACKBONE HINGES OF MYOSIN IN ISOLATED THICK FILAMENTS FROM LIMULUS STRIATED MUSCLE. S. F. Fan, M. M. Dewey and B. Chu. Department of Anatomical Sciences and Department of Chemistry, SUNY at Stony Brook, NY 11794.

Contemporary views of the mechanism of muscular contraction hold that during activation, the S_2 segment of the crossbridge swings out toward the thin filament, and the S_1 segment reacts with the thin filament and moves cyclically. Using a quasi-elastic light scattering technique, we have described an increase in $\bar{\Gamma}$ values from a suspension of thick filaments isolated from the myosin-regulated, striated muscle of Limulus following the addition of Ca^{2+} or depletion of ATP in the suspending medium where $\bar{\Gamma}$ is the value of the average linewidth of the photoelectron count autocorrelation function of light scattered. From the differences in the effect of heat denaturation (42°C, 10 min), phenylmethylsulfonyl fluoride (PMSF) and trifluoperazine (TFP) on the increase of the $\bar{\Gamma}$ values and of electron micrographs of negatively stained filaments, we conclude that Ca^{2+} in the presence of ATP elicits the active motion of the S_1 segment around the S_1-S_2 hinge (motion I) and depletion of ATP results in movement of the whole crossbridge around the S_2-backbone hinge as a result of thermal agitation (motion II) (J.M.B. 166:329 '83; Biophys. J. 47:809, 468a '85; BBA, 827: 101 '85). We further found that D_2O not only suppresses motion I (BBA, 827:101 '85) but also suppresses motion II. Thiourea has no effect on motion I but suppresses motion II. 2,3-butanedione monoxide (BDM), which has been suggested to depress crossbridge cycling (Mulieri & Alpert, Biophys. J. 45:47a '84; Warren et al., ibid 47:195a '85), has no effect on either motion I or II. In summary, PMSF and heat treatment only suppress the active motion of S_1 segment, thiourea only suppresses the thermal motion of the whole crossbridge, D_2O and TFP suppress both, and BDM has no effect on either.

T-Pos6 THE ISOLATION AND CHARACTERIZATION OF TROPONIN AND TROPOMYOSIN FROM BALANUS NUBILUS MUSCLE. James D. Potter, Priscilla F. Strang and Christopher C. Ashley*, Dept. of Pharmacology, Univ. of Miami School of Medicine, Miami, FL and *Univ. Lab. of Phys., Oxford, UK

It has been known for many years that elevation of free sarcoplasmic Ca^{2+} is required for muscle activation and that there are receptors for Ca^{2+} on the thin filament which are responsible for initiating the events which lead to muscle contraction. Much of our knowledge of the first event has come from studying free Ca^{2+} changes in barnacle fibers and relating these temporally to force development. The barnacle is ideally suited for this type of study since it has large single muscle fibers which can be injected with Ca^{2+} sensitive indicators and readily voltage clamped. Unfortunately, very little is known about the proteins involved in Ca^{2+} regulation in the barnacle. Regulation is thought to be thin filament linked (Lehman et al. (1973) Cold Spring Harbor Symp. 123, 604) and not to involve thick filament mechanisms (W.G.L. Kerrick, personal communication). To learn more about this, troponin (Tn) and tropomyosin (Tm) from barnacle have been isolated. Using an ether powder from barnacle muscle (Potter, J.D. (1982) Meth. Enz. 85, 241) a troponin like fraction was isolated which contained essentially three major components (TnT, $M_r \cong$ 50,000; TnI, $M_r \cong$ 35,000; and TnC, $M_r \cong$ 15,000). A tropomyosin fraction contained essentially one band of $M_r \cong$ 39,000. The Tm fraction alone slightly inhibited rabbit acto-HMM ATPase and was not affected by Ca^{2+}. The Tn fraction alone had no effect ($\pm$ Ca^{2+}) on the ATPase activity and when both fractions (Tn:Tm 1:1) were used the acto-HMM ATPase became Ca^{2+} sensitive. Thus both of these fractions behave as Tn and Tm isolated from other sources. Work is in progress to further characterize the Tn subunits. Supported by a grant from the MDA.

T-Pos7 Ca^{2+} TRANSIENTS DETECTED BY TnC_{IAANS} FLUORESCENCE IN SINGLE BALANUS NUBILUS MUSCLE FIBERS
†C.C. Ashley,†P.J. Griffiths,*P.F. Strang and*J.D. Potter University Laboratory of †Physiology, Oxford, U.K.,*Department of Pharmacology, Univ. Miami School of Medicine, Miami, FL33101

The calcium-binding subunit of troponin(TnC) can be labelled with 2-(4'-iodo-acetamido-anilino) naphthalene-6-sulphonic acid(IAANS)to produce the fluorescent species TnC_{IAANS} in which there is a decrease in fluorescence with calcium binding to the two calcium/magnesium sites. The calcium affinity of these sites is not substantially altered when this sub-unit is incorporated into the ternary complex and reconstituted onto the thin filament (Zot et al., Chem. Scrip. 21, 133, 1983). Thus free TnC_{IAANS} should give an indication of the time course of calcium occupancy of the calcium/magnesium sites on the thin filament. TnC_{IAANS} was injected into single barnacle muscle fibres (final internal conc. 50-100μM) and fiber fluorescence under voltage-clamp control was measured. The injection of TnC_{IAANS} causes the appearance of a fluorescence peak at 450nm upon excitation at 325nm. Fiber auto-fluorescence is maximal and the TnC signal minimal at 405nm, so this wavelength was chosen to monitor non-specific changes in fiber fluorescence. After scaled subtraction a net signal remained 450nm upon electrical excitation whose amplitude increased with intensity of stimulation. No detectable change was observed for single pulses of 200msec duration, unlike experiments with the calcium-specific site label, TnC_{DANZ}. (Griffiths et al., FEBS Letts ,176,144 ,1984).However 10msec pulses (10Hz) gave a fall in fluorescence. (halftime 1.2sec,n=19) compared to that for force development (2.1sec,n=19). Recovery from the fluorescence decrease upon cessation of stimulation had a halftime of 1.9sec(n=15) compared to the relaxation of force (halftime 1.1sec, n=18). These results are consistent with a slow loading and unloading of the high affinity calcium/magnesium sites during a tetanus . NIH HL226193A support.

T-Pos8 **CHARACTERIZATION OF CARDIAC MYOFIBRILS FROZEN IN THE "ON" STATE. Saleh El-Saleh, Mark Rocklin and R. John Solaro. Department of Physiology & Biophysics, University of Cincinnati, College of Medicine, Cincinnati, OH 45267-0576**

Earlier preliminary studies (Solaro and Rocklin, Biophys. J. (1983) 41, 265a) demonstrated that dog cardiac muscle myofibrils could be "frozen" in the "on" and "off" states following cross-linking with glutaraldehyde (GLA) of myofibrils in "rigor" and "relaxed preparations, respectively. GLA had been previously used to "freeze" reconstituted thin filaments in their "on" and "off" conformations (Mikawa, 1979). In this study we were able to freeze pig cardiac and rabbit skeletal muscle myofibrils in their respective "on" and "off" states over the physiological free (Ca^{2+}) range. ATPase levels of myofibrils frozen in the "on" state are equivalent to those produced under "rigor" conditions from covalent cross-linking by GLA of actin and myosin in reconstituted actin·myosin complex and to the ATPase of cross-linked desensitized myofibrils (free of Tm·Tn). Such ATPase levels were in turn equivalent to maximal ATPase (V_{max}) of actin-activated myosin·Mg^{2+}-ATPase at infinite actin concentration as deduced from double reciprocal plots of 1/ATPase vs 1/(actin). These results suggest that covalent actin-myosin interaction detected in frozen myofibrils in the "on" state could produce the conformation of reconstituted thin-filament preparations frozen in the "on" state. This is in line with other data from this study which shows that freezing of cardiac myofibrils in the "on" state increase the Ca^{2+}-affinity of the myofilaments in these states thus turning them on. (Supported by NIH #HL 07382-09.)

T-Pos9 **LACK OF EFFECTS OF ACIDIC pH ON CALCIUM ACTIVATION OF MYOFILAMENTS OF PERINATAL DOG HEARTS: EVIDENCE FOR DEVELOPMENTAL DIFFERENCES IN THIN FILAMENT REGULATION. R. John Solaro, Pankaj Kumar*, Edward M. Blanchard* and Anne F. Martin, University of Cincinnati, College of Medicine, Cincinnati, OH 45267**

We compared effects of acidic pH on Ca-activation of the ATPase activity of myofibrils prepared from adult and perinatal hearts. Our results show that Ca^{2+}-activation of myofilament preparations of dog heart in the perinatal period is unaffected by a reduction in pH from 7.0 to 6.5, which, in adult heart myofilaments, induces a 0.4 pCa unit rightward shift in the relation between pCa and myofibrillar ATPase activity. Acidic pH also had no effect on Ca^{2+} binding to myofibrillar troponin C (TnC) of perinatal hearts. The stoichiometry of TnC bound Ca^{2+} at full myofilament activation (about 3 mol Ca/mol TnC) was the same for adult and perinatal heart myofibrils, as was their myofibrillar TnC content. Moreover, there were no differences in isoelectric pH of TnC from adult and perinatal hearts. In adult and perinatal dog heart preparations, myosin heavy chain isoenzymes appeared the same as measured using native pyrophosphate gel electrophoresis. No evidence for thick filament related Ca^{2+}-regulation in the perinatal heart myofilaments was obtained, when tested using studies in which native thin filaments were displaced with a tenfold molar excess of pure actin. In preparations in which native thick filaments were displaced with a tenfold molar excess of pure skeletal muscle myosin, the effects of acidic pH on Ca^{2+}-activation were the same as in native adult and perinatal preparations. Our major conclusion from these results is that the perinatal heart myofilaments are likely to possess variations in thin filament activity and structure. Although not conclusive, preliminary investigations of this question by polyacrylamide gel electrophoresis of the adult and perinatal myofilaments in the presence of sodium dodecyl sulfate (SDS), or urea at basic pH and acidic pH provide evidence that there may be variants of TnI in the thin filaments of the perinatal hearts.

T-Pos10 PROTEIN SEPARATION OF CYTOSOLIC AND CYTOMATRIX FRACTIONS FROM SKINNED SKELETAL MUSCLE FIBERS. David Maughan, Cynthia Lord, and Gary Guilian*, Dept. of Physiology/Biophysics, Univ. of Vermont, Burlington, VT 05405 and *Dept. of Physiology, Univ. of Wisconsin, Madison, WI 53706.

We developed a microvolumetric method to determine the distribution of individual proteins between muscle cytosol and cytomatrix. To sample cytosol, we mechanically skin a frog semitendinosus fiber under oil and place several dry Sephadex beads (G-200) onto the skinned fiber surface. The beads hydrate, each withdrawing 0.2-0.9 nl of cytosolic fluid. In these experiments, the beads containing the cytosolic proteins were placed in denaturing SDS-sample buffer to yield a combined total sample volume of 1-2 nl and analyzed electrophoretically. The fiber was bisected, one half prewashed throughly with a relaxing solution (ionic strength 0.17 M; pH 7) to remove cytosolic proteins, and the residue (cytomatrix proteins) dissolved in sample buffer. The other half was solubilized directly in sample buffer (total proteins). SDS-PAGE (slab gels) with an ultrasenstive silver stain showed protein patterns with marked differences between the three samples. Cytosol contained 14 distinct bands (6-92 kD), 7 of which were also seen to various extents in cytomatrix. Cytomatrix contained many other bands as well (14-200 kD). Whole fiber samples (cytosol + cytomatrix) contained all bands seen in both fractions. Parvalbumin (11 kD, cytosol only), actin and myosin (42 and 200 kD respectively, cytomatrix only) were tentatively identified using purified standards. Parvalbumin standards stained linearly over the range 0.5-25 ng; cytosolic concentrations were 0.4-0.6 mM, in good agreement with literature values. Since parvalbumin appears only in the cytosol, it could be used as an internal marker for comparing amounts of proteins partitioned between the cytosol and cytomatrix. Supported by NIH RO1 AM33833.

T-Pos11 DEPOLARIZATION SPECTRUM OF DIFFRACTED LIGHT FROM SKINNED FIBERS: ELLIPSOMETRY MEASUREMENTS FOLLOWING MYOSIN EXTRACTION AND HMM LABELING. M. Jones, K. Burton, Y. Yeh and R.J. Baskin. Departments of Zoology and Applied Science, University of California, Davis, CA 95616 (Introduced by Dr. R. Nuccitelli).

In an effort to characterize the changes in molecular structure of skeletal muscle accompanying activity, we have applied the technique of optical ellipsometry to monitor the optical depolarization of chemically skinned frog single muscle fibers before and after extraction of myosin with a high ionic strength solution. Specifically the amplitude anisotropy (r) and phase angle (δ) were measured. Whereas r is a measure of intrinsic anisotropy, theoretically independent of the amount of material or optical path length, δ is dependent on both of these factors. Results obtained from rigor muscle fibers at a sarcomere length (SL) of 3.3 μm treated with a high ionic strength solution to disrupt the A-band are consistent with the theoretical considerations above. The δ value decreased by about 80% while r showed no significant decrease. Additionally the intensity of the first-order diffraction pattern of a non-myosin-extracted muscle fiber was determined following addition of a solution containing heavy meromyosin (HMM). HMM, isolated from rabbit skeletal muscle myosin treated with α-chymotrypsin, was added to a single muscle fiber in rigor (SL = 3.3 μm at a concentration of 5-7 mg/ml. The intensity showed a monotonic decrease to 50% of the initial value, supporting the idea that HMM bound to the exposed thin filaments resulted in a denser I-band.

T-Pos12 Monoclonal Fab Probe of Myosin Filament Assembly. Prokash K. Chowrashi, Beth Maguire and Frank A. Pepe. Department of Anatomy, University of Pennsylvania, Phila., PA 19104.

Myosin filaments were assembled from chicken skeletal muscle myosin, in the presence of the Fab fragment of a monoclonal antibody specific for the S2 portion of the myosin rod, (McFabS2). In the absence of the McFabS2 a single peak was obtained in the length distribution at around 1.5 um. With an McFabS2:Myosin molar ratio of 1:1, peaks were obtained at about 0.5 um and 1.4 um. The diameter of the filaments assembled in the absence of McFabS2 is about 25 nm. Filaments assembled in the presence of McFabS2 and with lengths around 1.4 um have diameters around 34-37 nm. The 9-12 nm increase in diameter corresponds well to the presence of Fab molecules, with dimensions of about 3 x 6 nm, on the surface of the filaments. The filaments around 0.5 um in length had diameters over a wide range with clusters around 20 nm and 37 nm. Assuming that the McFabS2 is bound to the surface of these filaments as well, the cluster with a diameter of around 20 nm would represent filaments with a diameter of about 8 nm to which the McFabS2 is bound. The 8 nm diameter is similar to that of the minifilaments described by Reisler et al (J. Mol. Biol. 143:129, 1980). These observations suggest that the McFabS2 is capable of blocking further assembly at a length of about 0.5 um and a diameter of about 8 nm. The assembly of these units by side to side interactions would produce the other cluster of filaments with a diameter of about 25 nm and a length of 0.5 um. It is possible that other monoclonal Fab probes will detect other macromolecular units in the assembly process. This work was supported by NIH grant HL 15835 to the Pennsylvania Muscle Institute.

T-Pos13 THE EXTRAOCULAR MUSCLES EXPRESS AN UNUSUAL COMBINATION OF FAST AND SLOW TROPONIN T SPECIES. M.M. Briggs,* J. Jacoby,† J. Davidowitz,† G.E. Moore* and F.H. Schachat* Department of Anatomy,* Duke University Medical Center, Durham, NC 27710 and Department of Opthalmology,† NYU Medical Center, New York, NY 10016 (Intr. by J.J. Blum).

Extraocular muscle (EOM) exhibits a more complex array of fibers than most skeletal muscles. Based on ultrastructural, physiological and histochemical analyses at least five classes of fibers are commonly defined. Studies on myosin heavy chain (mhc) expression (Wieczorek et al. [1985] J. Cell Biol. 101:618) show that all the striated muscle mhcs, including embryonic and cardiac mhcs, and one novel mhc are expressed. To determine whether these muscles also express an unusual pattern of thin filament proteins, we used monoclonal antibodies and two-dimensional gels to investigate the troponin T (TnT) species present in rabbit EOM. Analysis of myofibrils from pooled oblique and rectus muscles indicated that TnT_{3f} and TnT_{2s} are the predominant fast and slow TnT species, respectively. Although both TnT species are present in the epaxial and limb musculature, this is the first muscle in which they are the dominant species. In order to better understand the distribution of these TnTs in different extraocular fiber types, several regions of the EOM were dissected. The lateral arm portion, composed almost entirely of multiply-innervated fibers (mifs), expresses both TnT_{3f} and TnT_{2s}. This pattern of TnT expression in EOM is likely to be a consequence of either their different innervation or embryonic lineages. However, observation of a similar pattern in the small number of promiscuous fibers found in epaxial muscles suggests that somitic versus neural crest lineage is not the basis for this pattern of expression.

T-Pos14 MICROHETEROGENEITY IN CREATINE KINASE ISOENZYMES. Pan,Z.K., Iyengar,C.W.L. and Iyengar,M.R.(Intr. by Dr. J. Vanderkooi) Department of Animal Biology, Univ. of Pennsylvania, Phila. Pa. Preparations of creatine kinase(CK) from rabbit skeletal muscle(Sigma & Boehringer-Mannheim) migrate as a single active band in nondenaturing polyacrylamide gels(0.05 M tris-phosphate, pH 8.6) and as a single band with M_r=40,000 in SDS-PAGE. HPLC on gelfiltration columns(TSK 3000) & elution with 0.1 M potassium phosphate(pH 7.4) showed a single assymetric peak of MW of about 80,000. Chromatofocussing with polybufferexchanger(Pharmacia) columns(26 cm x 1.2 cm) and succesive elution with polybuffers 96 & 74(Pharmacia) resolved the protein into three enzymatically active subpairs designated in the decreasing order of pIs M1-M2(pI 7.17-7.07), X1-X2(pI 6.64-6.56) and B1-B2(pI 6.39-6.17). The specific enzymatic activities of each peak was determined in the direction of ATP synthesis by coupling ATP to NADP reduction. The specific activity [$(\Delta A_{340}$(min/mg) x 10^{-4}] of M1(24.9) was lowerthan of M2(33.5). The specific activities of X1 & X2(12.6 & 11.9) were not significantly different. B2 the more acidic form of subgroup B was less active(11.2) than B1(19.6). M1 & M2 accounted for about 86% of the total activity and probably represent the muscleoform of CK(M-CK). CK activity from a partially fractionated brain cytosol eluted in the region of B1 & B2. Recently CK from brain has been resolved into two fractions. The more acidic form was found to be phosphorylated(Mahadevan, et. al, Biochem. J, 222, 139, 1984). The chemical nature of M1 & M2 are under study. Supported by Univ. of Penn. Research Fund.

T-Pos15 RECONSTITUTION OF TWO-STRANDED MYOSIN FRAGMENTS INCLUDING THE S1/S2 SWIVEL L.Nyitray, I. Boldogh*, M. Balint*, R. Lu, & J. Gergely, Dept. Muscle Res., Boston Biomed. Res. Inst., Dept. Biol. Chem. & Neurology, Harvard Med. School, and Dept. Neurology, Mass. Gen. Hosp., Boston, MA 02114; *Dept. Biochem., Eotvos Univ., Budapest, Hungary.

A 140 kDa fragment in which the 20 kDa head region is joined to the total rod chain is formed by tryptic digestion of myosin in 30 mM KCl and in the presence of 10 mM Ca^{2+} or Mg^{2+}. Using HMM instead of myosin a 60 kDa fragment consisting of the 20 kDa region joined to the short S2 chain is produced. The 60 kDa fragment can be further degraded into a 25 kDa peptide containing the 20 kDa region and a 5 kDa C-terminal stretch, presumably the swivel between S1 and the rod. The 140 kDa, 60 kDa and 25 kDa fragments were isolated under denaturing conditions and renatured using the method of Muhlrad & Morales (PNAS 81, 1003, 1984). The helical domains of the fragments reform the native two-chained coiled-coil structure as shown by tryptic digestion patterns. The renatured fragments that contain the 20 kDa region bind to actin as shown by sedimentation and crosslinking by 1-ethyl-3-[3-(dimethylamino) propyl] carbodiimide. On renaturation the 20 kDa portion regains its light chain binding ability, too, as tested by sedimentation, crosslinking with dimethyl suberimidate and gel electrophoresis under non-denaturing conditions. Reassociation of the light chains decreases the otherwise pronounced tendency of self-aggregation due to the head region. The functional properties of these reconstituted fragments may shed more light on the importance of the S1/S2 swivel and the putative domain organization of myosin heads. Supported by grants from NIH (HL-5949, AM-28401) and the MDAA.

T-Pos16 LC2 Involvement in the Assembly of Skeletal Myosin Filaments. Prokash K. Chowrashi, Suzanne Pemrick, and Frank A. Pepe. Dept. of Anatomy, Univ. of Penn., Phila., PA 19104, and Dept. of Biochemistry, SUNY Downstate, Brooklyn, NY 11203.

In vitro assembly of LC2 deficient myosin was studied using a standard procedure which produces myosin filaments with length distributions around 1.6 um comparable to native filaments. (Chowrashi and Pepe, Biophys. J. 47:307A 1985). Assembly of LC2 deficient myosin, control myosin and reassociated myosin was compared. Rabbit skeletal myosin was prepared as described by Pemrick (Biochem. 16:4047, 1977). The ATPase activity of the LC2 deficient, control and reassociated myosins were all within normal ranges (nmoles Pi/sec/nmole site: 0.033-0.050 Magnesium, 1.11-1.33 Calcium and 14.3-15.1 K^+/EDTA ATPases). Filaments were assembled with and without the presence of 1 mM Magnesium ATP since Magnesium ATP leads to a sharpening of the length distribution around 1.6 um (Chowrashi and Pepe, Biophys. J. 47:307A, 1985). Myosin filaments assembled from control and reassociated myosin gave similar lengths around 1.6 um. Filaments assembled from LC2 deficient myosin gave length distributions around 1.1-1.2 um both in the presence and absence of Magnesium ATP. The most significant findings of these studies are the following: a) The LC2 chain is required for assembly of myosin filaments to the native length of about 1.6 um. LC2 deficient myosin assembles to about 1.2 um. The significance of this length is unknown. b) Reassociation of the LC2 chain with LC2 deficient myosin restores the assembly to the native length of 1.6 um. This work was supported by NIH Grants HL 15835 to the Pennsylvania Muscle Institute and HL 22401 to S.P.

T-Pos17 HEAVY CHAIN ISOENZYMES OF MYOSIN SUBFRAGMENT-1: ISOLATION AND PROPERTIES. Mathoor R. Sivaramakrishnan and Morris Burke, Department of Biology, Case Western Reserve University, Cleveland, Ohio 44106.

Chymotryptic SF1 preparations of fast muscle can be resolved into four distinct fractions by anion-exchange HPLC. Fractions 1 and 2 each contain 95K dalton heavy chain and 21K dalton (A1) light chain while fractions 3 and 4 each contain 95K dalton heavy chain and 16.5K dalton (A2) light chain. Peptide mapping showed that the 95K dalton heavy chains in fractions 1 and 3 are similar but distinct from fractions 2 and 4 which are themselves similar. Isolation of the chymotryptic N-terminal nanopeptide of the heavy chains from fractions 1 and 2 (Starr and Offer, J. Mol. Biol. 81, 17(1973)) indicate that at position 8, fraction 1 contained val whereas fraction 2 contained ile. This result suggests that the resolution of SF1 into four fractions is primarily based on the heavy chain and light chain isozymic forms, namely HC1A1, HC2A1, HC1A2 and HC2A2 respectively. Ca2+, K+/EDTA and actin activated ATPase activities show little difference if any between the HC isozymic forms. The pH dependence on the Ca2+ATPase activity was also similar for these isoenzymes. Limited proteolysis of the native isoenzymes by papain showed that cleavage at the 29K/27K junction was faster in HC1 compared to that of HC2 containing fractions. Differences in HC1 and HC2 species are also apparent from the relative amounts of 27K and 29K fragments produced by trypsin. Small differences can also be discerned at their 75K/21K junction by trypsin. In conclusion, it is now possible to isolate myosin SF1 into two heavy chain isozymic species, which have similar catalytic function but which are conformationally distinct from each other. This work was supported by UPHS grants AM 33327 and NS 15319.

T-Pos18 MYOSIN ISOZYMES IN EMBRYONIC CHICKEN ADDUCTOR PROFUNDUS MUSCLE. Yatian Zhang and and S.A. Shafiq. Biophysics Graduate Program and Department of Neurology, SUNY Downstate Medical Center, Brooklyn, N. Y. 11203.

The myosin composition of the adductor profundus (AP) muscle, a newly characterized slow muscle of the chicken was studied and compared with those of the fast pectoralis major (PM) muscle at several embryonic and post-hatching stages. A new monoclonal antibody (McAb), ALD-84, was produced against the slow myosin of chicken and its specificity for the myosin light chain 1 (LC1) was established by radioimmune assay, immunoautoradiography and immunoflurorescence. It was used in conjunction with previously reported anti-slow myosin heavy chain (ALD-58,ALD-88 and ALD-180), anti-fast myosin heavy chain (MF-14 and MF-20) and anti-fast myosin light chain 2 (LC2f) (MF-5) monoclonal antibodies. In the AP muscle of 16-day embryo two MHC bands were seen which show quantitative changes in their ratio during late embryonic and post-hatching stages similar to those described in the ALD muscle (Matsuda et all, 1982). In immunoblots the myosins of the embryonic and adult AP muscles reacted with anti-slow myosin McAbs whereas those of PM did not. By epitope analysis these four myosins presented distinctive patterns. Thus, these results, in contradistinction to those of previous studies (e.g.,Matsuda et al., 1982) indicate that the MHC of 16-day embryonic slow muscle represents an isoform different from those of adult slow and fast muscles. The newly characterized McAb, ALD-84 identifies the LC1s of both the embryonic and adult AP muscle. With the anti-LC2f McAb, Mf-5, however, a clear difference is seen in the light chains of embryonic and adult AP muscle in that two light chains react in the embryonic and only one in the adult stage.

T-Pos19 STRUCTURAL STUDIES OF MYOSIN AND ITS LIGHT CHAINS. Tsuyoshi Katoh and Susan Lowey. Rosenstiel Center, Brandeis University, Waltham, MA 02254.

Thiol modification of the heavy and light chains has provided a basis for obtaining structural information about myosin. Cross-linking the reactive thiols of the heavy chain, SH1 and SH2, by DTNB results in the formation of a disulfide bond between residues separated by as much as 25 Å in the native molecule (Wells and Yount, 1980, Biochemistry 19, 1711). This region of high flexibility was examined by electron microscopy of rotary-shadowed cross-linked myosin. No change was observed in the dimensions of the head, suggesting that any conformational changes taking place are too small to be visualized by this technique. The structure of the light chains has also been studied by introducing a fluorescent probe (IAF) into the single thiol located near the C-terminal end of the alkali light chain. Titration of the IAF-labeled light chain with anti-fluorescyl IgG antibodies caused extensive quenching of the fluorescence (up to 90%), from which it was possible to calculate a binding constant of $\sim 10^9 M^{-1}$. When the light chain was first reacted with an antibody specific for the N-terminus (Silberstein and Lowey, 1981, J. Mol. Biol. 148, 153), the affinity of the IAF-hapten for anti-fluorescein increased by greater than 10-fold, suggesting an interaction between the N- and C-terminal regions of the molecule. Complexes of antibody and light chain could be visualized by electron microscopy. This modified light chain will be exchanged into myosin, and the orientation and interactions of the light chain with the heavy chain will be investigated by a combined approach of spectroscopy and immunoelectron microscopy.

T-Pos20 MYOSIN ISOZYMES IN THE AVIAN POSTERIOR LATISSIMUS DORSI MUSCLE. J. I. Rushbrook, C. Weiss, and S. Ruo-qian. Dept. Biochemistry, SUNY-Downstate Medical Center, Brooklyn, N.Y. 11203.

The avian pectoralis major muscle (PM) has been well characterized histochemically. The bulk of it contains only fast twitch muscle fibers possessing a well characterized myosin molecule. The nature of the myosin present in the posterior latissimus dorsi muscle (PLD), also containing mainly fast twitch fibers, is unclear. Work from several laboratories has shown differences in the peptide maps of heavy chains from the two sources. One study concluded that the differences were due to post-translation modification differences (Bandman, E., Matsuda, R. and Strohman, R.C. (1982) Cell 29, 645), while the other, working with the rod portion of the protein which has not been shown to possess such modifications, concluded that the PLD myosin resembled a mixture of PM adult and post-hatch myosin, but contained some differences (Lowey, S., Benfield, P., LeBlanc, D. and Waller, G.S. (1983) J. Muscle Res. Cell Motility 4, 695).

We have explored the differences between the heavy chains from the two sources using reverse-phase HPLC fractionation of their S-1 tryptic fragments. The method used is able to differentiate 20kDa and 50kDa fragments of PM adult and post-hatch myosins. The PLD myosin possesses a single 50kDa fragment eluting with the same retention time as that of the adult PM myosin. However, it possesses two 20kDa fragments, one with elution characteristics like that from the adult PM myosin, the other resembling that of the PM post-hatch myosin. These preliminary results are consistent with the adult PLD myosin possessing two fast-twitch heavy chain isozymes, one similar to that in the adult PM muscle, the other, in overall characteristics, differing from both adult and post-hatch PM species.

T-Pos21 EXPRESSION OF SLOW MYOSIN ISOFORMS IN PRIMARY GENERATION MUSCLE CELLS OF THE DEVELOPING RAT HIND LIMB. M. Narusawa, J. Leferovich, N. Rubinstein and A. Kelly, Pennsylvania Muscle Institute, University of Pennsylvania, Philadelphia, PA.

We have prepared heavy chain peptide maps with column purified myosin from adult soleus, soleus and masseter at birth and from 18 day fetal hind limb muscle. Digests were transferred to nitrocellulose and reacted with a monoclonal antibody (HS) specific to subfraction 2 of slow myosin (donated by Dr. J. Hoh). Identical peptides stain in each preparation. Hence the same antigenic determinants recognized by HS in adult slow myosin are expressed throughout development.

Sections of hind limb muscles were stained with HS and with a monoclonal antibody, 2G3, which reacts with embryonic, neonatal and adult fast myosin but not with slow myosin. At 16 days gestation all primary generation myotubes of the Anterior tibial (AT) and Extensor digitorum longus (EDL) stain with both HS and 2G3. They all continue to stain at 18 days but primary myotubes in superficial regions stain less intensely with HS than do central myotubes. Secondary generation myotubes emerge at 18 days. They exclusively stain with 2G3. Primary cell switching from slow to fast myosin synthesis proceeds as a wave moving centrally; by 35 days only a small number of slow fibers remain.

In fetal animals made hypothyroid, primary cell slow to fast switching proceeds normally. Post partum, elimination of slow myosin is inhibited by hypothyroidism. The thyroid thus appears to assume control of isozyme expression in primary cells after birth. In the EDL of adult rats made hypothyroid, slow fibers increase. Their numbers and distribution simulates the EDL at birth. Plasticity in the adult thus may recapitulate early patterns of gene expression.

T-Pos22 EXPRESSION OF THE CALCIUM BINDING PROTEIN PARVALBUMIN DURING POSTNATAL RAT MUSCLE DEVELOPMENT. J.X. DiMario* and B.R. Unsworth (Dept. Biology, Marquette University, Milwaukee, WI 53233. *Dept. Zoology, University of California, Berkley, CA 94720).

Postnatal muscle differentiation is a temporally protracted process and offers an opportunity to monitor the acquisition of function. Rat limb muscles, whether destined to become fast- or slow-contracting in the adult, are slow at birth. A critical functional difference between fast and slow muscle is the ability of fast muscle to relax rapidly. The role of parvalbumin (PA) in the relaxation process is concentration dependent. Adult rat fast muscle contains high levels and adult slow muscle low levels of PA. We used specific, highly sensitive immunological techniques to quantitate PA in presumptive fast-twitch (extensor digitorum longus and plantaris) and slow-twitch (soleus) muscles during postnatal development.

No PA was detected in either the fast or slow muscles during the first 3 days of postnatal development using an ELISA assay. The EDL showed a steady accumulation of PA to reach about 2.5 mg/g in the adult. The plantaris PA concentration also increased postnatally, but accumulation of PA was delayed for 5 days and the adult value was less than half that attained by the EDL. The slow-twitch soleus accumulated PA from days 3 through 7, in parallel to that of the EDL, but a rapid decrease followed, resulting in the extremely low level characteristic of the adult soleus by 10 days postnatal. RIA analysis did not change the overall pattern of postnatal PA synthesis, but PA was detected in both slow and fast muscles from the time of birth. These results indicate that PA is synthesized by both presumptive fast and slow muscles, but over a different time course and expression is reduced to extremely low levels after 10 days in the postnatal soleus.

T-Pos23 STRUCTURAL STUDIES OF SKELETAL MUSCLE MYOSIN LIGHT CHAIN KINASES WITH MONOCLONAL ANTIBODIES. M. H. Nunnally, L. C. Hsu, M. C. Mumby, and J. T. Stull. Department of Pharmacology, University of Texas Health Science Center at Dallas, Dallas, TX 75235.

Monoclonal antibodies (MAbs) directed to rabbit skeletal muscle myosin light chain kinase (RSkMLCK; M_r = 87K) have been used to study the domains of this kinase. Epitope mapping of trypsin-digested RSkMLCK, by immunoblot, with nine MAbs to RSkMLCK indicates that two are directed to distinct sites within the inactive "tail" domain; seven MAbs are directed to the catalytic domain (M_r = 40K). Additionally, these seven MAbs react with sites that are clustered within a M_r = 14K fragment of RSkMLCK generated by V8 protease digestion. Three of the seven MAbs directed to the catalytic domain inhibit kinase activity (MAbs designated RSk2a, 9b and 12a). Inhibition of enzyme activity by Fab fragments of RSk12a is non-competitive with respect to Ca^{2+}-calmodulin activation. In contrast, inhibition of kinase activity by Fab fragments of RSk12a indicates competitive inhibition with respect to rabbit skeletal muscle myosin P-light chain, and competitive or "mixed" inhibition with respect to $MgATP^{2-}$. These data suggest that MAb RSk12a is binding to an epitope within or directly adjacent to the kinase active site, thereby blocking substrate binding. These data also support the contention that the catalytic and calmodulin-binding domains of RSkMLCK are distinct regions of the protein. The nine MAbs to RSkMLCK crossreact with other mammalian skeletal muscle MLCKs as determined by immunoblot of tissue extracts. However, there is no crossreaction with mammalian smooth muscle MLCKs. Thus, skeletal and smooth muscle MLCKs represent tissue-specific isoenzymes. (Supported by HL23990)

T-Pos24 MONOCLONAL IgM AND IgG ANTIBODIES DIRECTED AGAINST SKELETAL TROPONIN I. Kimbrough D. Warber, Priscilla F. Strang, and James D. Potter. Dept. of Pharmacology, Univ. of Miami School of Medicine, Miami, FL 33101.

Two monoclonal antibodies (McAb) against rabbit STnI have been studied. One (IVC8-B11) is an IgM (μ_2 κ_2) and one (IE7-B7) is an IgG ($\gamma 1_2$ κ_2). Both bind STnI and crossreact with cardiac TnI in enzyme-linked immunosorbent assay (ELISA). Neither reacts with TnT or TnC of either muscle type. Immunofluorescence data show the IgG McAb binds only at the I-band of fixed glycerinated rabbit psoas fibers; no binding by the IgM McAb was seen. As IgM McAb's against STnC can bind TnC in similar studies (see abstract by Strang, Warber, and Potter) the anti-STnI IgM McAb may recognize a determinant sequestered when STnI is in complex in myofilaments. Alternatively, both McAb's may recognize a determinant accessible *in situ* to a relatively small probe (IgG) but not to a larger probe (IgM). These data plus a unique ELISA of binding to myofibrillar proteins in "solution" show the IgG McAb binds STnI *in situ* more in the presence of Ca^{2+} than in its absence. Competitive inhibition ELISA data show a greater inhibition of McAb binding to adsorbed STnI by STnC·STnI complex with Ca^{2+} than without; inhibition by STnI alone was Ca^{2+}-independent. The IgG McAb binds STnI electroblotted onto nitrocellulose (immunoblot) while the IgM McAb does not, suggesting the IgM may be conformation-specific and the IgG may be conformation- or sequence-specific. Studies to identify determinant region(s) recognized by the IgG McAb and characterization of the IgM McAb will be presented. Also, six hybridomas producing anti-STnT IgM and IgG are being cloned and their partial characterization will be reported. Supported by NIH RO1 AM33427 and HL07188. K.D. Warber is a recipient of a postdoctoral fellowship from the American Heart Association, Florida Affiliate.

T-Pos25 MONOCLONAL ANTIBODIES THAT BIND SKELETAL TROPONIN C. Pricilla F. Strang, Kimbrough D. Warber, and James D. Potter, Department of Pharmacology, University of Miami School of Medicine, Miami, Florida 33101.

Monoclonal antibodies (McAb's) have been produced to the calcium binding protein of rabbit skeletal troponin (STnC). Five of these McAb's have been characterized to date. All are of the IgM class, containing kappa light chains. Preliminary results show that all five McAb's are crossreactive with other calcium binding proteins such as cardiac troponin C, calmodulin and parvalbumin. However, none are crossreactive with the other troponin subunits (TnT or TnI) from either rabbit skeletal or bovine cardiac muscle. Immunofluorescence experiments of the anti-STnC McAb binding to STnC in glycerinated myofibrils demonstrate that the McAb's are able to bind to the STnC antigen *in situ* as demonstrated by specific staining of the I-band region. The fluorescence intensity is dependent upon the metal (Ca^{2+} or Mg^{2+}) bound to STnC fixed *in situ*. Three of the McAb's appeared to be dependent on the presence of one of the metals (Ca^{2+}, clones F82 and B91; Mg^{2+}, clone F81) while two of the McAb's required either the absence of both metals (B102) or the presence of both metals (B_9D_9) for maximum fluorescence intensity. These data indicate that the five McAb's recognize different conformational states of STnC *in situ*. Work is underway to determine the antigenic determinants recognized by each McAb and what effects, if any, McAb's may have on STnC function in various troponin complex reconstitutions. Supported by NIH R01 AM 33427 03.

T-Pos26 VARIATIONS IN AFFINITY OF SYNTHETIC CALCIUM-BINDING ANALOGUES OF SITE III OF RABBIT SKELETAL TROPONIN C. B.J. Marsden, R.S. Hodges, and B.D. Sykes. Department of Biochemistry, University of Alberta, Edmonton, Alberta, Canada T6G 2H7.

Calcium is known to modulate many cellular events, such as muscle contraction, by acting as a chemical signal that alters the structure of regulatory proteins. The calcium-binding site, which is a highly conserved region of calcium-binding proteins, exists in a helix-loop-helix conformation. The six metal coordinating residues are found within the twelve residue loop region. To study the contribution made at each coordinating position to the metal binding affinity of the site, several 13-residue analogues of the calcium-binding site III of rabbit skeletal troponin C have been prepared by solid-phase synthesis. High field ^1H NMR spectroscopy has been used to study the events that occur within the calcium-binding site on the binding of La^{3+} ions. La^{3+} was used because it has a higher metal binding affinity than Ca^{2+}. The lanthanide affinities for the native sequence, AcSTnC (103-115) amide is $1.1x10^5M^{-1}$, for the synthetic analogues: Ac(Asp105)STnC amide (I), Ac-(Asn103, Asp105)STnC amide (II), Ac(Glu107)STnC amide (III), and Ac(Asn103, Asn107)STnC amide (IV) are: $1x10^6M^{-1}$, $1.25x10^5M^{-1}$, $5x10^4M^{-1}$, and $<1M^{-1}$, respectively. The chemical shift of several residues, such as, Gly 108, Tyr 109, Ala 106, and Ala 112 can be used to monitor the conformational change in these peptides upon metal binding. For example, the difference $\Delta\delta$ of the Gly 108 -protons, are for: the native peptide: +0.38 ppm, (I): +0.46 ppm, (II): +0.176 ppm, (III): +0.107 ppm, and (IV): -0.014 ppm. These results, except for peptide (III), follow the same trend as the metal binding affinities, suggesting that the conformational changes that occur on metal binding are different to those for the native peptide, peptide (I), and (II).

T-Pos27 EXCITATION ENERGY TRANSFER STUDIES ON INTERTROPONIN DISTANCES IN RECONSTITUTED THIN FILAMENTS. P.C. Leavis, E. Gowell and T. Tao, Dept. Muscle Research, Boston Biomedical Research Institute and Dept. Neurology, Harvard Medical School, Boston, MA 02114

We have employed excitation energy transfer to measure the distances between specific sites in the troponin complex. The fluorescent donor 1,5-IAEDANS was used to label either Cys 98 of troponin C or Cys 133 of troponin I from rabbit skeletal muscle. The chromophoric acceptor DAB-Mal (4-dimethylaminophenylazophenyl-4'-maleimide) was attached to the single Cys residue of bovine cardiac TnT (located between residues 50-70, Gusev et al. Biochem. J. 213, 123, 1982). Hybrid troponin complexes were made using various combinations of labelled and unlabelled components, and this troponin was incorporated with actin and tropomyosin to form reconstituted thin filaments. Using both fluorescence lifetime and steady-state measurements, energy transfer efficiencies of 3-5% were obtained for transfer between Cys 98 of TnC and TnT and between Cys 133 of TnI and TnT in the presence of either Ca^{2+}, Mg^{2+} or EDTA. Based on a critical transfer distance of 4 nm and on the assumption that the orientation factor, κ^2, has a value of 2/3, these efficiencies correspond to separation distances of ~6.5-7.0 nm between the labelled sites. In view of studies indicating that the length of TnT $\geq$ 13 nm (Ohtsuki, J. Biochem. 6,491, 1979; Flicker et al, J. Mol. Biol. 162, 495, 1982), our data suggests that the labelled portions of both TnC and TnI lie near the middle of the TnT molecule. (Supported by grants from NIH (AM21673 and HL20464) and the Muscular Dystrophy Association of America.)

T-Pos28 CHICKEN GIZZARD TROPOMYOSIN IS PREDOMINANTLY A βγ-HETERODIMER. Clive Sanders, Leslie D. Burtnick and Lawrence B. Smillie, MRC of Canada Group in Protein Structure and Function, Department of Biochemistry, University of Alberta, Edmonton, Canada T6G 2H7.

Chicken gizzard tropomyosin (gTM) when cross-linked with various N-hydroxy succinimide esters yields 4 dimeric species upon electrophoresis: γγ, γβ', γβ and ββ TMs. Since the γβ' species is also present in control experiments, where cross-linking and reducing agents are absent, it arises from intermolecular disulphide bond formation between cys36 on β-TM and cys190 on γ-TM. Densitometric scans of electrophoretograms of gTM cross-linked at 1 mg/ml and 0.1 mg/ml, ± 1 M NaCl at pH 7.5 with disuccinimidyl suberate indicate that the average ratio of γγ:γβ:ββ is 0.7:4.3:1. While pyrene labelling of denatured-renatured gTM, of the two homodimers, and of skeletal TM results in significant excimer fluorescence upon irradiation at 343 nm, similar labelling of native gTM, in agreement with previous observations (Lehrer et al. (1984) Biochemistry 23, 1591-1595) does not. These results indicate that the proportion of heterodimers present in native gTM is >70% and that the homodimeric species have sufficient flexibility to permit pyrene stacking. Circular dichroism measurements of molar ellipticities as a function of temperature show that the relative stabilities of the dimeric species is γγ<ββ, native gTM ≦ skeletal αα TM in agreement with predictions based on analysis of amino acid substitutions in "core" and "inner" positions of the several species (Sanders and Smillie (1985) J. Biol. Chem. 260, 7264-7275). Based on these results therefore, further evidence is required to assess the relative rigidities of the gizzard and skeletal TM species. (Supported by the Medical Research Council of Canada)

T-Pos29 FLUORESCENCE OF ACRYLODAN-LABELLED PLATELET TROPOMYOSIN. I.D. Clark and L.D. Burtnick, Department of Chemistry, University of British Columbia, Vancouver, B.C., Canada, V6T 1Y6.

Equine platelet tropomyosin (P-TM) was labelled with the sulfhydryl-specific fluorescent reagent acrylodan (AD). The extent of labelling at 4 ^{o}C could be regulated between 1.0 and 1.6 AD per P-TM chain by varying the reaction time from one to 4.5 hours. The reaction product, AD-P-TM, was highly fluorescent, having an emission maximum near 515 nm on excitation at 365 nm. Steady state measurements of polarization of the fluorescence of AD-P-TM in both low and high ionic strength solutions gave Perrin plots that exhibited sharp changes in slope near 52 ^{o}C, indicative of a sharp increase in mobility of the AD label at that temperature. This may be the result of a melting out of the coiled coil structure at the site of labelling. In solutions containing 150 mM KCl and 5 mM $MgCl_2$, addition of actin induced several changes in the emission from samples that contained AD-P-TM. Maximal fluorescence intensities and fluorescence polarization values increased with added actin up to a mole ratio of about 6 actins per P-TM. In addition, maximal emission was shifted to shorter wavelengths by about 5 to 7 nm. These changes indicate that actin does bind to AD-P-TM, the binding affects the environment of the AD label, making it more hydrophobic in nature, and the binding reduces motions of the label, probably because the AD is attached through P-TM to an extended F-actin filament.

Supported by the British Columbia Heart Foundation and the Natural Sciences and Engineering Research Council of Canada.

T-Pos30 RESONANCE ENERGY TRANSFER STUDIES OF TROPONIN I AND ITS COMPLEX WITH TROPONIN C. Chien-Kao Wang and Herbert C. Cheung. Department of Biochemistry, University of Alabama at Birmingham, Birmingham AL 35294

Molecular distances between specific residues in the troponin C (TNC) and troponin I (TNI) were determined by fluorescence energy transfer. The specific sites chosen were Met-25 and Cys-98 in TNC and Cys-133 and Trp-158 in TNI. The first three residues were labeled with either donor or acceptor probes, and the single tryptophan of TNI served as intrinsic fluorophore. The four chosen residues allowed determination of one distance in isolated TNC reported previously (Cheung, et al., 1982, Biochemistry, 21, 5135), one distance in isolated TNI, and six distances in the complex TNC·TNI that included two intrasubunit and four intersubunit distances. The two intrasubunit distances were (1) [Met-25 → Cys-98] and (2) [Trp-158 → Cys-133]. The distances, R(2/3), determined in EGTA, Mg^{2+}, Ca^{2+} were 38, 39 and 46 Å for (1), and 28, 27 and 20 Å for (2). Four intersubunit distances were measured: (a) Cys-98 → Cys-133, (b) Trp-158 → Met-25, (c) Trp-158 → Cys-98, and (d) Met-25 → Cys-133. The following separations, R(2/3), were obtained for cation-free, Mg^{2+}-saturated, and Ca^{2+}-saturated complex, respectively: (a) 57, 57 and 50 Å; (b) 25, 25 and 24 Å; (c) 29, 30 and 25 Å; and (d) 35, 34 and 44 Å. Of the six distances, distance (b) was insensitive to Ca^{2+} binding whereas the others were substantially perturbed by Ca^{2+}. However, all six distances were relatively insensitive to Mg^{2+} binding to the two high affinity sites. These results are compatible with the notion that the Ca^{2+} binding signal is transmitted via a cascade of global structural changes from troponin to the other thin filament proteins. (Support by NIH AM-25193).

T-Pos31 EFFECTS OF TROPONIN ON THE CONFORMATION OF PYRENE-TROPOMYOSIN.
Y. Ishii and S.S. Lehrer, Dept. of Muscle Research, Boston Biomed. Res. Inst., Boston Ma. 02114.

The excimer fluorescence (E) of tropomyosin labeled at Cys 190 with pyrene-maleimide (PTm) is the result of interchain pyrene-pyrene interaction. It increases with temperature in an unfolding pretransition at the expense of monomer fluorescence (M) from a low temperature value Eo to a value Emax associated with a localized chain-open state. Effects of troponin (Tn) on the PTm fluorescence were studied using two samples at different degrees of labeling, doubly labeled (E and M present) and singly labeled (only M present). Tn enhanced M of singly labeled PTm and decreased Eo of doubly labeled PTm, indicating that the environment of pyrene changed and that the pyrene-pyrene interaction was somewhat inhibited. In spite of the decreased Eo, E increased with temperature in a similar manner to PTm alone, indicating that the unfolding pretransition occurs in the Tn-PTm complex. Only a small Ca^{2+} effect on E was observed in the pretransition temperature range. For a TnT-PTm complex, the increase in E with temperature in the pretransition was less than for Tn-PTm, showing that TnT in the TnT-TnI-TnC complex interacts differently with Tm. The binding of the N-terminal chymotryptic fragment of TnT, TnT1, did not change the M fluorescence of singly labeled PTm, suggesting that TnT1 does not bind near Cys 190. The binding of TnT1 to doubly labeled PTm caused a ~10% decrease in Eo and a ~10% increase in Emax in the pretransition, suggesting conformational coupling between the TnT1 binding site and Cys 190 on Tm. (Supported by NIH and MDA)

T-Pos32 LOCALIZED UNFOLDING IN RABBIT SKELETAL α-α AND Nbs β-α TROPOMYOSIN. S.S. Lehrer, Dept. of Muscle Research, Boston Biomedical Research Institute, Boston MA 02114.

Rabbit skeletal tropomyosin (RSTm) is an α-helical coiled-coil consisting of $\alpha\alpha$ and $\alpha\beta$ molecules. The α-chain contains one Cys at #190; the β-chain has 2 Cys, at #36 and #190. Both chains contain 6 Tyr, 5 of which are located in the C-terminal half. RSTm was reacted with 5,5'-dithiobis(2-nitrobenzoate) (Nbs_2) to produce intrachain disulfide crosslinks at #190 for each molecule and an Nbs-blocked Cys at β 36 of the hetero-molecule. These are denoted α-α and Nbs β-α. To locate regions of differing stablility, the temperature dependence of the CD signal of the peptide in an α-helix (at 222nm) was compared with the CD bands of the Tyr (at 283nm) and the Nbs group (at 310nm) for both α-α and Nbs β-α in 10 mM phosphate buffer, pH 7.4, 0.6M NaCl. The helix unfolding profile of both α-α and Nbs β-α showed a pretransition near 32°, a main transition between 50°-60° for α-α and a somewhat broader main transition for Nbs β-α between 40°-60°. The Tyr CD band of both species was lost in a cooperative transition between 50°-60°. In contrast, the Nbs CD band of Nbs β-α was lost in a cooperative transition between 42°-52°. These data indicate that: i) the unfolding of each molecule in the pretransition temperature range does not appear to affect the C-terminal half or the region of the molecule near Cys 36 for Nbs β-α; ii) the unfolding of the Cys 36 region of Nbs β-α occurs prior to the main transition; iii) the C-terminal half of both molecules is unfolded in the main transition. (Supported by NSF, NIH and MDA.)

T-Pos33 PURIFICATION AND CHARACTERIZATION OF A TROPOMYOSIN KINASE. A.S. Mak and I. deBelle (Intr. by G. Côté) Dept. of Biochemistry, Queen's University, Kingston, Ontario, Canada

A kinase which phosphorylates skeletal muscle tropomyosin has been partially purified from 14 day-old chick embryo thigh muscle by DEAE, phosphocellulose, gel filtration and red dye chromatography. The tropomyosin kinase preparation consists of two bands of Mr ~ 78K and 69K determined by SDS-gel electrophoresis but it is eluted as a single peak of activity of Mr ~ 350K on a BioGel A ...5 M column under non-denaturing conditions. The activity of the tropomyosin kinase is dependent on Mg^{2+} and dithiothreitol but is independent on Ca^{2+} and cAMP. The pH optimum for the kinase activity is ~7.5 and its activity is reduced by 90% in the presence of 200mM KCl. The Km for skeletal α-tropomyosin and ATP is 120 μM and 200 μM respectively. The purest kinase preparation obtained phosphorylates skeletal α-tropomyosin and casein at similar rates but its activity towards histone and phosvitin is negligible. Skeletal α-tropomyosin is not phosphorylated by cAMP-dependent protein kinase, phosphorylase kinase nor smooth muscle myosin light chain kinase. The amino acid sequence around the phosphorylation site at serine-283 of tropomyosin bears little resemblance to other known phosphorylated sites. These properties together with its chromatographic behaviour suggest that the tropomyosin kinase is an unique kinase different from the casein kinase I and II.
Supported by MRC of Canada.

T-Pos34 Substructure of solid myosin filaments of insect flight muscles. Gernot Beinbrech, Francis T. Ashton and Frank A. Pepe, Zoologisches Institut, D4400 Munster, FRG, and Dept. of Anatmony, Univ. of Pennsylvania, Philadelphia, PA 19104.

Cross sections of 61 honeybee and 67 fleshfly myosin filaments from flight muscle fixed by a multistage fixation procedure (Ashton and Pepe, J. Microsc. 123:93, 1981), were digitized and processed by rotational averaging (Stewart et al., J. Mol. Biol. 153:381, 1981). In these filaments it was found that the symmetry of the core and the wall was not the same, with 85-90% of the filaments having 6-fold symmetry in the wall and about 95% having 3-fold symmetry in the core. The images of the filaments in each muscle were superimposed according to the 6-fold symmetry of the wall. These averaged images showed 6 pairs of subunits in their walls similar to what is found in the walls of tubular filaments. In fleshfly solid filaments 3 additional subfilaments were located in the core, positioned between two pairs of myosin subfilaments in the wall. In the bee filaments these three subfilaments were related to pairs of myosin subfilaments rather than between pairs, with an additional three located eccentrically in the core of the filaments. The extra subfilaments in the core of these filaments can be related to their paramyosin content (Aust et al., J. Muscle Res. Cell Mot. 1:448,1980; Beinbrech et al., Cell Tissue Res. 241:607, 1985). The different position of the three paramyosin subfilaments relative to the subfilaments in the wall may represent structural arrangements characteristic of the two species, or arrangements at different levels along the length of the filaments. Serial sections will resolve this. This work was supported by NIH grant HL 15835 to the Penn. Musc. Inst. and by travel support from the Deutsche Forschungsgemeinschaft to G.B.

T-Pos35 FIBER TYPES IN LIMULUS MUSCLE. R.J.C. Levine, S. Davidheiser, R.W. Kensler, A.M. Kelly & R.E. Davies. Department of Anatomy, Medical College of Pa., Philadelphia, PA 19129 & Departments of Animal Biology & Pathology, Univ. of Pa. School of Veterinary Medicine, Philadelphia, PA 19104.

By LM, EM and histochemistry we identify at least 2 fiber types in Limulus medial telson levators. Large fibers (mean x-sectional area = 2156μm^2) have 4.1μm A-bands, 2.15μm thin filaments and < 0.5μm Z-lines. Non-overlap sarcomeres average 11μm. Few mitochondria are present. These fibers react intensely for alkaline-stable myofibrillar ATPase activity but do not display β-NADH diaphorase activity. They comprise 54% of the fibers in a x-section and occupy 82% of the area. Small fibers (mean x-sectional area = 484μm^2) have 6.3μm A-bands, 3.1μm thin filaments and >0.5≤1.0μm Z-lines. Non-overlap sarcomeres average 15μm. Numerous mitochondria occur close to the Z-lines. Alkaline-stable ATPase activity is absent but these fibers react strongly for β-NADH diaphorase. They comprise 46% of the fibers in a x-section but occupy only 18% of the area. Some fibers are intermediate in size and histochemical reactivity. Two myosin isozymes appear on pp-PAGE of myofibrils, supporting the differences in ATPase reactivity. 20% of the thick filaments isolated from unstimulated muscle are very long (5-7μm), although the majority are 4.2μm. All have similar arrangements of myosin heads and similar diameters. We suggest that the small, long-sarcomere fibers contribute to the right-hand portion of the length-tension curve (Walcott & Dewey, JCB 87:204,'80; Davidheiser & Davies, Am.J.Physiol.242:R394,'82), allowing thick-thin filament interaction at full muscle extension. The 2 fiber types, however, do not explain the observed decreases in A-band and thick filament lengths in stimulated Limulus telson muscles. Supp. by USPHS grants: HL15835 to the Penna. Muscle Inst., AM30442 & NSF grant PCM82-17279.

T-Pos36 MUSCLE SEGMENT LENGTH MEASUREMENT BY DIRECT IMAGING. M.L. Denison and D.L. Morgan, Dept of Electrical Engineering, Monash University, Melbourne, Australia.

Fast tension transient experiments provide a basis for modeling the contractile process in muscle fibers. Best results are obtained using segment length control so that effects of tendon and mounting compliances are eliminated. Previous methods for measuring movement of fibers (hence segment length) have been invasive, limited by noise, or requiring specially uniform muscle segments. A measurement system that images the pattern of sarcomeres directly onto an array of photosensors and tracks its movement has been built. The heart of the system is a custom made integrated circuit (4.7mm x 3.1mm) which contains the photosensor array, image registers, and movement correlation circuitry. A laser illuminates the fiber and an image of 5-10 sarcomeres is projected onto the linear array of 50 photodiodes. Each diode is reset to a positive voltage which decays at a rate according to the intensity of light on that diode. A comparator converts this voltage to a binary output (light/dark). After optimum exposure, determined by the analog summation of the 50 comparator outputs, they are latched into the current image register and the diodes reset. Movement is detected by comparing the reference image with the current image and shifting the reference to best match the current image. Counting shifts gives a direct measure of the movement of the image. The maximum rate of movement that can be tracked is proportional to the cycle time of the circuit, determined by the intensity of the image on the array, as the comparison occurs concurrently with image formation. I have recorded image acquisition times of 1.8μs, faster rates can be achieved by increasing the light incident on the array.

T-Pos37 FREEZE-FRACTURE STUDIES OF CONTRACTING SINGLE FIBERS. Peter H.W.W. Baatsen and Gerald H. Pollack. Center for Bioengineering, WD-12, University of Washington, Seattle, WA 98195.

Single fibers were studied using an apparatus in which specimens could be quick-frozen. Sarcomere length was estimated prior to freezing by means of laser diffraction. Fibers were frozen by bringing Freon 22 (-157°C) around the fibers at a speed of ∿ 4 m/s. The frozen fibers were fractured, etched, replicated and subsequently observed in a Philips EM 420 electron microscope.

Activation of skinned fibers always resulted in irregular contraction along the length of the fiber; overstretched regions occurred next to supercontracted regions. Micrographs of the contracted regions were not readily interpretable in terms of myosin and actin filaments. Therefore, we turned to intact fibers. Initial sarcomere length was set at 3.1 - 3.3 μm. Fibers were tetanically stimulated through the mounting hooks and then allowed to shorten under a constant load. Fibers were frozen immediately after having reached a certain pre-set final length. In fibers allowed to shorten to ∿ 2 μm, sarcomeres became difficult to recognize. However, if shortening was terminated at ∿ 2.5 μm, well established features such as Z-lines, M-regions, H-zones and overlap zones of thick and thin filaments were easily discerned. In the H-zone, lateral structures (myosin heads) protruding from adjacent thick filaments sometimes appeared to touch each other and form lateral interconnections. Lateral projections were also observed on filaments of the I-band.

Additional experiments are underway to study structural changes associated with activated shortening.

T-Pos38 DIGITAL IMAGE PROCESSING OF MUSCLE STRIATIONS. David H. Burns, Ammasi Periasamy, William C. Everts & Gerald H. Pollack. Ctr. for Bioeng., WD-12, Univ. of Wash., Seattle, WA 98195.

We describe the use of digital image processing in optical microscopic studies of A- and I-band widths. Data were collected from two distinct preparations: In the first, single intact frog skeletal muscle fibers were imaged using a polarizing microscope. In the second, individual myofibrils isolated from rabbit psoas muscle and suspended between two micromanipulators were viewed under a phase microscope. The images obtained from these systems were collected with a vidicon camera and stored on an LSI-11/23 computer. Further analysis was done on a dedicated micro-VAX computer. The digital form of the data allowed the use of powerful image processing algorithms.

To estimate A- and I-band widths below the optical diffraction limit, the transfer function of each optical system was determined by imaging a step object and modelling the image with a combination of a Bessel and a Gaussian function. These transfer functions were used for subsequent digital deconvolution of striation images. Deconvoluted images demonstrated better distinction of fine structure than unenhanced images. To minimize aberrations caused by imperfections in the optical illumination and collection systems, a background subtraction method was also employed. Likewise, gray scale enhancement permitted better image visualization. Finally, the characteristic A- and I-band widths were determined by statistical analysis of the processed images.

Through application of these algorithms, we show that digital imaging allows both enhancement in the image quality and objective interpretation of results. Preliminary measurements obtained from relaxed fibers confirm the expected dimensional changes in both A- and I-bands with changes of sarcomere length. Currently, we are investigating A- and I-band widths in activated fibers.

T-Pos39 LATERAL CROSS-LINKS BETWEEN FILAMENTS IN THE H-ZONE AND IN THE I-BAND. K. Trombitas and G.H. Pollack, Center for Bioengineering, WD-12, University of Washington, Seattle, WA 98195.

A number of electron-microscopic studies have suggested that in the H-zone, myosin heads form cross-links between adjacent thick filaments. The early literature also contains evidence for the presence of bridges between filaments in the I-band. We reinvestigated these phenomena using two types of preparation: (1) conventionally fixed and embedded specimens from frog Sartorius and insect flight muscles; and (2) isolated A-segments and I-segments from rabbit skeletal muscles, prepared by negative-staining in the absence of fixatives.

Micrographs taken from frog Sartorius muscles that were stretched in the fully activated state revealed the presence of interconnections between thick filaments in the H-zones and between filaments in the I-bands; occasionally in regular arrangement.

In A-segments that had splayed like brushes at either end, distinct interconnections could be discerned between individual thick filaments. These interconnections were quite regular, and appeared to be responsible for the 14.3 and 43 nm periodicities observed in the A-segments that had remained intact. In isolated I-segments we could find no sign of interconnections. However, these segments contain only actin filaments. In the normal I-band an additional set of filaments, the so-called "connecting filaments," are also present, and these filaments, seen most clearly in rigor-stretched insect flight muscle, do show projections. Such projections appear, therefore, to be responsible for the lateral interconnections seen in the I-band.

Because A-band and I-band interconnections could be observed in both fixed and unfixed (negatively stained) preparations, they appear to be genuine. They may serve to stabilize the filament lattice and could play some role in sarcomere shortening.

T-Pos40 LASER DIFFRACTION OF INDIVIDUAL NEMATODES: T. ACETI AND C. ELEGANS. Victor Chen, Department of Biophysical Sciences,State University of New York, Buffalo, New York 14214

Single nematode (Turbatrix aceti or Caenorhabditis elegans)were anesthetized with either phenoxylpropanol or sodium azide. Larvae were not very sensitive to sodium azide. The individual nematode was then illuminated at normal incidence with a spatial filtered HeNe laser beam. The diffraction were recorded on film. The intensity and the substructure pattern of the first order diffraction were recorded. A major unit of light diffraction in these nematodes is the muscle sarcomere. The nematode has only longitudinal body muscles. The number and location of the muscle cells are fixed. The internal properties (structural factor) and the relative optical positions of the carcomeres (form factor) are the main determinents of the diffraction intensity. The oblique striations of the nematode muscle has a very prominent effect on the symmetry of the diffraction pattern. The right and left diffraction of the same order are not mirror images of the equatorial plane of the nematode.

T-Pos41 OPTICAL ELLIPSOMETRY OF DIFFRACTED LASER LIGHT FROM SINGLE FROG MUSCLE FIBERS STIMULATED TO ISOMETRIC TETANI. K. Burton, R.J. Baskin and Y. Yeh. Departments of Zoology and Applied Science, University of California, Davis, CA 95616.

Analysis of optical depolarization of laser light diffracted by single muscle fibers provides information on the structure and orientation of molecular components. Both the amplitude and phase anisotropy (r and δ, respectively) of the signals perpendicular and parallel to the fiber axis are useful in characterizing the intrinsic and form anisotropy of the signal. In previous reports detailing experiments on chemically skinned single fibers, we have presented evidence to show that the thick filaments are primarily responsible for the depolarization of the diffraction signal and that conditions which are thought to result in movements of crossbridges also result in changes in the depolarization signal. We have now extended these studies to electrically stimulated living fibers undergoing twitches and tetani. We have observed changes in tension, δ, and r with a time resolution of 20 μsec. or better. We have found that r decreases during an isometric contraction with a time-course which roughly parallels the rise and fall of tension. We also have observed a concomitant change in the δ signal. We are carrying out experiments to monitor the change in signal as a function of sarcomere length and to compare these data with the changes which occur as a fiber goes into rigor.

T-Pos42 DEPOLARIZATION SPECTRUM OF DIFFRACTED LIGHT FROM SKINNED FIBERS: ELLIPSOMETRY MEASUREMENTS OF THE ACTIVATED STATE. J. S. Chen, R. J. Baskin, K. Burton, Y. Yeh. Departments of Applied Science and Zoology, University of California, Davis, California 95616.

Differences in the total ellipsometry signal have been measured between the relaxed and the chemically activated states of skinned fibers from Rana pipiens. The activating solution which gives repeatable, sustained activation of the single fiber consists of potassium proprionate, 100 mM; TES, 60 mM; $MgCl_2$, 5 mM; EGTA, 30 mM; $CaCl_2$, 25 mM; creatine phosphate, 10 mM; CPK, 1 mg/ml; caffeine, 10 mM; pH = 7.1. Both the phase signal, δ, and the intrinsic depolarization factor, r, of the direct ellipsometry signal have been used to provide separate determinations of the relative changes in the intrinsic and form contributions to the total anisotropy signal. All signals are recorded during the middle phase of the activation cycle where the diffraction pattern is stable but broad. For all experiments, the relative change in the intrinsic contribution is negative: $(\Delta r/r_o) = -51.3 \pm 26.1\%$ over the entire sarcomere range. At the same time, the relative change in the form contribution is always positive: $(\Delta n_F/n_{F_o}) = 38.7 \pm 19.3\%$ The combined effect is consistent with the interpretation that as the fiber is activated, a significant part of the optically anisotropic element has rotated towards the f-actin filament while the mass content between the filaments has undergone appreciable redistribution. When the fiber was initially poised for activation in the low ionic strength state, then upon activation, $\Delta r/r_o \sim 0$ while $\Delta n_F/n_{F_o} > 0$.

Autocorrelation spectra of r(t) have also been obtained. Normal modes exist even when the fiber is relaxed. Upon rigor, there is a decrease in the number of modes while activation leads to further enrichment of the spectra. This work is supported by NIH under AM 26817.

T-Pos43 LIGHT DIFFRACTION STUDY DURING EQUILIBRATION PROCESS OF SINGLE MUSCLE FIBERS IN SOLUTIONS OF DIFFERENT TONICITIES. J.C. Hwang[1], Y.M. Cheung[1] and A.F. Leung[2]. [1]Department of Physiology, Faculty of Medicine, University of Hong Kong, Sassoon Road, Hong Kong and [2]Department of Physics, The Chinese University of Hong Kong, Shatin, Hong Kong.

Single fibers isolated from the semitendinosus muscle of frog were bathed in solution of 1.44R, 1.00R (normal Ringer) or 0.62R tonicity and illuminated normally with a He-Ne laser. The first-order diffraction intensity was measured continuously when the fiber's bathing solution was quickly replaced by a solution of 1.44R, 1.00R or 0.62R. When the original and final bathing solutions had the same tonicity, the diffraction intensity remained the same. A hypotonic replacement increased while a hypertonic replacement decreased the diffraction intensity. The time course of the intensity changes after replacement with a hypotonic or hypertonic solution followed closely a simple exponential time constant. This time constant was interpreted as the equilibration time constant (τ) for the muscle fiber equilibrating to the new bathing solution. When the normal Ringer solution (1.00R) was replaced by the 0.62R solution or vice versa, the equilibration time constant τ for (1.00R $\rightleftharpoons$ 0.62R) was about 40 s and about 20 s for (1.00R $\rightleftharpoons$ 1.44R). τ always decreased with sarcomere length. The equilibration process was attributed primarily to passive diffusion of water across the membrane system of the fiber. A proposed diffusion model could amount for the phenomena observed under the specified experimental conditions. (Supported in part by a research grant from University of Hong Kong to J.C.H.)

T-Pos44 **VISUALIZATION OF SARCOMERE DOMAINS IN SPATIALLY FILTERED IMAGES OF SKELETAL MUSCLE FIBERS.** C. L. Sundell[1], L. D. Peachey[1], Y. E. Goldman[2], H. Gonzalez-Serratos[3], and A. F. Huxley.[4] Depts. of Biology[1] and Physiology[2], Univ. of Pennsylvania, Phila, PA., Dept. of Biophysics, Univ. of Maryland, Baltimore, MD.[3], Physiological Laboratory, Cambridge Univ., Cambridge, England.[4] We have obtained images of sarcomere domains in single glycerinated rabbit psoas muscle fibers by spatially filtering the corresponding far-field diffraction patterns. These results provide direct evidence for the hypothesis that fine structure in skeletal muscle optical diffraction patterns arises from three-dimensional domains in the fiber that have uniform striation patterns. The spatial filtering system consists of a strip of quarter-wave retardation material superimposed over selected portions of the diffraction patterns. A low numerical aperture compound polarizing microscope forms a reconstructed image of the muscle fiber. When we select particularly bright and isolated fine structure lines in the diffraction patterns, we often observe single domains with tapered ends which are 220 to at least 1150 μm long and 18 to 63 μm wide (15 domains) in the reconstructed images. Observation of a fiber in the region of a domain with microscopes having numerical apertures of 0.25, oriented perpendicular to the fiber axis, revealed regular striations oriented as expected for Bragg reflection into the spatially filtered region. Often the diffracted light from two domains mutually interfered into the same region of the diffraction pattern to form two or more bright streaks separated by dark regions. As one of the domains was eliminated by masking the laser beam the dark regions separating the bright streaks increased intensity resulting in a single, wider fine structure line. These experiments provide direct confirmation of the domain hypothesis and information on the size and shape of selected domains. In addition they demonstrate that mutual interference from two or more domains influences the diffraction pattern such that one bright streak is not always correlated with a single domain in the muscle fiber. Grants: NIH GM7229, HL15835; MDA; AM26846.

T-Pos45 FLASH X-RAY MICROSCOPY OF CARDIAC MYOCYTES AND MYOFIBRILS. Joseph Dunn and Paul Paolini, Department of Biology and SDSU Heart Institute, San Diego State University, San Diego, CA 92182.

Flash X-ray contact microscopy (or transmission X-ray microscopy: TXM) has been used to produce high resolution X-ray transmission profiles of hydrated mammalian cardiac cells and myofibrils. Calcium-sensitive spontaneously active myocytes were isolated from adult rat heart by enzymatic dissociation. Myofibrillar fragments were prepared from whole heart homogenates and from skinned myocyte suspensions. Each type of preparation was deposited on a fine lithographic photoresist in an environmental chamber of 1 um depth. Single 100 nsec discharges from an imploding gas jet plasma X-ray source (LEXIS III, Maxwell Laboratories, Inc.) are produced at wavelengths in the "water window" between 2.3 nm and 4.4 nm by use of appropriate filter arrays mounted in front of the wet chamber. At this bandwidth, water is essentially transparent while biomolecules remain high in absorption, so that ultrastructural details can be contrasted. Exposed resists are then etched, metallized and examined by scanning electron microscopy. Image detail within contact TXM micrographs can be interpreted by comparison with differential interference contrast optical images and conventional SEM and thick section HVEM pictures. TXM micrographs of myocytes reveal the detailed substructure of myofibrillar bands, the arrangement of subsarcolemmal cisternae and the sarcotubular system surrounding the myofibrils. (Supported in part by an AHA, California Affiliate grant to P.P.)

T-Pos46 THE ULTRASTRUCTURE OF ISOLATED FISH SKELETAL MUSCLE THICK FILAMENTS. Robert W. Kensler. Department of Anatomy, The Medical College of Pennsylvania, Philadelphia, PA 19129.

We have previously demonstrated (Kensler and Stewart. 1983. J. Cell Biol. 96:1797-1802) that frog muscle thick filaments can be isolated with the helical arrangement of the myosin crossbridges largely preserved. As part of a comparative study of thick filament structure among the vertebrate classes, we have recently examined the structure of thick filaments isolated by a similar procedure from the lateral body wall of the goldfish (*Carassius auratus*). The negatively-stained fish thick filaments appear periodic with well preserved M-band regions and "end filaments". The crossbridge staining pattern along the filaments appears to repeat every third crossbridge level (43 nm) and is similar, but not identical, to that of isolated frog thick filaments. Optical diffraction patterns of images of the filaments show a series of layer lines indexing near the expected positions for a 43 nm helical (or near helical) repeat and appear consistent with previous X-ray diffraction data (Harford and Squire. 1982. J. Muscle Res. & Cell Motil. 3:481-482) for fish. The fish optical diffraction patterns typically differ from those of frog thick filaments in possessing a stronger 14.3 nm meridional reflection. This difference also appears to manifest itself in a strong 14.3 nm striping in the crossbridge region of isolated and negatively stained fish A-segments. These differences suggest that there may be subtle differences in the structure of the filaments of the two species. Our ability to isolate fish thick filaments with the helical ordering of the crossbridges preserved should allow these differences to be examined through a direct comparison of the filaments of the fish and frog. This work was supported by UPHS grant AM30442.

T-Pos47 X-RAY EVIDENCE FOR TWO DISTINCT MYOSIN HEAD ORIENTATIONS AND A TRANSITION BETWEEN THEM DURING ISOMETRIC CONTRACTION IN LIVING FROG SKELETAL MUSCLES J. Lowy and F.R. Poulsen (Intr. by G.F. Elliott) Open University, Oxford, UK.

The classical rotating myosin head model predicts a broad distribution of head orientations in the cross-bridge cycle. We have previously shown that the diffuse scatter present in X-ray patterns from frog skeletal muscles (Poulsen & Lowy, Nature 303, 146-152, 1983) and from threads of oriented synthetic myosin filaments (Poulsen et al., subm. for publ., 1985) contains information about the distribution of orientations of myosin heads. We found that in resting muscles (not stimulated for several hours) the myosin heads are practically randomly oriented; and that in full-overlap rigor muscles they have a preferred orientation. We have now investigated frog semitendinosus muscles during a series of isometric contraction cycles. In both the relaxed and contracted phases, tilt angles are concentrated around $|30°|$ and $|70°|$, the smaller angle being similar to that in rigor. During tension production, rotation about the long axis of the myosin head is restricted in about 40 % of the heads suggesting attachment to actin. The data indicate that a 'flip-flop' transition between tilt angles 70° and -30° produces a power-stroke of about 12 nm. We suggest that the two heads of each myosin molecule interact during the cross-bridge cycle making the return-stroke more efficient. We conclude that the rotating myosin head model is possible but that it operates in a manner not previously envisaged. Supported by MRC of UK and MDA of America.

T-Pos48 ANALYSIS OF HIGH RESOLUTION EQUATORIAL X-RAY DIFFRACTION PATTERNS FROM SINGLE SKINNED RABBIT PSOAS FIBERS L. C. Yu* and B. Brenner*†, *NIH, & †University of Tubingen.

Previously we have shown that an increasing fraction of crossbridges is attached to the thin filament as ionic strength (μ) decreases in a relaxed psoas fiber at 5°C (Brenner, et al, Biophys. J., 1984). To further characterize the structure of these weakly binding crossbridges (Brenner, et al, PNAS, 1982), equatorial diffraction patterns beyond the reflection [1,1] have been obtained in relaxed states at μ=100 and 20 mM, and in rigor at 100 mM. Fourier synthesis was performed by using reflections ([1,0],[1,1],[2,0],[2,1],[3,0]) with the phase combination (0°,0°,180°,0°,0°) (Yu, et al, Biophys. J., 1985). Density maps thus obtained showed that the thick filament is resolved into a backbone structure and an annular shell of mass, most likely that of crossbridges. Assuming phases remain the same for relaxed and rigor states, difference density maps showing mass transfers were constructed between (a) the two relaxed states and (b) 100 mM relaxed and rigor states. The mass increase at the thin filament site in (a) is approximately 1/2 that found in (b), and in (a) it occurs within a region ~150 Å in apparent diameter, whereas in (b) it occurs in a region of ~200 Å. A preliminary model, which includes the effect of the number of reflections being limited to [3,0] and produces density maps similar to experimental results, suggests that in axial projection, the increase of mass around the thin filament due to attachment of crossbridges is confined to a narrow area, probably 10-20 Å in the relaxed state, whereas in rigor, the attachment is probably confined to 20-35 Å. The narrower region of immobilization in relaxed state relative to rigor may reflect a higher degree of variability in attachment angle or crossbridge configurations.

T-Pos49 X-RAY DIFFRACTION AND RAPID STIFFNESS CHARACTERISATION OF MSL LABELLED RABBIT PSOAS FIBRES. Fajer,P., Brenner,B., Schoenberg,M., Yu,L. and Thomas,D., Biochem. Dept., Univ. of Minnesota, Minneapolis,MN 55455 and NIADDK, NIH, Bethesda, MD 20205.

In order to facilitate more direct comparisons between spectroscopic results (EPR) [1] and the X-ray diffraction and mechanical studies [2,3], the preparations used in EPR were characterised by the two latter techniques. In particular, the behaviour of fibres in rigor and under relaxing conditions at physiological μ (170 mM) and low μ (20 mM) was the object of this preliminary characterisation. Rapid stiffness of the unlabelled fibres in the presence of ATP at 170 mM was 8.4±1.7% of rigor stiffness and did not change on labelling with maleimide spin label (MSL). The speed-dependence of rapid stiffness at low salt was the same in labelled and unlabelled glycerinated fibres and similar to that reported for freshly skinned (EGTA) preparations. However, the dependence of rapid stiffness on ionic strength was less pronounced in glycerinated fibres than in EGTA preparations [3]. The I_{11}/I_{10} values were 5.8±1.5 and 3.5±0.3 (S.E.M.) in rigor, 0.68±.05 and 0.76±0.1 in the presence of ATP (μ=170 mM) and 1.82±0.2 and 1.95±0.2 (μ=20 mM) for unlabelled and MSL fibres, respectively. S.E.M. values are of 4 fibres from three different animals; one labelled fibre did not give a diffraction pattern. This variability is greater than that reported for EGTA skinned fibres [3], and precludes an unambigous conclusion as to whether spin labelling and/or skinning procedures significantly affect the X-ray data.

[1] P. Fajer et al. Biophys. J. 47, p. 380a, 1985
[2] B. Brenner et al. Proc. Natl. Acad. Sci. 79, p. 7288, 1982
[3] B. Brenner et al. Biophys. J 46, p. 299, 1984

T-Pos50 HIGH RESOLUTION DETECTION OF MUSCLE CROSSBRIDGE ORIENTATION: EPR OF GLYCERINATED PSOAS FIBERS MODIFIED BY DEUTERATED SPIN LABELS. V. A. Barnett, P. Fajer, C. F. Polnaszek, D. A. Momont & D. D. Thomas. Dept. of Biochem., Univ. of Minn. Medical School, Mpls., MN 55455.

Vertebrate Skeletal muscle consists of hexagonally packed actin and myosin filaments. Muscle contraction is proposed to involve the cyclical attachment and "rotation" of myosin crossbridges (myosin "heads"). Therefore, the orientation distribution of the myosin heads in rigor, and changes in that distribution due to contraction, or relaxation of the muscle fiber are of fundamental importance to the understanding of the mechanism of muscle contraction. In the present study, we have used ^{2}H-spin probes to specifically modify myosin at SH_1 in glycerinated rabbit psoas fibers and subfragment-1 (S-1). The advantage of the ^{2}H-probes is the removal of lineshape broadening due to the unresolved superhyperfine coupling to hydrogens in protonated probes. The narrower linewidth of the ^{2}H spin probe increases spectral resolution by a factor of two. Conventional EPR was used to measure the orientation distribution of the probed heads in rigor, relaxation, and in fibers decorated with labeled S-1. Using non-axial tensors we have simulated the spectra of relaxed and rigor fibers, and also the spetra of fibers decorated with labeled S-1 + ADP. These simulations allow the assignment of axial and azimuthal distributions of the spin label orientation. We wish to thank Dr. Al Beth of Vanderbilt Univ. for providing us with the ^{2}H-label.

T-Pos51 MUSCLE FORCE AND STIFFNESS DURING ACTIVATION AND RELAXATION. F.V. Brozovich and A.M. Gordon, Department of Physiology and Biophysics, Univ. of Wash., Seattle, WA 98195.

The calcium sensitivity of muscle force and stiffness was measured during isometric contractions of single skinned skeletal muscle fibers. In these experiments, single frog toe muscle fibers were isolated in chilled Ringer's solution and then transferred to relaxing solution (pCa=8, MgATP=5mM, μ=0.2M) where small Al foil T-clips were attached near the myotendon junctions. The preparations were then mounted between a force transducer (resonant at 10kHz) and a length driver (step response of 500μsec), and chemically skinned for 30 sec in CHAPS. Fibers were activated and then relaxed with quick changes of solution (T=5-8°C) in which free [Ca^{2+}] was controlled between 10^{-3} and 10^{-5}M using EGTA. Muscle stiffness was measured from the magnitude of the force change produced by small (<1%) 1 kHz oscillations in muscle length imposed during each force steady state. Sarcomere length was computed from the striation image by a phased locked loop device. For each pCa going up and coming down in [Ca^{2+}], force and stiffness was measured in the steady state. Using Hill's equation to fit the data, the plot of pCa vs force or stiffness during activation (increasing pCa) had pk's of 5.53 and 5.51 with n values of 3.4 and 3.8, respectively. During relaxation (decreasing pCa), the plot of pCa vs force or stiffness had pk's of 5.51 (n=3.0) and 5.53 (n=3.1), respectively. Therefore, during the steady state, no difference in the calcium sensitivity of force or stiffness was observed with increasing or decreasing [Ca^{2+}]. Also, the slope of plots of force vs stiffness was 1 for both activation and relaxation, implying that the force per cross-bridge is the same at all levels of calcium activation. Thus, cross-bridge attachment and force production appear to be regulated by Ca^{2+} binding to the same site. (Supported by grants from the MDA and NIH, NS08384 and HL07403.)

T-Pos52 THE ROTATIONAL DYNAMICS OF MYOSIN HEADS IN MYOFIBRILS IN THE PRESENCE OF ATP AND ATP ANALOGS DETERMINED BY TRANSIENT PHOSPHORESCENCE ANISOTROPY. Richard D. Ludescher, William B. Nelson, and David D. Thomas, Departments of Biochemistry and Physiology, University of Minnesota Medical School, Minneapolis, MN. 44544.

We have labeled myosin in intact muscle fibers with a triplet probe, eosin-5-iodoacetamide, which specifically labels the fast reacting sulfhydryl, SH_1, in isolated myosin. Polarized phosphorescence of myofibrils prepared from labeled fibers can measure rotational dynamics of the myosin head in the micro- to millisecond time range. The transient phosphorescence anisotropy (TPA) of myofibrils in rigor buffer (150 mM ionic strength, pH 7.0, no ATP) is flat and constant over hundreds of microseconds, indicating that the myosin heads are not rotationally mobile. In the presence of 5 mM MgATP, however, the TPA decays over several microseconds to a constant value that is smaller than that seen in rigor buffer. Upon hydrolysis of the ATP, the TPA reverts to that characteristic of rigor myofibrils. The TPA decay of relaxed myofibrils appears similar to that seen for synthetic myosin filaments. These data indicate that the myosin heads in relaxed myofibrils undergo microsecond rotational motions with significant amplitude. The TPA of myofibrils in the presence of AMPPNP and PPi also differs under some ionic conditions from that seen under rigor conditions. The dynamic state of myosin heads in myofibrils in the presence of ATP and ATP analogs will be discussed in light of the current theories of muscle contraction.

T-Pos53 AMPPNP, GLYCOL, AND PP_i EFFECTS ON CROSSBRIDGE ORIENTATION AND MOTIONAL PROPERTIES. N. Brunsvold, E. A. Fajer, P. Fajer, V. Barnett, S. Johnson, A. Le and D. D. Thomas, Dept. of Biochem., Univ. of Minnesota, Minneapolis, MN55455.

X-ray diffraction, EM and mechanical studies suggest that AMPPNP, glycol, and PP_i induce myosin crossbridge states intermediate between rigor and relaxation. Combining both AMPPNP and glycol induces a conformation similar to that of the relaxed state. We have examined the orientional effects of PP_i, AMPPNP and/or glycol on MSL spin-labeled fibers using conventional electron paramagnetic resonance (EPR). In the presence of 2-10 mM AMPPNP or 4mM PP_i (at 5-6 C, pH=7, u=100 mM), 30% of the myosin probes (one per head) are disordered. Glycol (50% v/v) produces a similar disordering. A combination of AMPPNP and glycol results in spectra identical to those of relaxed fibers (i.e., in the presence of ATP). Motional effects of AMPPNP, glycol, and PP_i on crossbridges were examined using saturation transfer EPR. These studies show that orientational disorder is accompanied by increased motion relative to rigor. The lack of an effect of AMPPNP on stiffness has been interpreted to show that no crossbridges are dissociated by AMPPNP (Tregear and Clarke, Adv. Exp. Med. Biol., 170, p. 177, 1984.). Therefore the present results imply that AMPPNP either (a) produces an attached crossbridge state that is dynamically disordered or (b) dissociates a fraction of myosin heads without dissociating crossbridges (e.g., dissociation of single heads of the double-headed crossbridge).

T-Pos54 THE EFFECTS OF PYROPHOSPHATE AND GLYCEROL ON MUSCLE FIBER STIFFNESS AND ON THE SPECTRA OF SPIN PROBES ATTACHED TO MYOSIN HEADS. E. Pate and R. Cooke, Department of Mathematics, Washington State University, Pullman WA 99164 and Department of Biochemistry and Biophysics, and CVRI, University of California, San Francisco, 94143-0448.

We have measured the orientation of a spin probe attached to the reactive sulfhydral on the myosin head in glycerinated rabbit psoas muscle. Step changes were applied to the fiber length to measure the stiffness of the fibers. All EPR spectra can be resolved into two components, one representing an ordered angular distribution of probes characteristic of myosin heads attached to actin and one representing an isotropic angular distribution characteristic of states in which myosin is bound weakly or not at all to actin. The concentrations of pyrophosphate (PPi) and glycerol were varied at 0° C in the presence of Ca and 0.18 M ionic strength. The presence of either PPi (0-2mM) or glycerol (0-50%), induced a decrease in the ordered component of the spectra (approximately 25%) with a concomitant increase in the disordered component and no change in stiffness. Both PPi and glycerol induced a a further shift towards the disordered component. Approximately half of the probes became random without a change in stiffness, but stiffness fell to a low value as the remaining fraction of probes became random. Two explanations can account for these results: 1) approximately one half of the myosin heads are only weakly bound to actin and can be dissociated without affecting fiber stiffness, or 2) there is a domain of the myosin molecule that is highly disordered by PPi and glycerol with the head still attached to actin. Supported by grants from the USPHS AM30868, HL32145, from the NSF PCM 8208292, and from the Research and Arts Committee of W.S.U.

T-Pos55 RESTING TENSION AND SARCOMERE-ASSOCIATED CYTOSKELETAL MATRIX IN SKELETAL MUSCLE: EFFECTS OF A-BAND EXTRACTION. K. Wang, R. McCarter, M. Hydorn (Intr. by J.T. Herlihy). Clayton Foundation Biochem. Inst. and Dept. Chemistry, UT, Austin and Dept. Physiol. UT Health Sci. Ctr., San Antonio, TX

Resting elastic properties of skeletal muscle were measured using mechanically skinned single rabbit psoas fibers. Isolated myofibrillar bundles were stretched to 200% rest length (4.6μm sarcomere spacing), and were then relaxed in calcium-free relaxing buffer solutions at room temperature (20°C). Control experiments demonstrated little change in elastic stiffness during several successive stretch-relax cycles. Extraction of A-bands with a sequence of solutions containing increasing amounts of KCl, up to a maximum of 0.5M KCl (Higuchi and Umazume, Biophys. J. 48:1985) resulted in marked increase in resistance to stretch of the preparations. The increased resistance exhibited two components: the first component was present for initial stretch from zero tension length and was labile, i.e. not observed in subsequent cycles. The second component resulted in higher peak rest tension for a given sarcomere spacing than control. When sequential extraction was carried out at a length correspondong to non-overlap of thick and thin filaments (4.2 μm) component 1 remained but component 2 was not present. Both components were eliminated by the presence of phosphate ion in the range 5-100 mM. Indeed resting tension decreased to less than 20% control after sequential extraction with solutions containing phosphate ion. An additional intriguing feature of component 1 is that tension is generated in a clearly stepwise manner during this phase of stretch. These results are consistent with involvement of sarcomere cytoskeletal matrix in the genesis of resting tension in myofibrils.

T-Pos56 RESTING TENSION AND SARCOMERE CYTOSKELETAL MATRIX IN SKELETAL MUSCLE: MYOFIBRILLAR ORIGIN OF HYSTERESIS. R. McCarter, K. Wang, M. Hydorn (Intr. by T.C.Smith). Dept. Physiol., U.T. Health Sci. Ctr., San Antonio and Clayton Foundation Biochemical Inst. and Dept. Chemistry, U.T., Austin, TX

To assess the role of sarcomere-associated cytoskeletal matrix in elastic properties of skeletal muscle, we have characterized the resting tension of single rabbit psoas fibers mechanically skinned in a relaxing buffer containing protease inhibitors. These myofibrillar bundles (0.8 mm long, 2.38 μm sarcomere spacing at rest length) were stretched at a rate of 10% of rest length in 30 seconds in a continuously perfused chamber. In control experiments there was little change in peak tension developed (1.8±0.1 kg-wt/cm^2, n=20) or in the areas of hysteresis loops obtained when myofibrils were subjected to 9 successive stretch-relax cycles, stretching to just beyond overlap of thick and thin filaments (4.2 μm sarcomere spacing). However, when myofibrils were extracted with 0.5M KCl solution, peak tension and area of hysteresis declined by 50%. Following further extraction with 0.6M KI, there was little change in peak tension but further reduction in amount of hysteresis. Finally, extraction with 6M guanidine hydrochloride resulted in purely elastic behavior (zero hysteresis) with preparations developing 10% control rest tension. The results indicate that the hysteresis phenomena of skeletal muscle are associated with myofibrillar components other than actin and myosin and that a truly elastic component of myofibrillar structure exists which is highly resistant to chemical extraction.

T-Pos57 DECREASE IN HEAT PRODUCTION DURING TRANSIENT TENSION RESPONSES TO SMALL RELEASES IN ACTIVE MUSCLES. Susan H. Gilbert & Lincoln E. Ford*, Dept. of Anatomical Sciences, SUNY at Stony Brook, Stony Brook, NY 11794, & *Dept. of Medicine, U. of Chicago, Chicago, ILL 60637

Huxley & Simmons (CSHS 1973) suggested that heat produced during quick releases, traditionally attributed to the thermoelastic effect (Hill, Proc. R. Soc. B 1953), could instead arise from enthalpy changes associated with transitions between attached crossbridge states, which they interpreted as length changes within a Voigt element in series with the rapid crossbridge elasticity. The two could be distinguished by measuring heat production during very slow releases. Thermoelastic heat would scale with the tension change and enthalpy changes with the length change. In these experiments three types of small releases were imposed on sartorius muscles contracting isometrically at 0C: releases of 3.2 to 12.9 nm/half-sarcomere (HS) (1) complete in 4 ms and (2) at a constant velocity of 0.8 μm/s per HS and (3) releases of 9.6 to 16 nm/HS complete in 100 ms. Tension and heat production were measured and isometric heat subtracted from the heat records. Extra heat was produced during all sizes and speeds of release and was a linear function of the tension change. For releases (1) and (2) the intercept of the line was about zero and its slope -0.014±0.001, the same as the thermoelastic heat-tension ratio measured in rigor muscles (Gilbert & Ford, 1985, in press). The line determined for release (3) had an intercept of -0.61±0.07 ($p<0.05$) and a slope of -0.016±0.001. Thus the amount of heat produced during the slow releases was substantially less than that produced during smaller, faster ones. The results show that at least part of the thermal response to releases is of thermoelastic origin and that any shortening in the postulated Voigt element is associated with absorption rather than production of heat.

T-Pos58 ASYMMETRY OF THERMAL RESPONSES DURING TENSION RECOVERY FOLLOWING SMALL STRETCHES AND RELEASES IN ACTIVE MUSCLE. S. H. Gilbert & L. E. Ford* (Intr. by Benjamin Walcott), Dept. of Anatomical Sciences, SUNY at Stony Brook, Stony Brook, NY 11794, &*Dept. of Medicine, U. of Chicago, Chicago, ILL 60637

If early stages of tension recovery following small stretches and releases are produced by reversible biochemical transitions on attached crossbridges (Huxley & Simmons, CSHS 1973), the thermal responses that accompany them should be symmetrical. Small length changes ($\leq$6.5 nm/half-sarcomere in 4 ms) were applied to frog sartorius muscles contracting isometrically at 0C. Tension and heat production were measured and isometric heat subtracted from heat records. Phase 2 of tension recovery was slower following stretches than releases (Ford, Huxley & Simmons, J. Physiol. 1977). Thermal responses measured at the end of the length changes were a linear function of the tension changes with an intercept of about zero and a slope of -0.0137 ± 0.0005. During the next 80 ms the thermal responses decreased in size and became positive after stretches. Between 80 and 160 ms the direction of the thermal responses reversed again, so that at 160 ms less heat was recorded than at 80 ms after stretch and more heat recorded than at 80 ms after release. During 160 ms after the length changes heat was produced after stretch and absorbed after release. The amount of heat produced after stretch was greater than that absorbed after release, although the extent of tension recovery was slightly less. While the processes occurring during tension recovery from length changes of opposite sign have enthalpy changes of opposite sign, the enthalpy changes do not bear the same ratio to the extents of tension recovery, suggesting that an additional heat-producing reaction may occur after both directions of length change.

T-Pos59 SKINNED SINGLE FIBERS FROM CHICKEN SLOW MUSCLE: VELOCITY OF SHORTENING (V_{max}), MYOSIN ISOZYMES AND DEVELOPMENTAL IMPLICATIONS. Peter J. Reiser, Marion L. Greaser and Richard L. Moss, Department of Physiology, School of Medicine and Muscle Biology Laboratory, University of Wisconsin, Madison, WI 53706.

V_{max} of single, chemically skinned fibers from the slow anterior latissimus dorsi (ALD) muscle of chickens was measured at 15°C using the slack test. For 16 adult fibers, the mean V_{max} was 0.24 $\pm$ 0.13 (SD) muscle lengths/s (ML/s) with a ten-fold range from 0.05 to 0.52 ML/s. (The mean V_{max} of 6 adult posterior latissimus dorsi (PLD) fibers, which are fast-twitch, was 3.28 $\pm$ 0.53 ML/S.). The myosin heavy chain (MHC) composition of the same fibers was examined using SDS-PAGE. Most of the adult ALD fibers contained two MHC's which were distinct from the MHC's in the PLD fibers. Previously, Matsuda, Bandman and Strohman (Differentiation 23: 36-42, 1982) demonstrated that the ratio of the amount of the two slow MHC's of ALD muscle (SM1 and SM2) changed during maturation. Specifically, the amount of SM1 decreased with increasing age. In our study, the relative amount of SM1 increased with V_{max} among the individual adult ALD fibers. There were no apparent differences in the regulatory protein or myosin light chain content on the SDS gels among these ALD fibers. This would suggest that the mean V_{max} of single fibers at early stages of development, where it has been shown that the amount of SM1 is greater than that of SM2 (Matsuda, et al., 1982), would be greater than that of the mean V_{max} of adult ALD fibers.
Supported by grants from NIH and the American Heart Association.

T-Pos60 THE INFLUENCE OF pH ON FORCE-CALCIUM RELATIONS IN SKINNED SKELETAL FIBERS AT VARIOUS LENGTHS. D.A. Martyn, A.M. Gordon. Center for Bioengineering and Department of Physiology and Biophysics, University of Washington, Seattle, Washington 98195.

Force-calcium relations for glycerinated rabbit psoas fibers were measured at several sarcomere lengths (2.3, 2.7, 3.1 and 3.4 μm) in bathing solutions at pH 6.0 and 7.0, with and without 3% Polvinylpyrrolidone (PVP). Bathing solutions all contained 133 mM K^+ proprionate, and 1.0 mM Mg^{+2}, 4.0 mgATP with appropriate Ca^{+2} and pH buffers. For experiments at pH 7.0, Ca^{+2} was buffered with EGTA (17 mM) and H^+ with MOPS. At pH 6.0, Ca^{+2} was buffered with CDTA (17 mM) and H^+ with MES. The MOPS or MES concentrations were adjusted at various pCa's to keep ionic strength at 200 mM. At pH 7.0 the Hill fit parameters obtained for sarcomere lengths of 2.3, 2.7, 3.1 and 3.4 μm were (for n) 3.12 ± .13, 3.02 ± .16, 2.45 ± .10, 1.86 ± .14 and (for K) 5.76 ± .006, 5.81 ± .007, 5.92 ± .007, and 6.01 ± .01, respectively. At pH 6.0, and the same lengths, the values were (for n) 3.85 ± .10, 4.24 ± .20, 3.62 ± .30, 3.1 ± .20, and (for K) 5.36 ± .006, 5.40 ± .006, 5.50 ± .011 and 5.51 ± .01, respectively. Lowering the pH resulted in force-calcium curves shifting to higher Ca^{+2} concentration, having generally steeper slopes and having K values which exhibited less length dependence. Absolute maximum force was also reduced in pH 6.0. Addition of 3% PVP (known to shrink fiber diameter to in vivo size) caused a uniform increase in Ca^{+2} sensitivity at all lengths, except 3.4 μm, in pH 7.0, but caused no change in the curves at pH 6.0. The results indicate that myofilament charge may have a strong influence on contractile Ca^{+2} sensitivity.
NS 08384, HL 31962-02.

T-Pos61 THE [$H_2PO_4^{1-}$] MAY DETERMINE CROSS-BRIDGE CYCLING RATE AND FORCE PRODUCTION IN LIVING FATIGUING MUSCLE M. Joan Dawson*, Susan Smith#, and D.R. Wilkie° (intr. by George Phillips*)
*Dept. of Physiology and Biophysics, Univ. of Illinois; #Dept. of Biochem., Univ. of Arizona; °Dept. of Physiology, Univ. College, London.

We have used ^{31}P nuclear magnetic resonance to determine intracellular pH and concentrations of phosphorous metabolites in repetitively stimulated anaerobic gastrocnemius muscles of rana temporaria. In an earlier study (Dawson, Gadian, and Wilkie, Nature 274: 861, 1978), we found that force development is proportional to the rate of ATP-utilization and that the decline in these parameters as muscles fatigue is correlated with buildup of products of ATP hydrolysis (ADP, inorganic phosphate [Pi], and H^+). We have recently repeated the earlier study using a wider range of stimulation patterns and have obtained essentially the same results. Further, we have found that as the muscles fatigue there is a strong linear relationship between the concentration of the acid form of Pi ($H_2PO_4^-$) and the decline in force development. These results suggest a product inhibition of force generation by $H_2PO_4^-$ and that the effect of H^+ on force development is due to acidification of Pi. Our results in living muscle are consistent with the conclusion of Hibberd, Dantzig, Trentham, and Goldman (Science 228: 1317, 1985) that formation of the dominant force generating cross-bridge state may be coupled to release of Pi in a reaction that is readily reversible.

T-Pos62 ADP BINDING TO MYOSIN CROSSBRIDGES AND ITS EFFECT ON CROSSBRIDGE DETACHMENT RATE-CONSTANTS. M. Schoenberg and E. Eisenberg†, NIADDK and NHLBI†, NIH, Bethesda, MD, 20892

Previously we showed that in the presence of PPi, AMP-PNP, or ATP, the tension induced by stretch of skinned rabbit psoas fibers decays to zero as strained crossbridges detach and then reattach in positions of lesser strain. Here we report that crossbridges with ADP at the active site behave differently. To eliminate the tension producing effect of contaminant ATP in the ADP, it was necessary to add Ap_5A, glucose and hexokinase to our solutions; 200 μM Ap_5A alone was not always sufficient. In the presence of 4 mM PPi the tension induced by a 2-nm/half-sarcomere stretch decays with a half-time < 1 s. In contrast, in the presence of 2 mM ADP, the tension induced by a 2-nm stretch decays slowly with a half-time > 500 s, a rate of tension decay comparable to that in rigor. Therefore, the binding of ADP appears to have little effect on the detachment rate of crossbridges. Because ADP alone has such a small effect, we could study the ability of ADP to inhibit the relaxing effect of PPi, thereby calculating an apparent K_i for ADP binding. Inhibition increased with increasing [ADP]; adding 0.25-0.75 mM ADP to 4 mM PPi caused as much inhibition as reducing [PPi] from 4 to 1 mM. In a single experiment, adding 4 mM ADP to 4 mM PPi reduced the decay rate as much as reducing [PPi] from 4 to 0.25 mM. Assuming that PPi and ADP show simple non-cooperative binding to the active site and that the rate of tension decay depends upon the number of crossbridges with bound PPi, these numbers suggest a K_i for ADP binding of 0.1-0.3 mM. We conclude 1) that unlike AMP-PNP or PPi, ADP at most slightly increases the crossbridge detachment rate-constants relative to those in rigor and 2) that ADP binds to attached crossbridges with an apparent dissociation constant of 0.1-0.3 mM. It is of interest that this dissociation constant measured in fibers is similar to that for ADP binding to actomyosin-S1 in solution.

T-Pos63 **KINETICS OF ACTIVATION OF SKELETAL MUSCLE FIBERS BY PHOTOLYSIS OF CAGED ATP IN THE PRESENCE OF MgADP** J.A.Dantzig*, D.R.Trentham†, and Y.E.Goldman* Dept. of Physiology* University of Pennsylvania, Phila., PA 19104 and NIMR†, Mill Hill, London NW7 1AA, England.

We previously reported that relaxation of glycerol-extracted rabbit psoas muscle fibers from rigor by laser pulse photolysis of caged ATP in the absence of Ca^{2+} is markedly slowed by addition of 0.05-1 mM MgADP to the photolysis medium (Biophys. J. 45:8a, 1984). In those experiments the relaxation showed strong evidence of cooperativity among cross-bridges. The figure shows results from a corresponding experiment with ~30 μM free Ca^{2+} present. Single glycerol-extracted fibers were put into rigor and then Ca^{2+} and caged ATP (10 mM) were added to the medium. Each panel shows an isometric trial (i) and one in which the muscle fiber was stretched (s) by 0.4%, 1 s before the laser pulse (arrows). In the absence of MgADP, liberation of ~0.6 mM ATP from caged ATP caused a tension dip and then rapid onset of active force production. The data can be fit by a simple kinetic model (circles): **Caged ATP → ATP; AM + ATP → D → F**, where D = detached, F = active force (J. Physiol. **354**:605, 1984). In the presence of MgADP, the tension dip is suppressed and activation is slowed by formation of AM.ADP complexes. The above model with the added reaction **AM.ADP ⟷ AM + ADP** does not fit the transients unless the state **D** is assumed to produce force (circles). The results suggest that in the presence of MgADP, ATP-initiated cross-bridge cycling involves cooperativity among sites. Supported by the MDA and NIH grants HL15835 to the Pa. Musc. Inst. and AM00745.

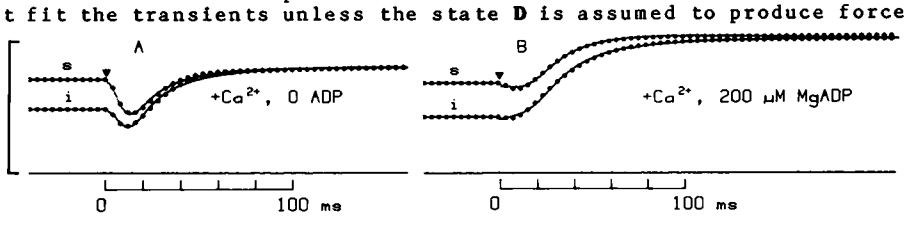

T-Pos64 INORGANIC PHOSPHATE INHIBITION OF FORCE IN MUSCLES. J.W. Lacktis and E. Homsher, Physiol. Dept., UCLA Med. School, Los Angeles, CA 90024.

During an isometric tetanus, force progressively declines. Godt et al. (Biophys. J. 47,293a,1985) showed that inorganic phosphate (P_i) inhibits force production in skinned frog muscle fibers and suggested that P_i accumulation may be responsible for muscle fatigue. To test this hypothesis isometric force ($F(t)$) and inorganic phosphate content ($P_c(t)$) of frog sartorius were measured at various times (t) during a 20 sec. tetanus. Normalized force ($F(t)/F_{max}$) was related to $P_c(t)$ by the equation $F(t)/F_{max} = 1.31[P_c(t)]^{-0.20}$. In other experiments using maximally activated skinned frog fibers at 5°C ($r/2 = 0.16$) force generation in the absence of P_i (F_o) was compared to force observed (F_p) at varying P_i concentrations. The relation between force and P_i was given by the equation $F_p/F_o = 0.91[P_i]^{-0.22}$. Considering that unstimulated muscle contains 3.2 μmol P_i/gm, we conclude that P_i dependent force inhibition quantitatively accounts for the decay of force during a maintained tetanus. The effect of P_i on isometric force was also measured in skinned rabbit fibers at 5°C and 24°C. The rabbit fibers behaved similarly to the frog fibers and maximal inhibition of force was about 25% at 24°C and 65% at 5°C. Hibberd et al. (Science, 228, 1317, 1985) have suggested that P_i reduces force by reversal of a force generating step assocciated with P_i release. Our data suggest that there are at least two strongly attached force generating crossbridge states subsequent to P_i release. Supported by NIH Grant AM 30988.

T-Pos65 ATTACHED CROSS-BRIDGES INCREASE CA BINDING TO THE ACTIVATING SITES. E.B. Ridgway and A.M. Gordon, Department of Physiology and Biophysics, Medical College of Virginia, Richmond, VA 23298 and Department of Physiology and Biophysics, University of Washington, Seattle, WA 98195.

When a barnacle single muscle fiber, microinjected with the Ca luminescent protein, aequorin, is stimulated under voltage and length control and allowed to shorten during the declining phase of the resultant Ca transient, extra Ca is observed. This extra Ca probably comes from the activating sites on the myofilaments because the time course of the extra Ca for shortening steps at different times is intermediate between free Ca and force. One explanation for the observed extra Ca is that Ca binding is sensitive to muscle length and/or force. An argument supporting length-dependent Ca binding is that the amplitude of the extra Ca depends on initial muscle length. However, the ratio of the extra Ca to active force is relatively independent of initial length so that the data do not distinguish between an effect of length on (1) Ca binding directly or (2) cross-bridge attachment (through a geometrical factor). The amplitude of the extra Ca increases with the size of the shortening step but saturates for steps greater than 8-9% of the initial muscle length arguing that Ca binding is not just length sensitive (if at all) but depends on muscle force. The extra Ca seen following stretch to higher forces is little increased over the control and is far less than that seen after stimulation to this higher force. Thus cross-bridge attachment appears to be more important than force per se. After a step decrease in length, the extra Ca seen after a second shortening step increases with a time course parallel to the force redevelopment implying that the bound Ca is increased by cross-bridge reattachment. Although our experiments do not exclude a simple length-dependent Ca binding, they argue strongly for an effect in which attached-active cross-bridges increase Ca binding to the activating sites. Supported by NIH, AM-35597 and NS-08384, and the American Heart Association.

T-Pos66 FILAMENT OVERLAP AFFECTS EXTRACTION OF TNC FROM SKINNED MUSCLE FIBERS. L.D. Yates, V. Koval and A.M. Gordon. Department of Physiology and Biophysics, Univ. of Washington, Seattle, WA 98195.

Recent studies on calcium regulation of muscle contraction selectively extract troponin C (TnC) from skinned skeletal muscle fibers with a low ionic strength solution containing a Ca^{2+}/Mg^{2+} chelator. Since previous results from this lab and others demonstrate a cross-bridge effect, especially rigor, on many of the properties of TnC, the effects of filament overlap on TnC extraction from skinned rabbit psoas muscle fibers were investigated. Force-pCa relationships at a sarcomere length (SL) of 2.7μm were determined before and after a 5 min TnC extraction at SL of 2.7, 3.1 or 3.5μm with 20mM Tris, pH 7.8, 5mM EDTA. The decrease in maximum Ca^{2+} activated force, an indicator of the amount of TnC extracted, was linearly related to overlap with decreases of 63±6% (n=14), 78% (n=2), and 89±4 (n=12) for extractions at SL of 2.7, 3.1 and 3.5μm, respectively. The smaller fiber diameter at the longer SL could facilitate diffusion. However, the wide range of measured diameters, ≈40-120μm, did not correlate with the observed force decrement and shrinking the fiber with polyvinylpyrrolidone did not increase the force decrement. Thus, TnC is preferentially extracted from non-overlap than overlap regions of the sarcomere. There were significant differences ($P>0.95$) between the Hill coefficients, pK and N, of the force-pCa relationships, measured at 2.7μm, for fibers extracted at 2.7 (pK=5.66±0.6) and 3.5μm (pK=5.55±0.08, N=3.0±0.6). However, the significance may result from a bias introduced by the low forces of the 3.5μm extracted fibers. All extracted fibers recovered force and Hill coefficients to control levels with added TnC. These results further indicate that rigor cross-bridges affect TnC other than Ca^{2+} binding and that under the conditions used here, retard its extraction. Supported by NIH grants HL31962 and NS08384.

T-Pos67 CYCLING CROSSBRIDGES INCREASE THE Ca^{2+} AFFINITY OF TnC. K. Guth, K. Winnikes, and James D. Potter, Dept. of Pharmacology, Univ. of Miami School of Medicine,Miami, FL

Previous studies by Bremel and Weber (Nature New Biol. 238: 97, 1972) have clearly demonstrated that rigor bridges increase the affinity of troponin for Ca^{2+}, however, little is known about the effect of force generating crossbridges on Tn Ca^{2+} affinity. We have investigated this question using the technique of TnC extraction and replacement by TnC_{DANZ} described previously (Zot, H.G., Guth, K. and Potter, J.D. (1985) Biophys. J. 47, 473a) followed by simultaneous measurements of fluorescence and force development. Measurements of fluorescence were also carried out in the rigor (no ATP) state. In the presence of ATP the steepness of the Ca^{2+} dependence of fluorescence and force (Hill Coeff. $\cong$ 3) was greater than could be accounted for by Ca^{2+} binding to TnC alone. A simple model has been developed which assumes only that, Ca^{2+} binding to either Ca^{2+}-specific site produces the fluorescence change, that there is no cooperativity in Ca^{2+} binding between these sites, that binding at both of these sites is required for activation and that the observed cooperativity comes from the interaction between adjacent regulatory units (7 actin: Tm:Tn). By using paired fluorescence and tension points we have calculated using this model, that there is a ten-fold Ca^{2+} dependent increase in TnC affinity over the pCa range of 7-5. This accounts fully for all of the cooperativity seen without invoking cooperative Ca^{2+} binding to TnC. This model is supported by the fact that in rigor no cooperativity in the fluorescence response was observed. Further support for the model comes from the fact that the Ca^{2+} dependence of TnC_{DANZ} fluorescence in reconstituted thin filaments is also not cooperative (Zot, A. and Potter, J.D. (1986), Biophys. J. (this meeting), Supported by NIH HL22619-3A.

T-Pos68 TITIN SPACING IN MYOFIBRILS FROM CARDIAC AND SKELETAL MUSCLES, S.-M. Wang and M. L. Greaser, Muscle Biology Laboratory, University of Wisconsin, Madison, WI 53706. A monoclonal antibody against bovine cardiac titin has been used to stain myofibrils of rabbit psoas (P) and bovine (B) cardiac muscle. Strips of muscle were tied to sticks at rest length (RL), at 150% of rest length (stretched) (S), and at 200% of rest length (overstretched) (OS). Strips were soaked in 75 mM KCl - 10 mM Tris (pH 6.8) - 2 mM EGTA - 2 mM $MgCl_2$ - 0.1 mM PMSF - 0.1% Triton X-100 to allow the muscle to go into rigor. Myofibrils were prepared and stained with anti-titin and fluorescein-labeled secondary antibody. The antibody stained two stripes per sarcomere which were perpendicular to the long axis of the myofibril. Most P and B myofibrils from the RL and S groups showed an increase in titin spacing (within a sarcomere) from about 1.65 microns to about 2.0 microns as sarcomere lengths increased from 2.0 to 3.0. The OS myofibrils (sarcomere lengths > 3.5 microns) had changes in titin spacing equivalent to changes in sarcomere length. The distance between titin bands in adjacent sarcomeres increased with sarcomere length up to about 3.5 microns but remained constant at about 1.5 microns at sarcomere lengths from 3.5 to 7.0 microns. Myofibrils from P - OS with sarcomere lengths from 2.6 to 3.5 microns often had titin spacings of 1.6 to 1.65 microns. However, B myofibrils from the OS group showed titin stretch dependence like the R and S groups. The results are interpreted to mean (1) that titin attachments may be broken at either the M line end or Z line end upon stretch (2) the breakage occurs at the M line end in very long sarcomeres, and (3) the breakage at the Z line end occurs with much greater frequency in rabbit psoas than bovine cardiac muscle. (Supported by AHA and NIH.)